Stratigraphic Investigations into the Late Miocene-Early Pliocene of the Northern Aorangi Range, Wairarapa

by

Tamsin Lesley Beatrice Bertaud-Gandar

A thesis submitted to the Victoria University of Wellington as partial fulfilment of the requirements for the degree of Master of Science in Geology

School of Geography, Environment and Earth Sciences

Victoria University of Wellington

October 2015

Abstract

The late Miocene-early Pliocene geology of the Makara and Ruakokoputuna Valleys in the northern Aorangi Range, south-east Wairarapa, is described in detail. In this area, a succession of Neogene sedimentary units laps onto basement rocks of Cretaceous age, and late Miocene-early Pliocene stratigraphy varies markedly, from bathyal mudstone to high energy coastal environments, over distances of only a few kilometres. Sections were measured at four key locations, which provided reference sites for stratigraphic changes across the study area. Additional detailed field mapping was carried out around Te Ahitaitai Ridge. Depositional environments were interpreted using grain size analysis, macrofossil and foraminiferal assemblages, and palynology. Foraminiferal biostratigraphy was used to constrain the ages of samples. Data obtained by these methods were combined with previous authors' work to produce a synthesis map, unit correlations, and geological cross-sections of the Makara and Ruakokoputuna Valleys. Late Miocene-early Pliocene geological history is interpreted, and a depositional model is proposed to explain the presence of giant cross-beds in the Clay Creek Limestone.

Despite major differences in lithology, the Clay Creek Limestone and Bells Creek Mudstone are shown to be partially laterally equivalent, while the overlying Makara Greensand is shown to be a diachronous unit which ranges from late Miocene (Kapitean) to early Pliocene (Opoitian) in age. This revised stratigraphy raises questions about the current classification of the Palliser and Onoke Groups, and provides new insights into regional geological history. The late Miocene-early Pliocene stratigraphy records a history of regional subsidence, punctuated by episodes of deformation which caused localised uplift and erosion. Previous seismic imaging studies identified one such episode of accelerated crustal shortening and deformation in the Wairarapa region near the Miocene-Pliocene boundary. The Clay Creek Limestone has proven to be a useful marker horizon for constraining the timing and style of deformation, which is interpreted to have occurred prior to 7.2 Ma. Major differences in stratigraphy between the upthrown and downthrown sides of the Mangaopari Fault indicate that the fault was active during this deformational episode. Lithostratigraphic units from the study area have been correlated with units in other parts of the Wairarapa, and these correlations suggest that late Miocene deformation in the region may have propagated from south to north.

Acknowledgements

Firstly, I would like to thank my supervisors, Cliff Atkins and Mike Hannah, for their guidance, support, and encouragement throughout this project. Thanks also to John Collen and Katie Collins at Victoria University, and to Alan Beu and Martin Crundwell at GNS Science, for their assistance with macro- and microfossil identification, to Bill McLea and Matt Ryan for pollen identification. Thanks to all the VUW staff members who have helped me in one way or another: Rob McKay for MATLAB wrangling, Stewart Bush for preparing thin sections, Dene Carroll for help with microscope work, Andrew Rae for help with GIS, and to Jane Chewings and Sandra Fogliani for their help in the lab and the library respectively.

Thanks to everyone who has accompanied and assisted me in the field: my supervisors, Ben, Katie, my dad, and Helen. I would also like to thank the other members of my 2012 ESCI 341 mapping group, Juliet, Russell, and Elliot, who were there when it all began; my officemates from CO421; and all the staff and students in the geology department who have provided feedback, advice, and camaraderie.

Thanks to Stuart and Caroline Ross at Birch Hill Station, and to Leigh and Wayne Ross at Greycliffs Station, for permitting us to work on their land. Thanks also to Simon and Liz Beveridge at Mangapari Station for providing accommodation during field work.

Special thanks go to my partner Tom, for providing tea, moral support, and assistance with forams and faunal lists, to my dad, for writing and study advice and for reminding me not to panic, and to my sister Rhiannon. Finally, I would like to dedicate this thesis to the memory of my mum, my aunt Janet, and my grandma, all of whom encouraged my interest in science from a young age. Thank you.

Contents

List of figures

A note on place names

Some of the Māori place names in the study area have alternate spellings, or spellings that have changed over the years. Previous geologists have sometimes used the spelling 'Ruakokopatuna' for the Ruakokoputuna River and Valley; the spelling used here is the one recognised by Land Information New Zealand (LINZ). The Aorangi Range has previously been referred to by some authors as the Haurangi Range, but Aorangi is recognised by LINZ as the correct Māori name, and is the name which appears on contemporary maps.

The spelling 'Mangaopari' is here used for Mangaopari Stream, although LINZ uses the spelling 'Mangapari' for this stream. The Plio-Pleistocene section in Mangaopari Stream has been studied extensively by geologists, and the spelling 'Mangaopari' has always been used in geological literature, although some early authors rendered the name 'Manga-o-pari'. I have been advised that the spellings 'Mangaopari' and 'Mangapari' are both sensical, and have chosen to use 'Mangaopari' in this study, for consistency with previous geological literature.

Chapter 1 Introduction

1.1 General introduction

Late Miocene to early Pliocene stratigraphy in the northern Aorangi Range varies greatly over distances of only a few kilometres (Vella and Briggs, 1971). This variability is particularly pronounced in the case of the Clay Creek Limestone, which partly overlies Cretaceous basement and partly overlies late Miocene sedimentary rocks (Vella and Briggs, 1971, Beu, 1995). Seismic reflection studies in the Wairarapa region (e.g. Cape et al., 1990, Nicol et al., 2002) show evidence for an episode of uplift and accelerated tectonic shortening during the latest Miocene or early Pliocene, and the Clay Creek Limestone may be a useful marker horizon for this event. An improved understanding of late Miocene-early Pliocene stratigraphy in the northern Aorangi Range will allow for better constraints on the paleogeography and tectonic history of the region during this time interval.

1.2 Aims

This study aims to reconstruct late Miocene-early Pliocene geological history in the northern Aorangi Range, and to place this in the wider context of the Neogene evolution of the southern Hikurangi Margin. In order to achieve this aim, the following objectives have been identified:

- Collect data and measure sections in key locations in the field;
- Interpret depositional environments based on lithology, grain size, and paleontology;
- Use biostratigraphy to constrain the ages of late Miocene-early Pliocene units in key sections;
- Correlate units across the field area;
- Combine data collected in this study with data from previous studies to produce a synthesis map and stratigraphic interpretation;
- Interpret late Miocene-early Pliocene geological history in the region;
- Constrain the timing and style of tectonic activity during this time interval.

1.3 Study area

The Aorangi Range is the southernmost of a series of coastal ranges which extend along the eastern side of the Wairarapa region. The study area is located on the range's northern margin, approximately 12 km south of Martinborough. The area is about 75 km^2, and encompasses the valleys of the Ruakokoputuna and Makara Rivers, and their tributaries Blue Rock Stream, Clay Creek, Bells Creek, and Mangaopari Stream (Figure 1.1).

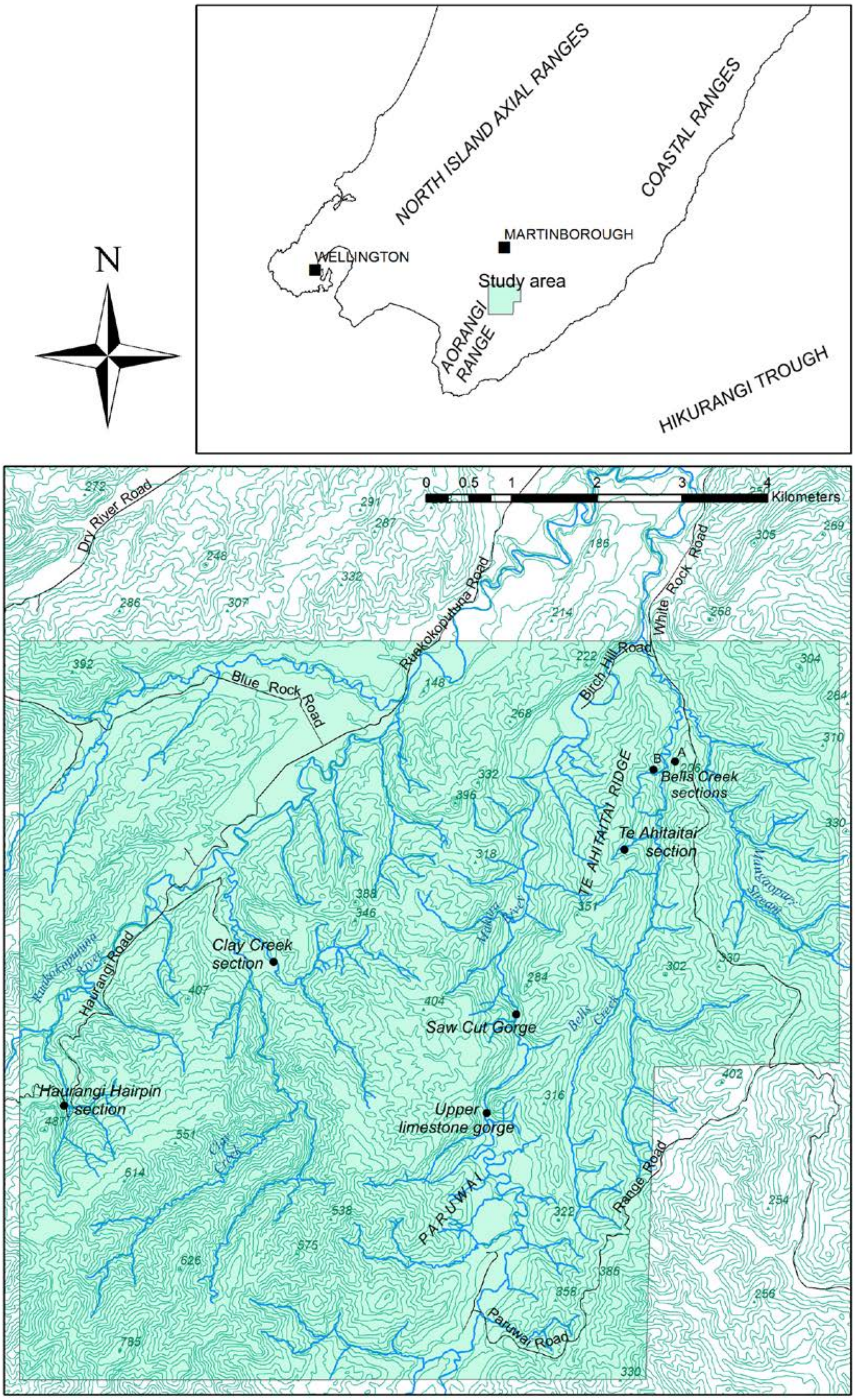

Figure 1.1: Study area, showing locations of key sections. 20 m topographic contours and spot heights (in metres) are also shown.

1.4 Geological setting

The study area is part of the southern Hikurangi Margin, where the Pacific Plate is being obliquely subducted beneath the Australian Plate. The forearc region of the Hikurangi Margin can be divided into several key structural components: a subduction trench (the Hikurangi Trough), a 150 km wide accretionary prism, and a zone of uplifted basement rocks forming the North Island axial ranges (e.g. Cole and Lewis, 1981, Beanland et al., 1998, Nicol et al., 2002). Deformation associated with the plate boundary is partitioned into a zone of strike-slip faulting in the axial ranges, and a fold-and-thrust belt extending from the inner forearc to the subduction trench (e.g. Cape et al., 1990, Nicol et al., 2002). The study area is located near the southern end of the forearc basin, within the fold and thrust zone (Figure 1.2).

Basement rocks of Late Permian to Early Cretaceous age are exposed in the axial and coastal ranges. In the East Coast forearc basin, these basement rocks are overlain by Paleogene and Neogene sediments. The Neogene sequence records the development of the plate boundary zone, starting in the Miocene (Begg and Johnston, 2000). This sedimentary record has allowed the paleogeography of the eastern North Island to be reconstructed in some detail through the Pliocene and Pleistocene (e.g. Kamp et al., 1988, Beu, 1995, Trewick and Bland, 2011). However, rocks of Miocene age in the southern East Coast Basin are less widespread than younger sediments, and few paleogeographic details are known for this time interval (Beu, 1995).

One of the defining features of the East Coast Basin Neogene sedimentary record is the presence of several coarse-grained, barnacle-dominated limestones, which are mostly of Pliocene age, but range from late Miocene to early Pleistocene (e.g. Beu, 1995, Kamp et al., 1988, Nelson et al., 2003). Barnacle plate limestones are rare globally, and the East Coast Basin limestones may be the most extensive barnacle limestones in the world (Beu, 1995). By volume, these limestones account for <10% of Neogene sediments in the basin, which consist mostly of terrigenous sandstone and mudstone (Nelson et al., 2003). Despite their relatively small volume, however, the barnacle-dominated limestones are a distinctive, widespread, and recurring facies throughout the onshore portion of the basin. This barnacle-dominated limestone facies is known as the Te Aute Lithofacies (Beu, 1995). The Pliocene Te Aute limestones have been interpreted as having been deposited on the margins of a narrow, tide-swept forearc seaway known as the Ruataniwha Strait (Kamp et al., 1988, Beu, 1995, Trewick and Bland, 2011) (Figure 1.3).

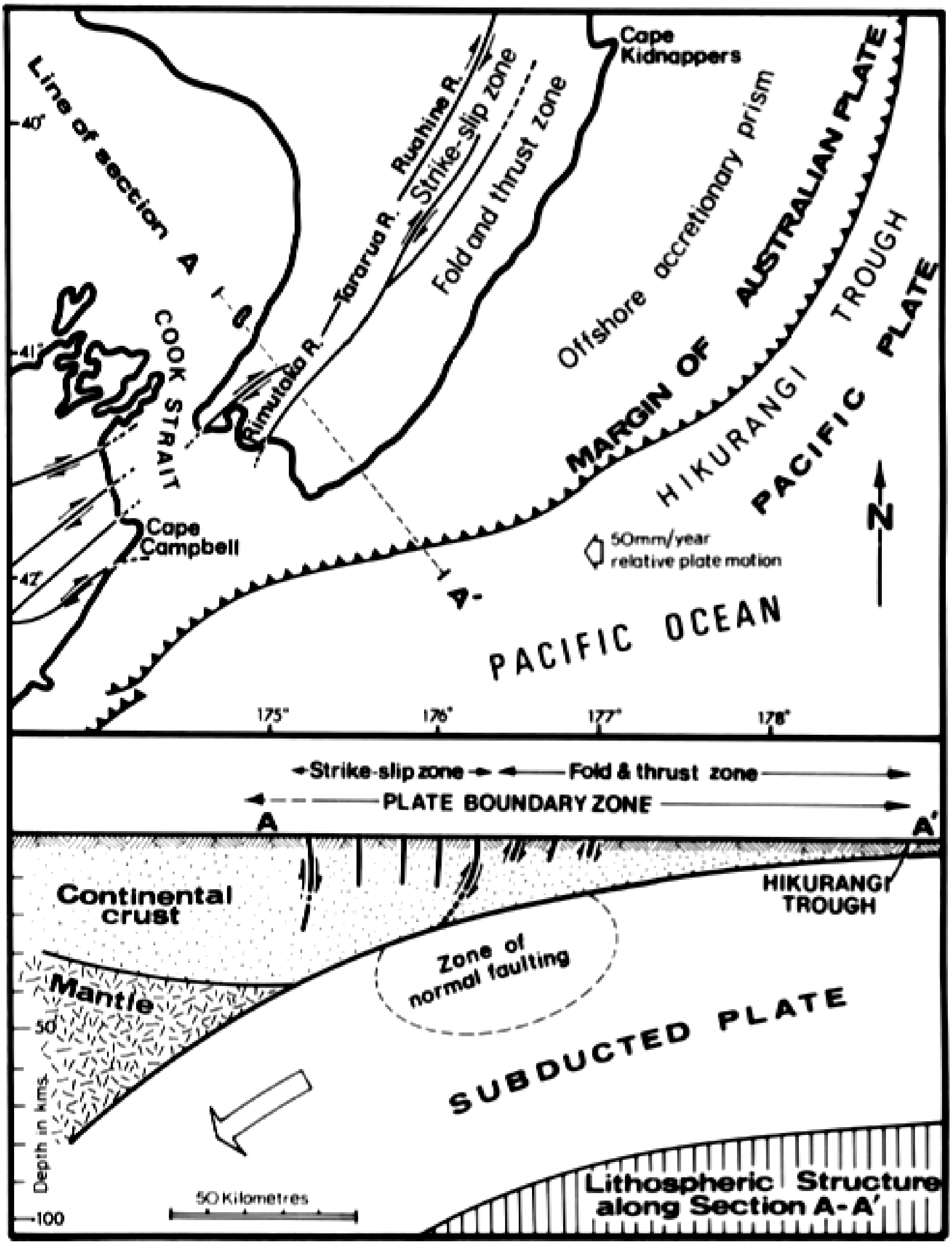

Figure 1.2: Map and cross section of the plate boundary zone in the lower North Island, showing zones of strike-slip and reverse faulting. From Cape et al. (1990); cross-section after Lamb and Vella (1987).

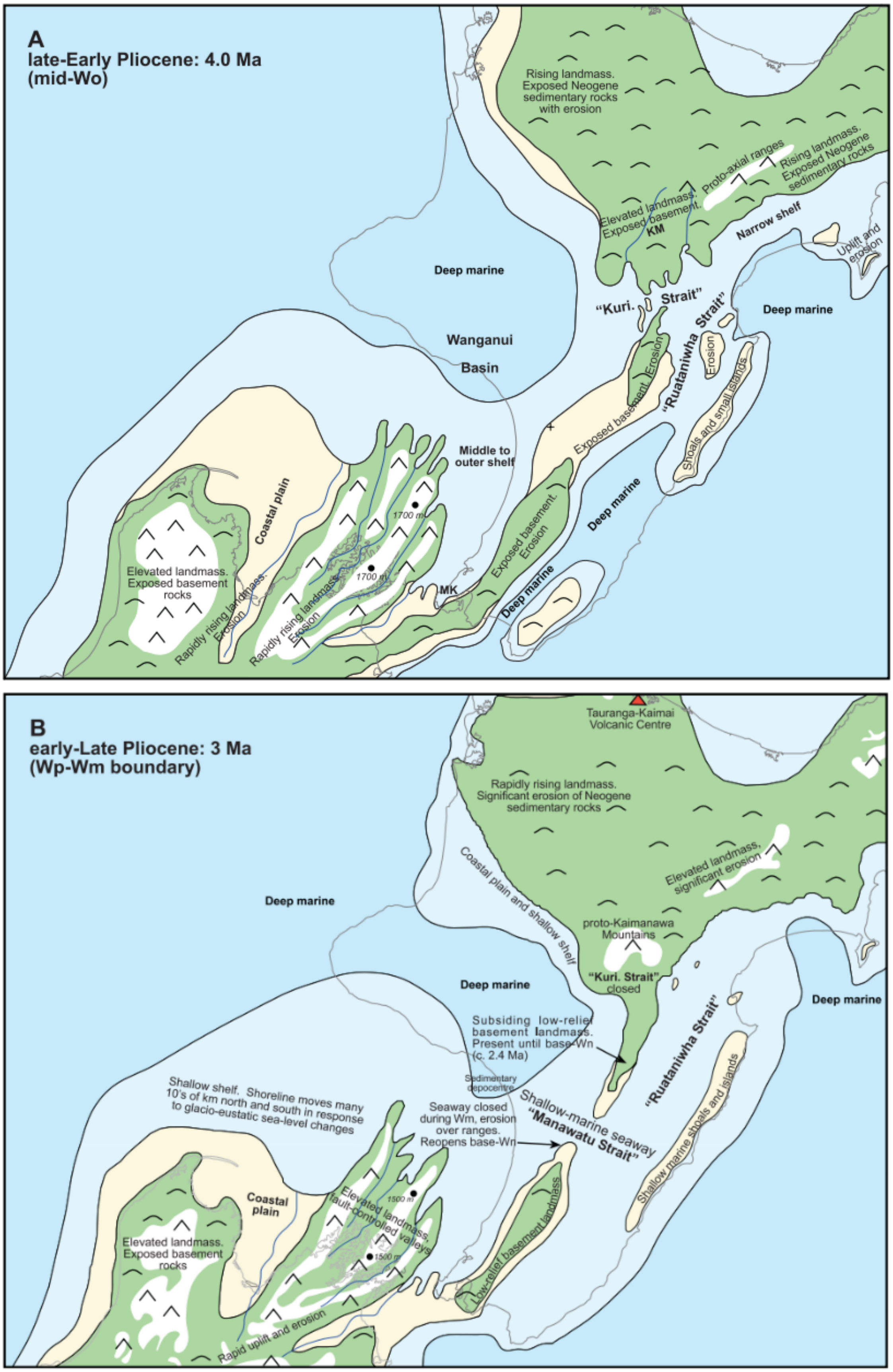

Figure 1.3: Paleogeographic reconstruction of central New Zealand during the early Pliocene (Opoitian stage, Wo) and Late Pliocene (Waipipian and Mangapanian stages, Wp and Wm) showing the development of the Ruataniwha Strait. From Trewick and Bland (2011).

1.5 Previous work

The history of geological research in the south-eastern Wairarapa stretches back more than a century. McKay (1878) conducted a reconnaissance survey of the eastern Wairarapa in which he noted Miocene and Pliocene limestone beds unconformably overlying greywacke basement on the margin of the Aorangi Range. Waghorn (1926) mapped part of the Ruakokoputuna Valley and suggested that the Tertiary sediments were deposited on a peneplain greywacke surface during an episode of marine transgression. King (1933) and Vella (1954) compiled faunal lists of molluscan fossils found in Tertiary rocks from the Ruakokoputuna and Makara valleys and from Palliser Bay.

Couper (1948) conducted the first detailed survey of the geology of the Makara and Mangaopari Valleys, and identified three main Tertiary lithological units. Larger-scale mapping studies were carried out by McLean (1953), who mapped an area between Dry River and Tuturumuri, and Bates (1967), who mapped an area between Lake Ferry and Makara River. Areas of key mapping studies from 1948 onwards are shown in Figure 1.5.

Vella and Briggs (1971) described and named 12 Cenozoic lithostratigraphic units in the Northern Aorangi Range. They noted that Cenozoic stratigraphy varies significantly over distances of only a few kilometres in the Ruakokoputuna-Makara area. Vella and Briggs's (1971) stratigraphy was revised by Vella and Collen (1984) based on new biostratigraphic data and tuff marker beds.

Several Victoria University students carried out projects in the Ruakokoputuna-Makara area between the 1960s and 1990s. Rodley (1961) studied the geology and paleoecology of Late Pliocene-Early Pleistocene sediments near the confluence of the Ruakokoputuna and Makara Rivers. Abbas (1971) studied the sedimentology of Miocene and Pliocene rocks, with a focus on the Sunnyside Conglomerate and the Bridge Sandstone Member of the Mangaopari Mudstone. Anderson (1976) studied the Upper Haurangi Limestone and Bull Creek Limestone at the Haurangi Hairpin section in Ruakokoputuna Valley, while Dobbie (1976) studied the Clay Creek Limestone, Makara Greensand, and Lower Haurangi Limestone at the same section and in the Makara and Blue Rock Stream Valleys. Crundwell (1979) studied the Makara Greensand at several locations across the northern Aorangi Range. Fittall (1979) mapped an area between Mangaopari and Whakapuni Streams, while Eggo (1979) studied biostratigraphic zonation in the mudstones in the southern part of Mangaopari Stream. Green (1981) and Hatfield (1981) mapped late Miocene to early Pliocene sediments at Paruwai in the southern Makara River Valley. Most recently, Henry (1996) mapped an area around the confluence of the Makara River, Bells Creek and Mangaopari Stream, and Clark (1998) studied the biostratigraphy of the Pukenui Limestone in the Makara and Ruakokoputuna Valleys.

The Mangaopari Stream section has been used in several studies of Pliocene-Pleistocene climate fluctuations. Devereux et al. (1970) combined oxygen isotope ratios from foraminiferal tests with coiling ratios of *Neogloboquadrina pachyderma* to produce a record of fluctuations in ocean temperature during Plio-Pleistocene times. Data from this section were also used in a landmark study by Kennett et al. (1971), which demonstrated that magnetostratigraphy could successfully be applied to Cenozoic marine sediments exposed on land, as well as constraining the ages of climate events reported by Devereux et al. (1970).The Mangaopari section was also included in studies of glacio-eustatic cycles by Beu and Edwards (1984) and Gammon (1997).

Beu (1995) conducted an in-depth study of Te Aute Lithofacies limestones of the eastern North Island, including in the northern Aorangi Range. He reviewed and revised the stratigraphic nomenclature for these limestones, and discussed their lithological characteristics, depositional environments, and pectinid biostratigraphy. He noted that the Clay Creek Limestone is of particular interest because it sits partly on Cretaceous basement and partly on Miocene mudstone.

Crundwell (1997) revised the definitions of some of the stratigraphic units in the study area, including the Makara Greensand, to better integrate the Aorangi Range stratigraphy with stratigraphy in other areas of the southern Wairarapa.

Several studies have examined the structural geology and tectonic history of the Wairarapa region. Wells (1989a) studied the burial history of Neogene basins in the Wairarapa and identified two cycles of subsidence followed by rapid uplift in the last 15 Ma. A seismic reflection study by Cape et al. (1990) identified buried folds in Miocene sediments which are unconformably overlain by Pliocene to Quaternary sediments which have also undergone folding. Nicol et al. (2002) used outcrop and seismic reflection data to study the growth of contractional structures in the Wairarapa over the last 10 Ma. They found that most deformation occurred during three episodes of accelerated shortening. The oldest of these episodes occurred during the latest Miocene, between about 8 and 6 Ma, with subsequent shortening episodes occurring between 3.4 and 2.4 Ma and from 1.8 Ma to the present day.

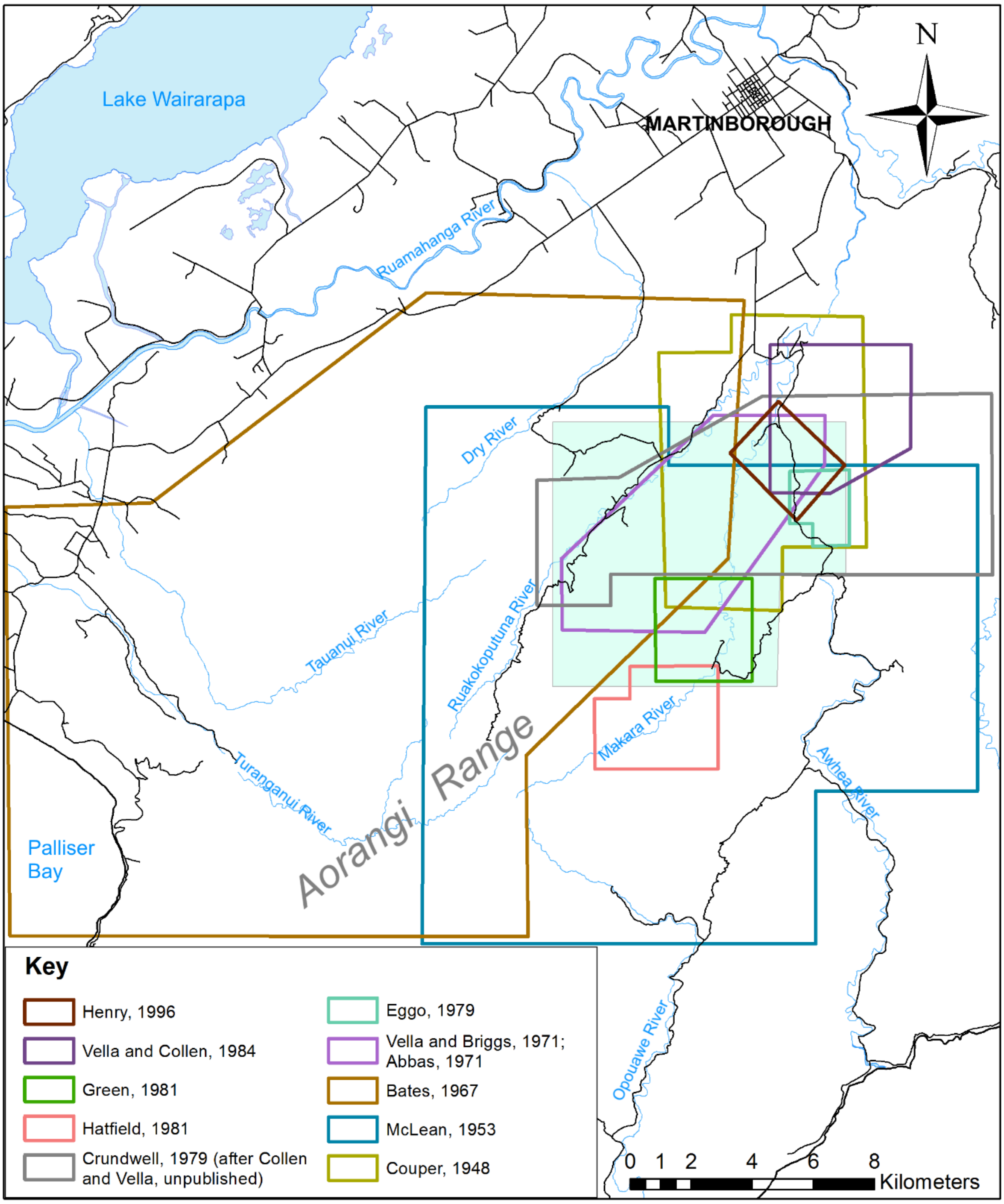

Figure 1.4: Map showing areas of previous mapping studies in the northern Aorangi Range from 1948 to 1996. The area of the current study is shaded.

Chapter 2 Methods

2.1 Mapping

In preparation for field study, maps produced in previous studies of the Northern Aorangi Range were scanned and the images were imported into ArcMap. Images were manually georeferenced to the NZMS260 rivers vector dataset. A draft compilation map was digitised from these data, and was used to correlate units and to identify key locations for field study. The area around Te Ahitaitai Ridge was identified as a key location in need of more detailed field mapping due to the dramatic changes in stratigraphy between the Makara River and Bells Creek.

Detailed field mapping was carried out along Te Ahitaitai Ridge and in the adjacent Makara River valley. Station locations, outcrop lithology, and strike and dip data were plotted on a 20 m topographic contour map in the field. No GPS was used, but bearings to key landmarks were taken and used when plotting locations on the field map. A draft geological map and cross-section of the Te Ahitaitai area were constructed over the course of the field campaign.

In creating the final Te Ahitaitai map (Figure 4.3), data from the field map were combined with high-resolution aerial photography acquired by the Greater Wellington Regional council, and made available through Land Information New Zealand. Aerial imagery was used to locate key features with greater accuracy than could be achieved with topographic contours alone. The map was manually digitised in ArcMap 10.

This Te Ahitaitai map was incorporated into the larger-scale compilation map. The compilation map incorporates data from most of the previous studies listed in Chapter 1. Some maps were omitted from the final compilation. The map by McLean (1953) was omitted because the Neogene rocks were mapped by New Zealand stages rather than by lithology, and the Miocene-Pliocene limestones were not differentiated and were all assigned to the now-antiquated Waitotaran stage. Some other maps were omitted due to duplication: the map of Vella and Briggs (1971) is very similar to that of Abbas (1971), and the latter could be obtained as a better-quality image, so the Vella and Briggs (1971) map was omitted. The map by Anderson (1976) was also omitted due to its similarity to the Vella and Briggs (1971) and Abbas (1971) maps. The map by Fittall (1979) was also omitted as the same area was mapped in greater detail by Vella and Collen (1998). The map by Henry (1996) was omitted because it was partly duplicated and partly contradicted by field observations from this study.

The remaining maps included in the compilation agreed well in some areas and were mutually contradictory in others. Where maps contradicted field observations made in this study, the field observations were given priority. The main areas of conflict were the Te Ahitaitai area, where data from this study were prioritised over all older maps, and the Makara River-Clay Creek interfluve. For the latter area, and at other locations of conflict, the following strategies were employed:

- Check to see if any of the conflicting maps include additional data for these locations, such as strike and dip of faults or bedding;
- If so, prioritise the map with more details plotted at the conflicting location;
- If no map is clearly more detailed in the area of conflict, check the aerial photography for any indicators of which lithologies may be present;
- Plot inferred geology for the area in question, based on aerial photography, topography, and interpolation from nearby areas of known geology;
- Attempt to construct a cross-section, and adjust the mapped geology as necessary for the cross-section to work;
- Indicate uncertainty on the map with appropriate symbology.

Strike and dip data from previous maps were also used in the compilation, along with strike and dip data from this field study. As these maps displayed the strike of beds visually, the bearing of strike had to be estimated when the symbols were digitised. For this reason, strike and dip data from older maps were omitted for areas where georeferencing distorted the original maps.

The cross-sections that accompany the maps were created using topographic data extracted from the 15 m digital elevation model (DEM) produced by the Otago University School of Surveying.

2.2 Measured sections and sample collection

Sections were measured at four key localities: the Haurangi Hairpin, Clay Creek, Te Ahitaitai Ridge, and Bells Creek. These sections provide key reference sites for changes in stratigraphy from southwest to northeast across the study area. Sections were measured using a 30 m tape measure, geological compass, Jacob's staff, and Abney level. Sections were described from outcrop and shallow excavation where required, using standard terminology and symbols after Andrews (1982). Fossil and bulk rock samples were collected and their heights recorded in the section descriptions. Additional samples were collected during field mapping around Te Ahitaitai Ridge. Samples were taken back to Victoria University for processing. A table of sample numbers, sample locations, and VUW locality numbers is presented in Appendix 1.

2.3 Sample processing

2.3.1 Grain size analysis

Grain size analysis was based on the methodology of Dunbar and Barrett (2005).

Grain size analysis was only carried out for sandstone and mudstone samples. Limestone and greensand were omitted, as the sizes of shell fragments and glauconite grains do not reflect hydrodynamic properties of depositional processes. The less cemented sandstone and mudstone samples were crushed between wooden blocks. Some samples proved to be too well-cemented for this method; they were crushed using a hydraulic press.

50-100 g of from each crushed sandstone or mudstone sample was measured out for grain size analysis. These samples were placed in beakers which were then filled with 0.5 g/L Calgon and disaggregated in a sonic tank for 15 minutes. The samples were then wet-sieved through 60 µm mesh to separate the sand and mud components. The separated sand and mud were then dried in a 40°C oven. The dried sand fractions were then weighed, and the weight percentage of sand calculated. Sand components were then placed in a sieve stack with 0.5 ϕ intervals and shaken in a Fritsch sieve shaker for 15 minutes. The sediment retained in each sieve was weighed, and the weights recorded in a spreadsheet.

The dried mud fractions were manually disaggregated using a spatula, and 4 g of each sample measured out into beakers. A 0.5 g/L Calgon solution was added to each beaker and samples were further disaggregated in the sonic tank prior to being run through SediGraph 5100. The SediGraph data were then combined with the sieve data to obtain full grain size distributions, and statistics were calculated using a MATLAB script. Grain size data are presented in Appendix 2 as per cent frequency figures for each 0.5 ϕ size class, summary statistics, and per cent frequency histograms.

2.3.2 Macro- and microfossils

Some macrofossils were picked in the field and others were extracted from disaggregated bulk sediment samples. The less well-cemented limestone samples were disaggregated by crumbling under running water, and macrofossils and clasts were removed and set aside. Cemented limestone samples were broken apart with a sledgehammer and crushed in a hydraulic press. Greensand samples were crushed with wooden blocks and macrofossils extracted. Macrofossils were identified with assistance from Dr. Katie Collins (VUW) and Dr. Alan Beu (GNS Science).

For micropaleontological analysis, crushed and disaggregated sediment samples were rinsed through two sieves: a 2 mm sieve to remove sediment coarser than sand, and a 64 µm sieve to remove mud. Samples were then dried in an oven at 40°C. A census of 300 foraminifera was picked from each sample where possible and mounted on slides, producing a total of 16 censuses. Three additional samples yielded some foraminifera, but not enough for a census. Other notable microfossils, such as ostracods and micro-brachiopods, were also picked and mounted on these census slides. Foraminifera were identified with assistance from Dr. John Collen (VUW) and Dr. Martin Crundwell (GNS Science).

In several cases the initial foraminiferal census data did not adequately constrain the age and paleodepth of samples, and further analysis of the residue from the picked samples was necessary. The residue was sieved at 150 µm to remove juvenile specimens and speed up the picking process. It was then searched for species which are key age indicators (e.g. the *Globoconella miotumida-Globoconella puncticulata* lineage) or paleodepth indicators as identified by Hayward et al. (2010). Four key samples were further processed in this way, and the specimens mounted on separate slides from the initial censuses.

2.3.3 Palynology

Three bulk rock samples collected in the field (19A, BC1, and 28A) contained significant amounts of visible organic matter, and these samples were processed for pollen. 10-11 g of each crushed sample was measured out and placed in a beaker. Two sub-samples were taken from sample 28A in order to balance the centrifuge.

Samples were first soaked in 10% HCl for 30 minutes. 30 mL of 40% HF was then added to each sample, and samples were left to digest for two days. Samples were then topped up with filtered water, stirred, left to settle, and drained, and this process was repeated four times. Sediment from the beakers was emptied into 50 mL tubes and spun in a centrifuge at 2600 rpm for 8 minutes. Samples were drained and topped up with filtered water, and this process was repeated four times, with samples only placed in the centrifuge for 5 minutes the second two times.

A few drops of 10% HCl were added to each sample, and topped up with filtered water. Samples were again centrifuged at 2600 rpm for 5 minutes, drained, and topped up with filtered water, and this process was repeated three times, and samples were drained of water. A sodium polytungstate (SPT) solution with a specific gravity of 1.85 was then added to each sample. Samples were centrifuged at 1800 rpm for 15 minutes, and left to settle overnight.

Organic matter floating at the top of the SPT solution was collected from each tube and transferred to smaller tubes, which were topped up with water. These tubes were placed in the centrifuge at 3000 rpm for 3 minutes. Samples 19A and BC1 separated well, and were drained and topped up with water. The two sub-samples of 28A did not separate well, and were not drained. All four samples were centrifuged again, drained, and topped up, and this process was repeated six times.

Because sample 28A contained a large amount of very fine organic material, it was then filtered through a 6 µm mesh to remove this fine component. The coarse material from the mesh was then washed into centrifuge tubes and spun at 3000 rpm for 3 minutes. All samples were mounted on glass microscope slides. Pollen grains were identified by Matt Ryan and Dr. Bill McLea (VUW).

Chapter 3 Stratigraphic framework

3.1 Introduction

This chapter summarises the stratigraphic framework for dividing the Neogene rocks present in the study area. The Neogene stratigraphy of the northern Aorangi Range has been extensively studied since the early 20th Century. However, the most detailed studies (e.g. Devereux et al., 1970, Kennett et al., 1971, Vella and Collen, 1984) have focused on the Pliocene-Pleistocene succession, with relatively little attention paid to the less widespread late Miocene-early Pliocene units. The definitions and interpretations of some late Miocene-early Pliocene units, especially the Clay Creek Limestone and Makara Greensand, have proven to be problematical. Section 3.2 outlines and discusses previous authors' interpretations of the late Miocene-early Pliocene rocks in this area. Section 3.3 lists and briefly describes the stratigraphic units recognised in this study. Most of the lithostratigraphic units recognised are after Vella and Briggs (1971).

The lithostratigraphic units in the study area have been defined and correlated using the stages of the New Zealand Geological Timescale. The New Zealand stages have been revised several times since they were first defined by Finlay and Marwick, (1940, 1947), and changing stage definitions are an additional source of uncertainty in correlating units. The currently recognised stages and their 2015 age calibrations are listed in Appendix 3. The biostratigraphic basis for some stage correlations is discussed further in Chapter 6.

3.2 Previous interpretations

Previous authors' interpretations of late Miocene-early Pliocene lithostratigraphy in the Makara-Ruakokoputuna area are summarised in Figure 3.1.

Couper (1948) was the first geologist to divide the rocks of the northern Aorangi Range into lithostratigraphic units. The oldest of Couper's Cenozoic units, the Makara Formation, consisted of basal conglomerate and limestone, overlain by mudstone; he considered the limestone and conglomerate to be laterally equivalent. He assigned the Makara Formation to the Tongaporutuan stage, and noted an apparent absence of Kapitean sediments from the area. The Makara Formation was disconformably overlain by the Manga-o-pari Formation, the lower part of which he assigned to the Opoitian stage.

McLean (1953) and Bates (1967) both mapped the Cenozoic rocks in the Aorangi Range on the basis of New Zealand stages rather than lithostratigraphic units. McLean (1953) assigned the limestones of the Ruakokoputuna and Makara valleys to the now-antiquated Waitotaran stage (equivalent to the modern Waipipian and Mangapanian stages), though he noted the presence of an apparently Tongaporutuan limestone in the lower limestone gorge of Makara River. Bates (1967) was the first to recognise Kapitean sediments in the area, in the form of a thin bed of glauconitic limestone and shelly glauconitic mudstone in the hills between Clay Creek and the Makara River. However, he considered the limestones of the Ruakokoputuna Valley to belong to the Opoitian and Waitotaran stages.

The first formally recognised Cenozoic lithostratigraphic unit found in the study area was the Hurupi Formation, which was initially described as the Hurupi Series by King (1933), and renamed the Hurupi Formation by Vella (1954). Vella and Briggs (1971) defined twelve lithostratigraphic units in the northern Aorangi Range, and divided the Neogene units into two groups. The oldest units, the Sunnyside Conglomerate and Bells Creek Mudstone, were placed with the Hurupi Formation in the Palliser Group, while all younger units were placed in the Onoke Group, with the two groups separated by an angular unconformity in the northern Aorangi Range, but conformable at other locations in the Wairarapa. Most of the units recognised in this study follow Vella and Briggs (1971).

The Clay Creek Limestone has proven problematical. It was defined by Vella and Briggs (1971) as the basal unit of the Onoke Group in the northern Aorangi Range, and was assigned to the Kapitean stage. This is in sharp contrast to Couper (1948), who placed this limestone at the base of his Makara Formation, stratigraphically below what is now recognised as the Bells Creek Mudstone, and assigned it to the Tongaporutuan stage. Previous studies have also reported widely varying stratigraphic thicknesses for the Clay Creek Limestone, from a maximum of 10 metres (Vella and Briggs, 1971) to over 100 metres (Green, 1981).

Hatfield (1981) and Green (1981) described the Clay Creek Limestone as unconformably overlying the Hurupi Formation in the southern Makara River valley, and grading stratigraphically and laterally into a unit of neritic to bathyal sands, muds, and shellbeds belonging to the Kapitean and Opoitian stages, which they informally named the Paruwai Formation.

According to Vella and Collen's (1984) revised stratigraphy, the upper Bells Creek Mudstone at Hinakura Road is Kapitean to lower Opoitian in age and a lateral equivalent of both the Clay Creek Limestone and Makara Greensand. The Bells Creek Mudstone was redefined to include all mudstones underlying the Opoitian Hikawera Tuff marker bed and overlying either the Hurupi Formation or Torlesse basement. This definition would include at least the lower part of the Paruwai Formation (Figure 3.1).

Crundwell (1987) mapped the Neogene rocks of Wainuioru Valley, approximately 50 km northeast of Ruakokoputuna. In this area, he found the Palliser and Onoke Groups to be separated by an angular unconformity associated with the Makara Greensand, which he inferred to belong to the Kapitean stage. Later, Crundwell (1997) revised the definitions of the Palliser and Onoke Groups in order to better integrate the stratigraphy of the Wainuioru area with that of the Aorangi Range. He found the Hikawera Tuff to be an unsuitable marker horizon for separating the two groups due to its limited distribution, and redefined the base of the Onoke Group as the base of the Makara Greensand where present, or the first appearance of Kapitean fossils in sections where the greensand is absent. As Kapitean fossils are present in the Clay Creek Limestone, Crundwell considered the greensand overlying the limestone to be a separate unit from the Makara Greensand. The greensand overlying the Clay Creek limestone was given informal status as an unnamed glauconitic bed. This redefinition of the late Miocene-early Pliocene greensands was also used by Field et al. (1997), but Begg and Johnston (2000) grouped the greensand overlying the Clay Creek Limestone with the Makara Greensand for mapping purposes.

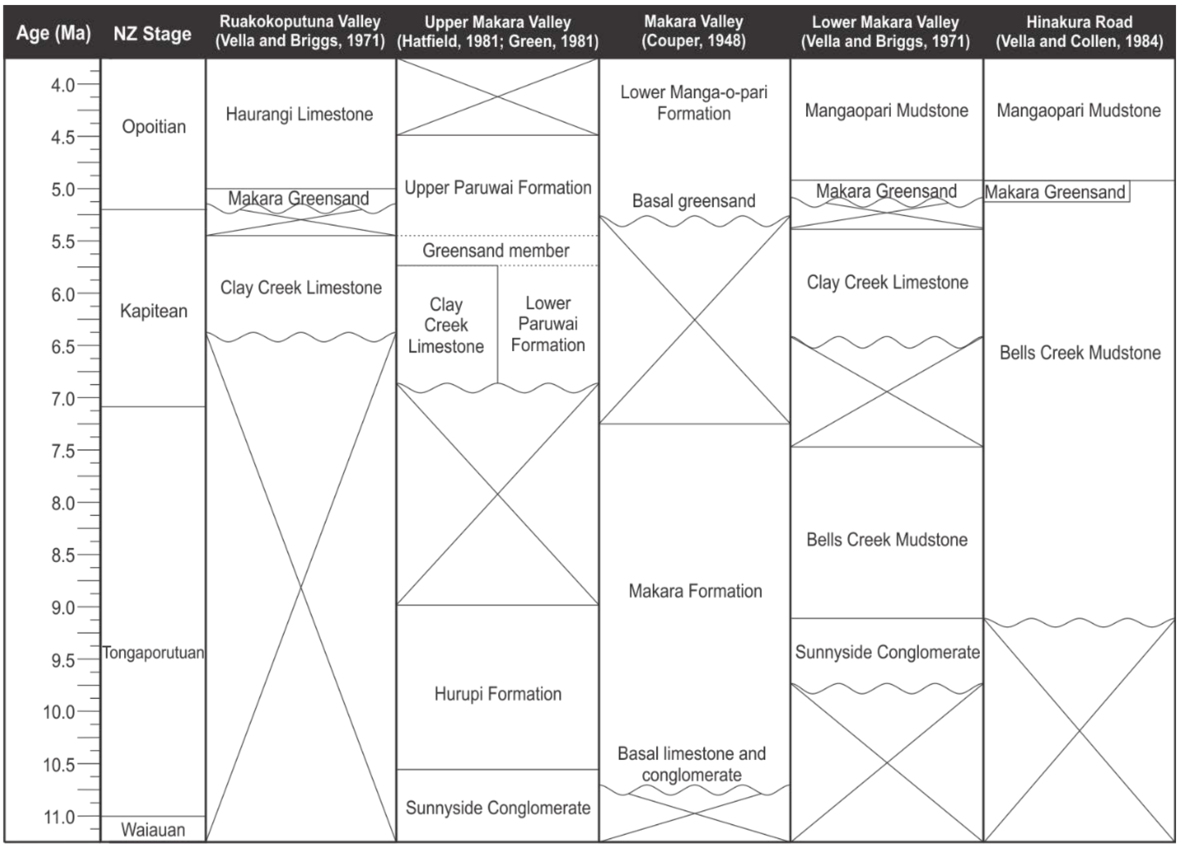

Figure 3.1: Previous authors' interpretations of late Miocene-early Pliocene stratigraphy at various locations in the northern Aorangi Range, arranged from southwest to northeast. Ages in Ma are approximate and based on the 2015 calibrated ages for NZ stage boundaries (Raine et al., 2015)

3.3 Stratigraphic units recognised in this study

3.3.1 Cretaceous

The basement rocks in the study area are of Early Cretaceous age, and belong to the Pahau Terrane and overlying Pahaoa Group of the Torlesse Composite Terrane (Moore and Speden, 1984, Begg and Johnston, 2000). They consist mainly of indurated quartzose sandstone and argillite, which is highly sheared and brecciated at some locations. Rare igneous rocks are also present within the Torlesse basement in the study area; most notably, a band of spilite forms prominent bluffs in Mangaopari Stream, adjacent to the Mangaopari Fault. The Torlesse rocks are not differentiated in this study.

3.3.2 Sunnyside Conglomerate

The basal unit of the Neogene sequence in the northeast of the study area is the Sunnyside Conglomerate, which overlies the Cretaceous basement with an angular unconformity (Vella and Briggs, 1971). The Sunnyside Conglomerate is a poorly sorted conglomerate, consisting of pebble- to boulder-sized clasts in a light brown sandy matrix. Clasts consist exclusively of basement-derived, indurated sandstone and argillite, are sub-angular to well-rounded, and have generally high sphericity. The conglomerate is a mixture of matrix- and clast-supported, and is interbedded in some sections with friable sands and organic siltstone.

3.3.3 Hurupi Formation

The Hurupi Formation forms the base of the Neogene sequence in the southeast of the study area; like the Sunnyside Conglomerate, it overlies Cretaceous basement rocks with an angular unconformity. It consists mostly of grey sandstones and sandy mudstones, although sandy limestones and metre-scale beds of conglomerate are also present at some locations (e.g. Hatfield, 1981). The Hurupi Formation contains a distinctive molluscan fauna, with key species including *Glycymeris hurupiensis, Polinices huttoni, Eumarcia thompsoni,* and *Struthiolaria callosa* (Vella, 1954, Beu and Maxwell, 1990).

3.3.4 Bells Creek Mudstone

The Hurupi Formation and Sunnyside Conglomerate are both overlain by the Bells Creek Mudstone. The exact nature of the basal contact of the Bells Creek Mudstone is unknown, and its relationships to underlying units are discussed in Chapter 6. The Bells Creek Mudstone is a massive, blue-grey mudstone with a significant clay component. It was initially defined by Vella and Briggs (1971) as a calcareous mudstone containing a distinctive assemblage of sparse, scattered bivalves, gastropods, and scaphopods, but the definition was broadened by Vella and Collen (1984) to include laterally equivalent mudstones lacking this fossil assemblage.

3.3.5 Clay Creek Limestone

The Clay Creek Limestone is the basal unit of the Neogene sequence in the west of the study area, where it unconformably overlies Cretaceous basement rocks. In other parts of the study area, it variably overlies the Sunnyside Conglomerate, Hurupi Formation, and Bells Creek Mudstone. It is a coarse-grained, weakly-bedded, well-cemented coquina limestone, which is white to pale yellow-grey on fresh surfaces and weathers to dark grey. It contains sparse to very abundant pebbles and cobbles of basement-derived sandstone and argillite, and in some places resembles a calcareous conglomerate. It is the oldest of the Te Aute Lithofacies limestones present in this area.

3.3.6 Makara Greensand

The Makara Greensand is here recognised as disconformably overlying both the Clay Creek Limestone and Bells Creek Mudstone, for reasons that are discussed in Chapter 6. The Makara Greensand is a thin (<10 m), friable unit of glauconitic sandstone and mudstone, with scattered pebbles of basement-derived sandstone and argillite. Scattered to abundant shell fragments and rare intact shells are also present in the greensand at some locations.

3.3.7 Haurangi Limestone

The Haurangi Limestone overlies the Makara Greensand in the west of the study area, and is the second of the Te Aute Lithofacies limestones present in the area. It is a medium-grained, barnacle-dominated coquina limestone which is moderately well-cemented. Vella and Briggs (1971) informally divided it into two parts, the lower and upper Haurangi Limestone, although the latter was subsequently defined as a separate unit (see below). Many exposures of the Haurangi Limestone contain abundant specimens of *Towaipecten ongleyi* (Beu 1995).

3.3.8 Dyerville Limestone

The upper Haurangi Limestone was formalised as a separate formation by Beu (1995), who renamed it the Dyerville Limestone. The Haurangi and Dyerville Limestones are separated by a disconformity, which at some locations is marked by an unnamed greensand bed. The Dyerville Limestone is a yellow-grey, coarse-grained barnacle plate limestone which varies from well-cemented to poorly cemented, and often contains intact specimens of *Phialopecten marwicki*. The Haurangi and Dyerville Limestones are not differentiated on the large-scale map.

3.3.9 Mangaopari Mudstone

In the eastern, southern, and central parts of the field area, the Makara Greensand is conformably overlain by the Mangaopari Mudstone, the lower part of which is considered to be a deep-water lateral equivalent of both the Haurangi and Dyerville Limestones (Vella and Briggs, 1971, Beu, 1995). The Mangaopari Mudstone is a grey mudstone that is mostly massive. Vella and Briggs (1971) informally divided the Mangaopari Mudstone into lower, middle, and upper sub-units, and also formally recognised one member: the Bridge Sandstone Member of the lower Mangaopari Mudstone. The Bridge Sandstone Member consists of a sequence of well-sorted, friable sandstone beds, which are interbedded with grey mudstone on a centimetre to metre scale. Macrofossils are extremely rare in the lower Mangaopari Mudstone and the Bridge Sandstone Member, but molluscan species such as *Pelicaria vermis* become more common with increasing stratigraphic height. Bedding on a decimetre scale, and concretionary bands parallel to bedding, become apparent in the upper part of unit.

3.3.10 Greycliffs Formation

The Greycliffs Formation was defined by Vella and Briggs (1971) as a unit of interbedded grey sandstone and mudstone containing scattered to abundant molluscs and concretionary bands. It conformably overlies the Mangaopari Mudstone, and the two are often difficult to distinguish in the field. Its status as a formation is disputed: Crundwell (1997) and Field et al. (1997) both treat it as a member of the Mangaopari Mudstone, while Begg and Johnston (2000) call it a formation in its own right. For the purposes of this study, the Greycliffs unit is mapped as a formation.

3.3.11 Bull Creek Limestone

The Bull Creek Limestone is a variably cemented, coarse-grained, barnacle plate limestone which is grouped with the Te Aute Lithofacies. Vella and Briggs (1971) and Anderson (1976) assigned the Bull Creek Limestone to the Mangapanian stage and correlated it with the upper Mangaopari Mudstone, but Beu (1995) showed it to belong to the lower Nukumaruan stage, and interpreted it as a shallow-water correlative of the Greycliffs Formation.

3.3.12 Pukenui Limestone

The Pukenui Limestone is the youngest formation recognised in this study, and the fifth of the Te Aute Lithofacies limestones in the study area. It conformably overlies the Greycliffs Formation. It consists of a sequence of cyclothemic interbedded shoreface limestone and mid-shelf muddy sandstone belonging to the Nukumaruan stage (Beu and Edwards, 1984, Beu, 1995, Clark, 1998). For the purposes of this study, the Pukenui Limestone is not differentiated from younger units, such as the Hautotara and Te Muna Formations, which may also be present in the north of the study area.

Chapter 4 Mapping and key localities

4.1 Introduction

This chapter provides details of the lithostratigraphy, stratigraphic variation, and structural geology of the study area. Geological maps and cross-sections are presented and discussed in section 4.2, and the structural geology of the area is outlined. Sections 4.3-4.6 present data from detailed measured sections, which illustrate lateral changes in stratigraphy from southwest to northeast. Sections 4.7-4.9 describe changes in late Miocene-early Pliocene stratigraphy from north to south in the Makara River valley. Additional lithological data from samples collected at the described locations are also presented in this chapter.

4.2 Geological maps

Figure 4.1 shows the locations of observations made and samples collected over the course of this study. The geological map presented in Figure 4.2 is a synthesis, combining data collected from these locations with data from previous authors' maps (see chapter 2). The synthesis map shows several key features of Neogene geology in the area. A transition in lithologies is apparent, from limestone-dominated Miocene-Pliocene successions in the west of the field area to mudstone-dominated successions in the east; the Mangaopari and Bells Creek Mudstones both thicken significantly from west to east. The Clay Creek Limestone outcrops over large areas in the central part of the study area, between Clay Creek and the Makara River, but thins to the west and disappears entirely in the east.

In contrast to highly variable late Miocene-early Pliocene stratigraphy, the late Pliocene-early Pleistocene stratigraphy in this area is relatively uniform, with the Greycliffs Formation and Pukenui Limestone appearing as continuous, laterally extensive layers across the northern and central parts of the study area.

Structurally, the mapped area is dominated by large, northeast-southwest striking reverse faults and folds, most notably the Mangaopari, Ruakokoputuna, Blue Rock, and Nikorima Faults. The Nikorima Fault is an informal name used here for the first time. The northern and southern segments of this fault have been mapped previously by several geologists (e.g. Collen and Vella, unpublished, Crundwell, 1979, Eggo, 1979, Green, 1981), while the central segment connecting the two is inferred here based on the mapped geometry of the contact between the Cretaceous basement and overlying Neogene units. The Mangaopari Fault is inferred to split into two strands near the Makara River's upper limestone gorge at Paruwai. Field observations suggested that more than one fault might cut through the gorge, and a second fault is shown in cross-section B-B'. The extent of this second fault strand to the northeast is not known; it is inferred to diminish rapidly to the southwest of its mapped location, as offset of the Clay Creek Limestone across the Mangaopari Fault becomes negligible at the southern end of the upper limestone gorge, and remains so for a distance of 1 km along strike. The main expression of the Mangaopari Fault over this interval is a large monoclonal flexure in the Clay Creek Limestone, shown in Figure 4.5 and cross-section A-A' (Green, 1981). Further to the southwest, vertical offset across the Mangaopari Fault increases again (Green, 1981, Hatfield, 1981).

Cross-sections A-A', B-B', and C-C' (Figure 4.3) illustrate some of these structural features, especially the Mangaopari Fault and broad Mangaopari Anticline. Lateral variations in stratigraphy, and inferred lateral relationships between units, are also illustrated in these cross-sections.

The Te Ahitaitai map (Figure 4.4) shows the results of the detailed field mapping carried out in the area around Te Ahitaitai Ridge. This map shows major lateral changes in stratigraphy between the Makara River and Bells Creek. The Clay Creek Limestone overlies Torlesse rocks in the Makara River valley, and overlies Sunnyside Conglomerate on the western side of the ridge, but is absent in Bells Creek, where the Sunnyside Conglomerate is overlain by Bells Creek Mudstone, and on the eastern side of the ridge adjacent to the Mangaopari Fault, where the conglomerate is overlain by Makara Greensand.

The main structural features in the Te Ahitaitai area are the Mangaopari Fault and the northern part of the Mangaopari Anticline. Smaller-scale features include the McLeod Fault, which was mapped and discussed in detail by Vella and Collen (1998), the Birch Hill Syncline (new name), and the Makara Fault, which was mapped by Couper (1948) and Abbas (1971). The Makara Fault is shown as an inferred feature due to uncertainties around its precise location, age, and geometry. Faulted, brecciated, and sheared basement rocks were observed in Makara River to the south of Homestead Creek, consistent with Couper's (1948) description of the Makara Fault as a relatively broad zone of deformation running through the Cretaceous basement, sub-parallel to the river. Abbas (1971) mapped the fault with a more northeast-southwest strike than Couper, and showed it truncating the Sunnyside Conglomerate, but not the overlying Clay Creek Limestone. The faulting-out of the Sunnyside Conglomerate could not be confirmed in the present study, but is assumed to be correct. There is no sign of offset in the Clay Creek Limestone, so activity on the Makara Fault is assumed to postdate the deposition of the Sunnyside Conglomerate and pre-date the Clay Creek Limestone.

Observations from aerial photographs show a difference in strike of up to 20° between the Sunnyside Conglomerate and Makara Greensand in Bells Creek, and an angular unconformity is apparent between the Sunnyside Conglomerate and Clay Creek Limestone in the area around Homestead Creek. In this area, the Clay Creek Limestone dips to the northeast at 20°, while the outcrop pattern of the Sunnyside Conglomerate indicates that has a shallow dip to the east or southeast. Vella and Briggs (1971) considered the relationship between the Sunnyside Conglomerate and Bells Creek Mudstone to be conformable, and placed the angular unconformity between the Bells Creek Mudstone (the uppermost unit of the Palliser Group) and the Clay Creek Limestone (the basal unit of the Onoke Group). However, in this study, it is suggested that the Clay Creek Limestone is a partial lateral equivalent of both the Bells Creek Mudstone and Makara Greensand. Possible relationships and correlations between these units are discussed further in Chapters 5 and 6.

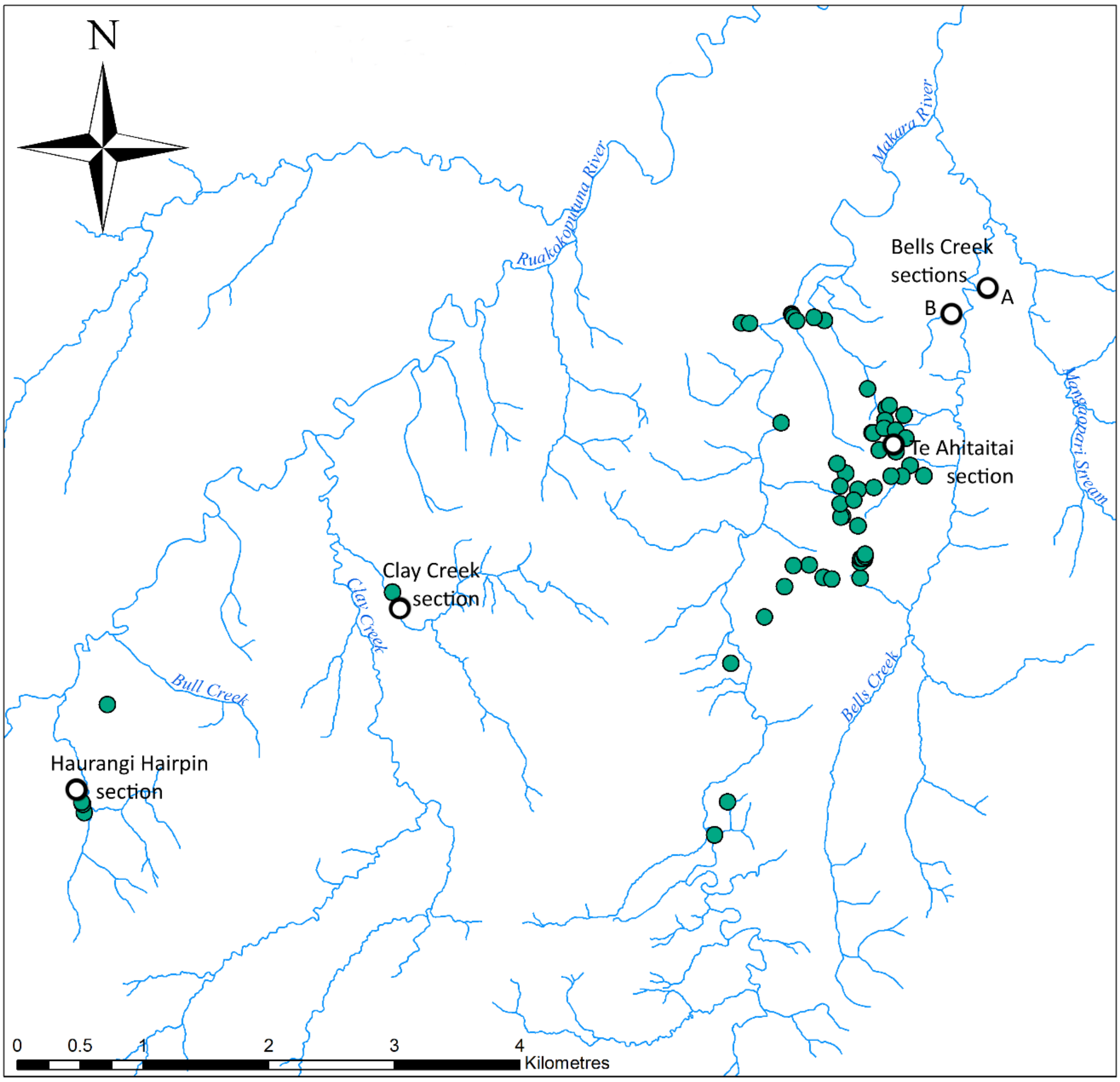

Figure 4.1: Map showing outcrop and measured section locations for this study.

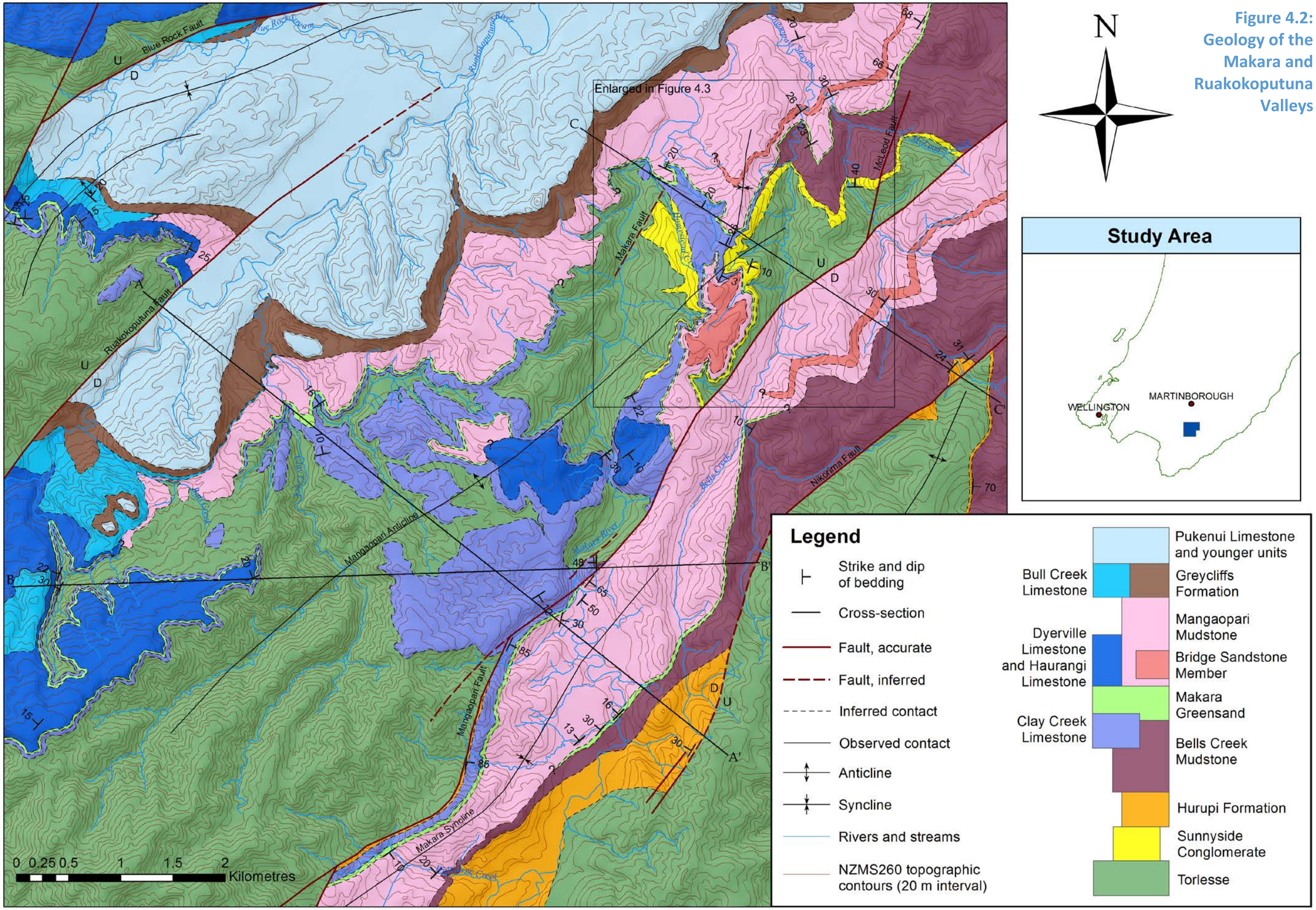

Figure 4.2: Geology of the Makara and Ruakokoputuna Valleys

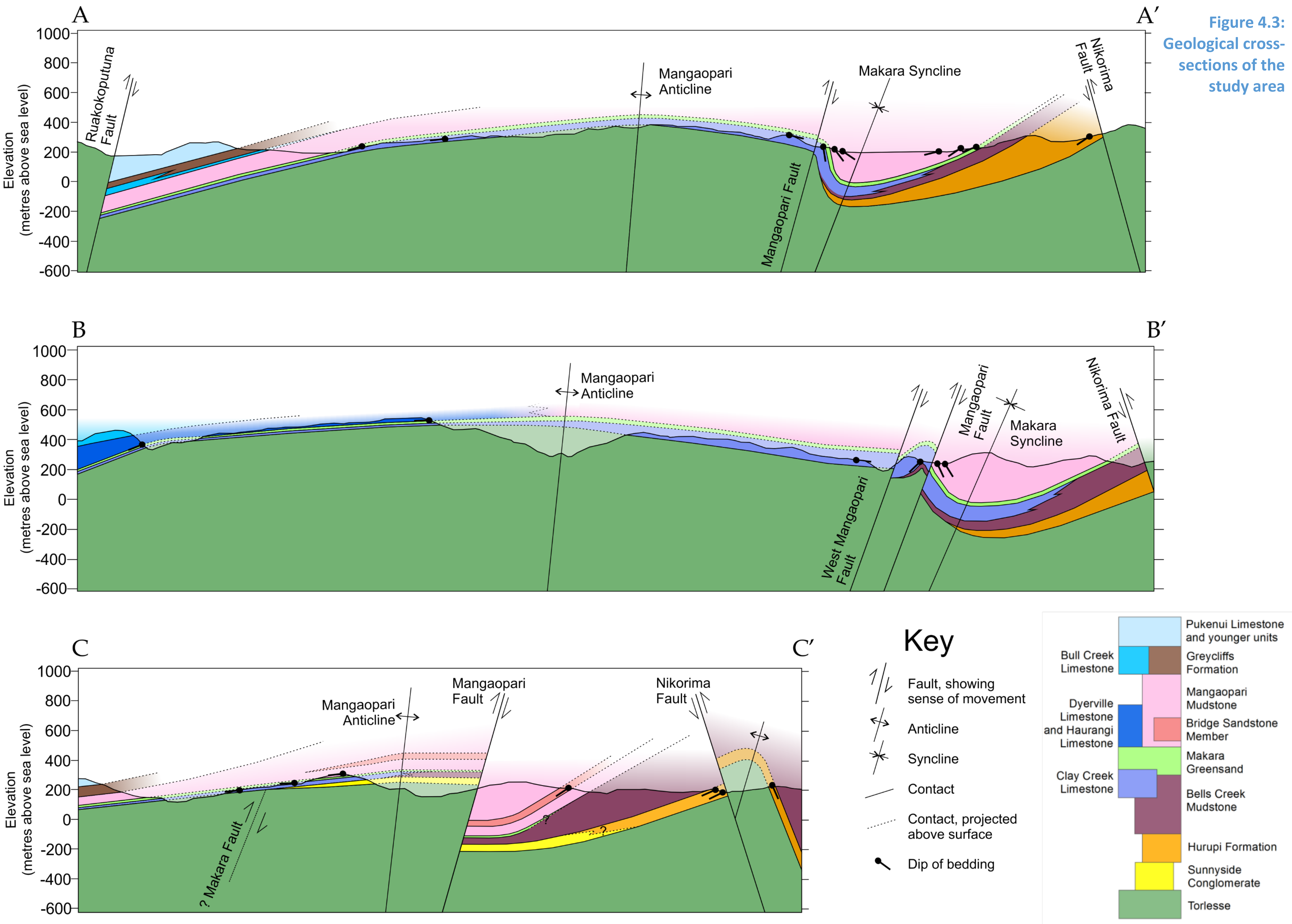

Figure 4.3: Geological cross-sections of the study area

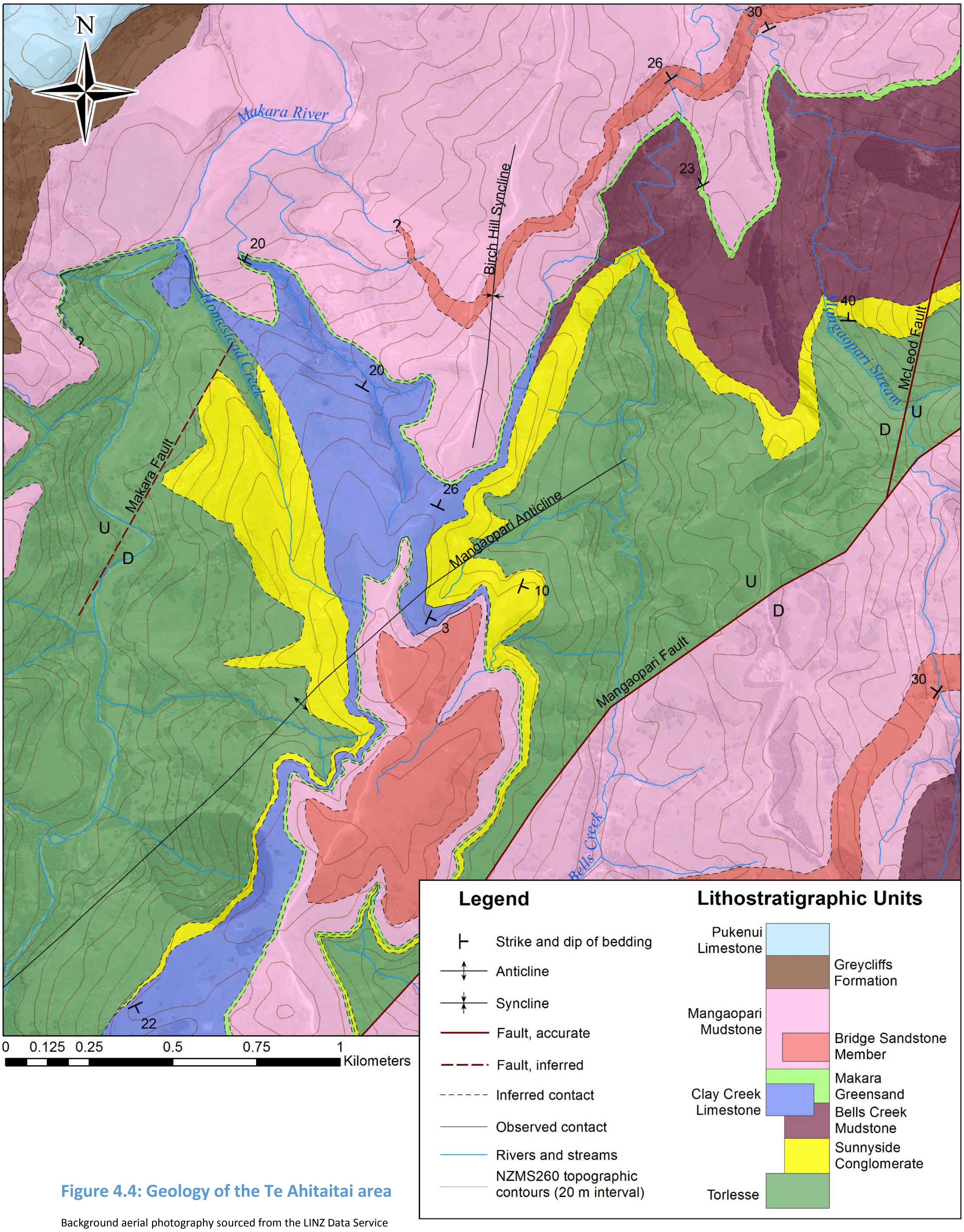

Figure 4.4: Geology of the Te Ahitaitai area

Background aerial photography sourced from the LINZ Data Service https://data.linz.govt.nz/layer/1870-wellington-03m-rural-aerial-photos-2012-2013/ and licensed by Wellington Regional Council for re-use under the Creative Commons Attribution 3.0 New Zealand licence.

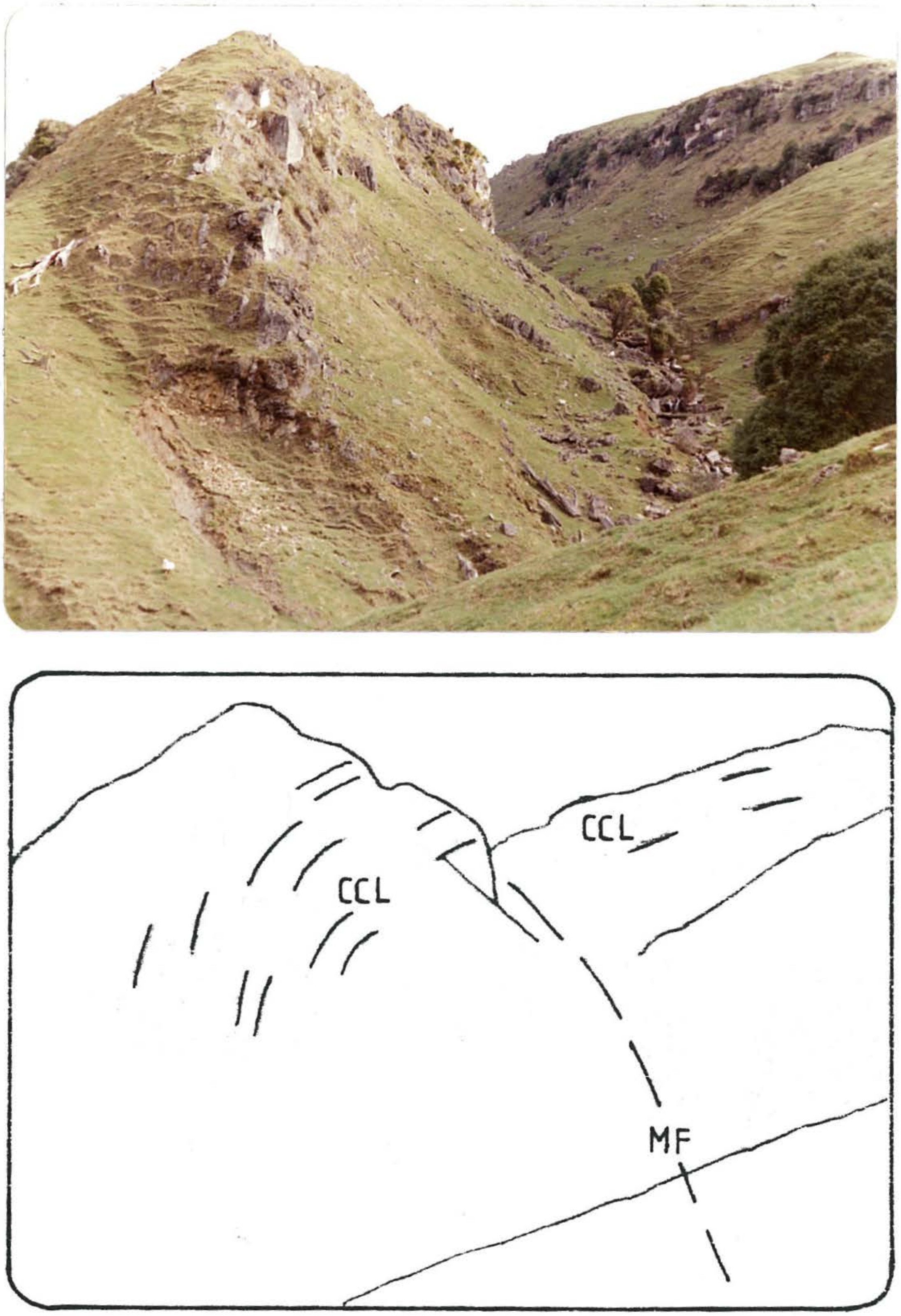

Figure 4.5: Clay Creek Limestone (CCL) forming a monocline across the Mangaopari Fault (MF). View looking southwest from the upper limestone gorge, Makara River. Modified from Green (1981). Photo coordinates: BQ34/050176.

4.3 Haurangi Hairpin section

The Haurangi Hairpin section is located in the south-west of the field area, on the southern side of a large hairpin bend in the Haurangi Road (NZTopo50 map ref. BQ33/001178). It consists of a sequence of limestones and greensands which unconformably overlie Torlesse basement rocks. At the time of writing, the lower part of the Neogene sequence is well-exposed in a new road cutting, allowing for more detailed study than has previously been possible. The section was measured along the road cutting (Figure 4.6), and extends from the Torlesse basement to the lower part of the Dyerville Limestone. The measured section is presented in Figure 4.7.

The Clay Creek Limestone is the basal unit of the Neogene sequence at this location, and overlies the Torlesse with an angular unconformity. It is 2.4 m thick, and is overlain by Makara Greensand. The greensand at this location can be divided into two sub-units: 60 cm of grey-green glauconitic mudstone overlain by 1.4 m of sandy glauconitic shell hash. The Makara Greensand is overlain by 22 m of Haurangi Limestone, a finer-grained and more pure calc-arenite than the Clay Creek Limestone. An unnamed greensand unit, which varies between 4 m and 6 m in thickness, separates the Haurangi Limestone from the overlying Dyerville Limestone. The presence of a greensand bed separating the Haurangi and Dyerville limestones has been noted before, and its thickness estimated at between 30 cm and 1 m (Beu, 1995, Vella and Briggs, 1971, Abbas, 1971). The measured section presented in Figure 4.7 shows that this greensand is significantly thicker than previously thought.

Figure 4.6: View of the Haurangi Hairpin section. The road cutting is approximately 5 m high. Photo: Cliff Atkins. Photo coordinates: BQ33/002189.

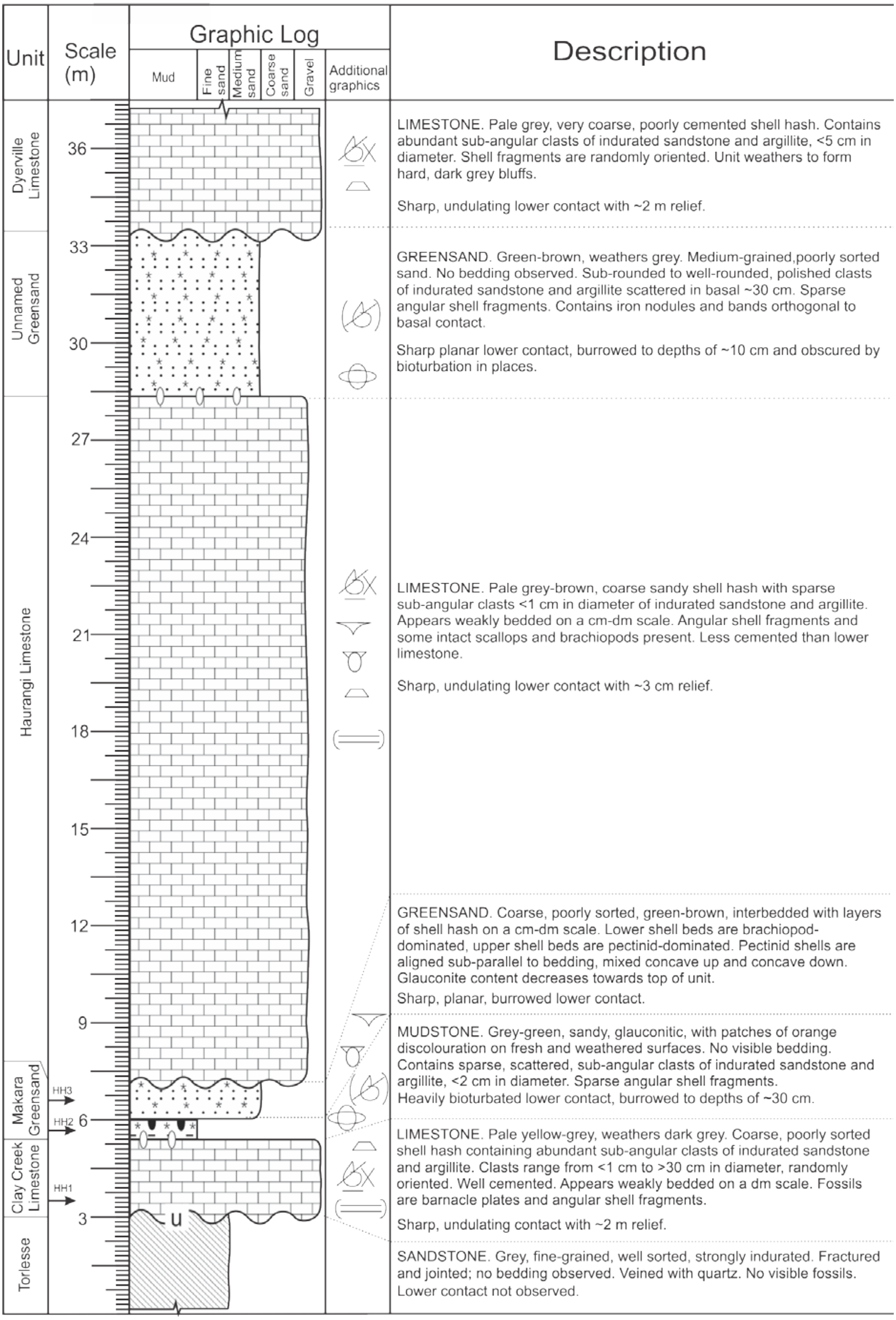

Figure 4.7: Haurangi Hairpin measured section. See Fig. 4.1 for location. Arrows denote sample heights.

The uppermost unit at this location is the Bull Creek Limestone, which is not included in the measured section. The Bull Creek Limestone overlies the Dyerville Limestone with an angular unconformity (Vella and Briggs, 1971, Abbas, 1971, Anderson, 1976). The thickness of the Bull Creek Limestone at this locality was reported as 52 m by Vella and Briggs (1971).

4.4 Clay Creek section

The Clay Creek Limestone was found to be poorly exposed at its type locality in Clay Creek, but a well-exposed section was found in a tributary 350 m along strike from the type locality (BQ33/026195), where a section was measured. At this section location, the Clay Creek Limestone forms a narrow gorge in the creek. The lower part of the limestone appears heavily recrystallized, and near the basal contact the walls of the gorge are covered by flowstone and stalactites. The basal contact with Cretaceous sandstone and argillite is unconformable and highly irregular, with up to 1 m of relief (Figure 4.8).

The Clay Creek Limestone is 13.4 m thick in this section, thicker than the 10 m reported by Vella and Briggs (1971) at the type locality (Figure 4.9). The thickness of the limestone can be reported with confidence despite the presence of a covered interval, as the top of the unit forms an obvious 'ramp' on either side of the stream at the downstream end of the limestone gorge. The Makara Greensand is assumed to be present in the covered interval, as it was recorded by Vella and Briggs (1971) overlying the Clay Creek Limestone in this area. The Mangaopari Mudstone in this section is a poorly-sorted mudstone with mean and modal grain sizes near the silt-clay boundary, and a negligible sand component (Figure 4.9).

Figure 4.8: Basal contact of the Clay Creek Limestone in the Clay Creek section. Hammer is 50 cm long. Photo: Cliff Atkins. Photo coordinates: BQ33/026195.

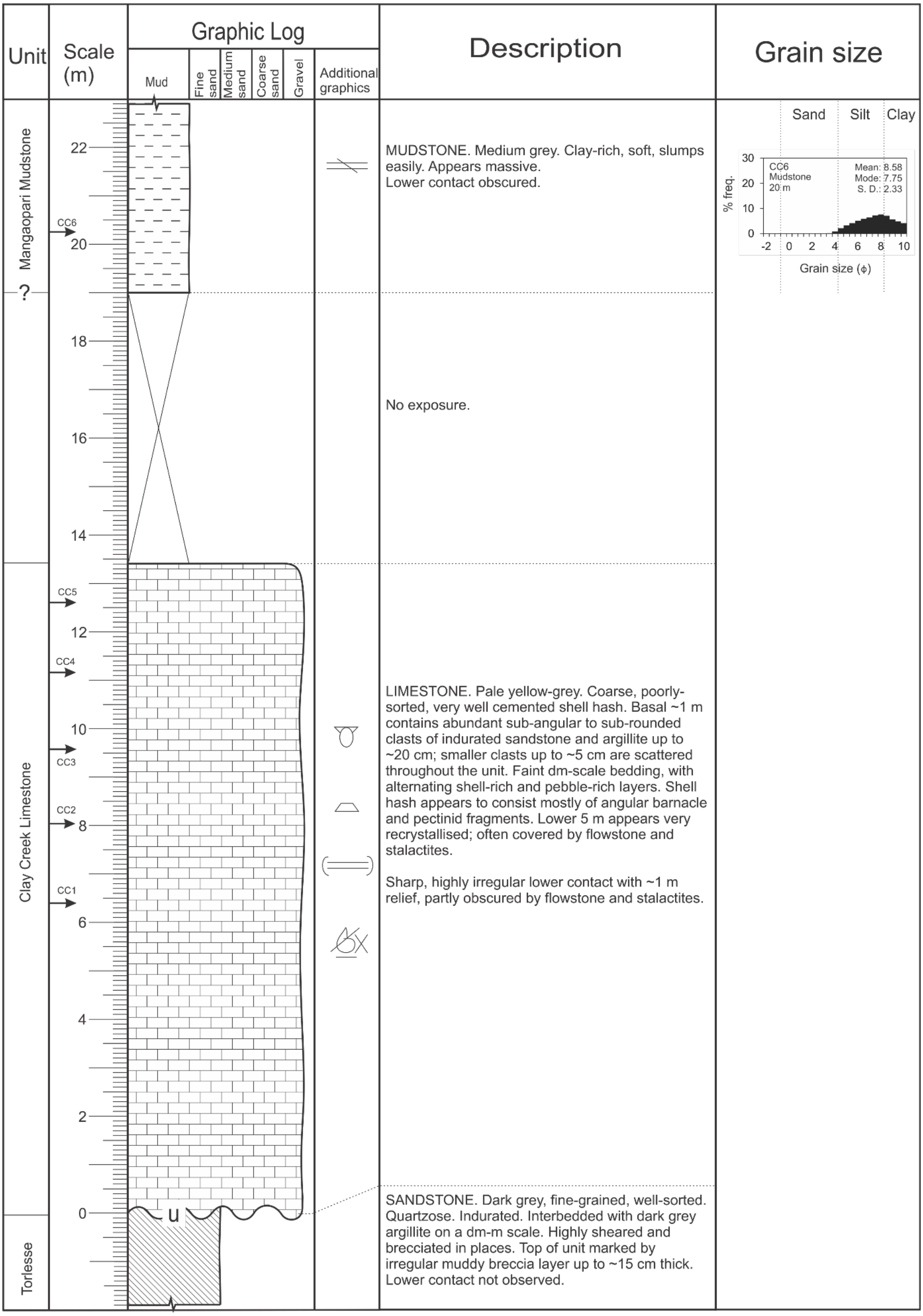

Figure 4.9: Clay Creek measured section. See Fig. 4.1 for location. Arrows denote sample heights.

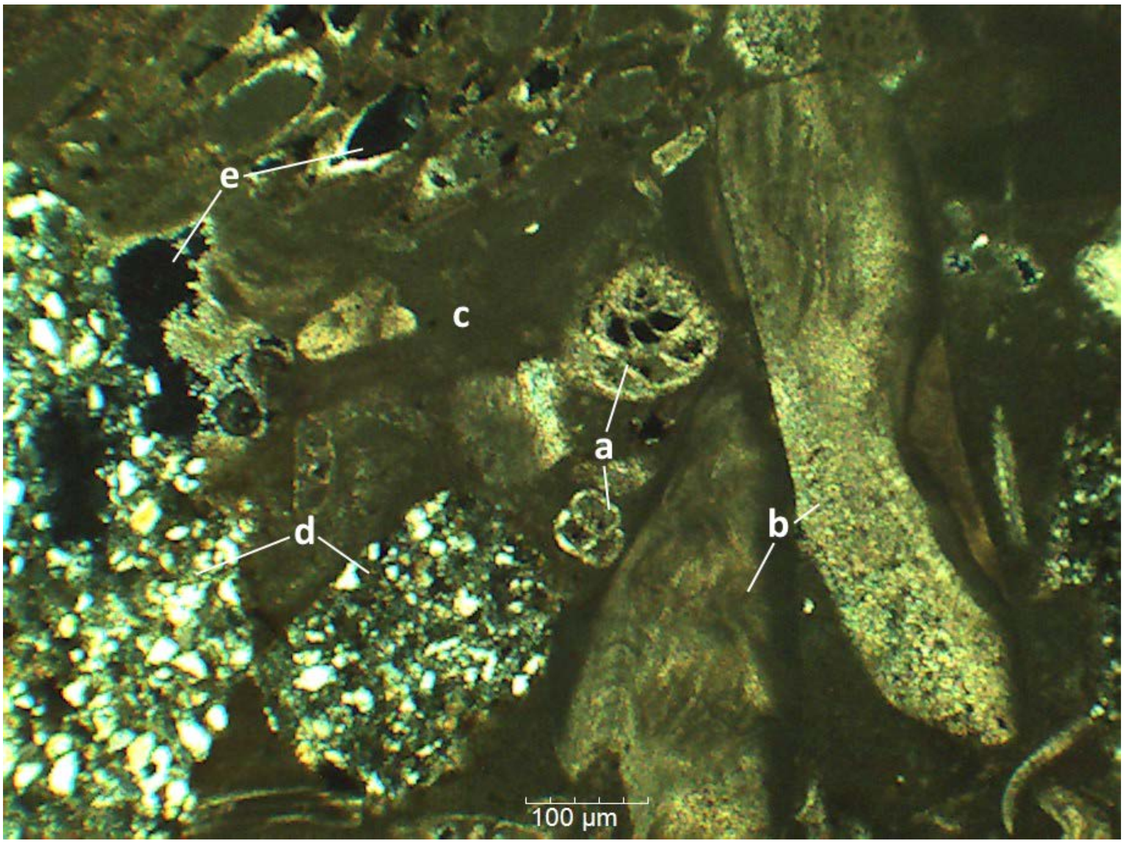

Figure 4.10: Thin section of Clay Creek Limestone, viewed in cross-polarised light. Notable features include (a) foraminifera, (b) shell fragments, some partly recrystallized, (c) micritic cement, (d) lithic sand grains derived from Cretaceous basement, and (e) pore spaces fringed with sparry calcite.

Five thin sections were cut from the Clay Creek Limestone samples collected at this location (samples CC1-CC5). In a typical thin section (Figure 4.10), the limestone is shown to have micritic cement, with small amounts of sparry calcite fringing some skeletal grains and pore spaces. Skeletal components include barnacle, mollusc, and bryozoan fragments and foraminifera. Large lithic sand grains are abundant, and are inferred to be derived from Torlesse sandstone and argillite. The sizes of grains within these lithic particles range from fine sand to mud, and their mineralogy appears to be dominated by quartz and feldspar. Feldspar veins were observed in some lithic particles. No significant variation was noted between limestone samples taken at different stratigraphic heights.

4.5 Te Ahitaitai section

The easternmost known exposures of pebbly, cemented Clay Creek Limestone are found on the eastern side of Te Ahitaitai Ridge. The section presented here was measured at the top of a gully 200 m east of the ridge top (BQ34/066207). The section is poorly exposed, and was studied using shallow excavation in addition to outcrop data. The measured section is presented in Figure 4.12.

At the base of the section, outcrops of Sunnyside Conglomerate are clearly visible in the hillside (Figure 4.11). Above these conglomerate outcrops is a poorly exposed interval of friable quartzose sandstone. The sandstone lacks any shell material, and is considered to be a sandy facies within the Sunnyside Conglomerate. Grain size analysis (see Figure 4.12) shows that the sandstone is poorly sorted, with a modal peak in the fine sand range. The lower sample collected from this sandstone interval has a significant coarse sand and grit component which is absent in the upper sample. This is interpreted as evidence for a vertical gradation from conglomerate to sandstone. The extended mud tails on the grain size distributions are likely to be diagenetic, as the samples were collected near the surface of a heavily weathered outcrop.

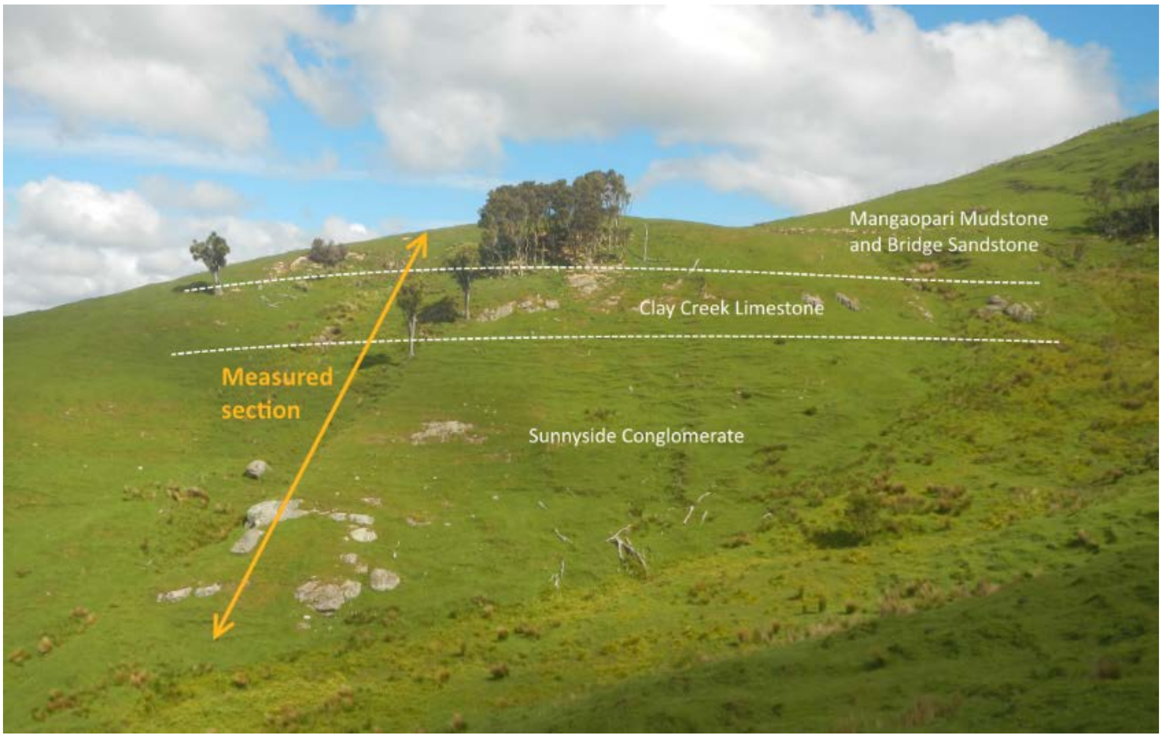

Figure 4.11: View of the Te Ahitaitai section. Photo: Ben Hines. Photo coordinates: BQ34/066209.

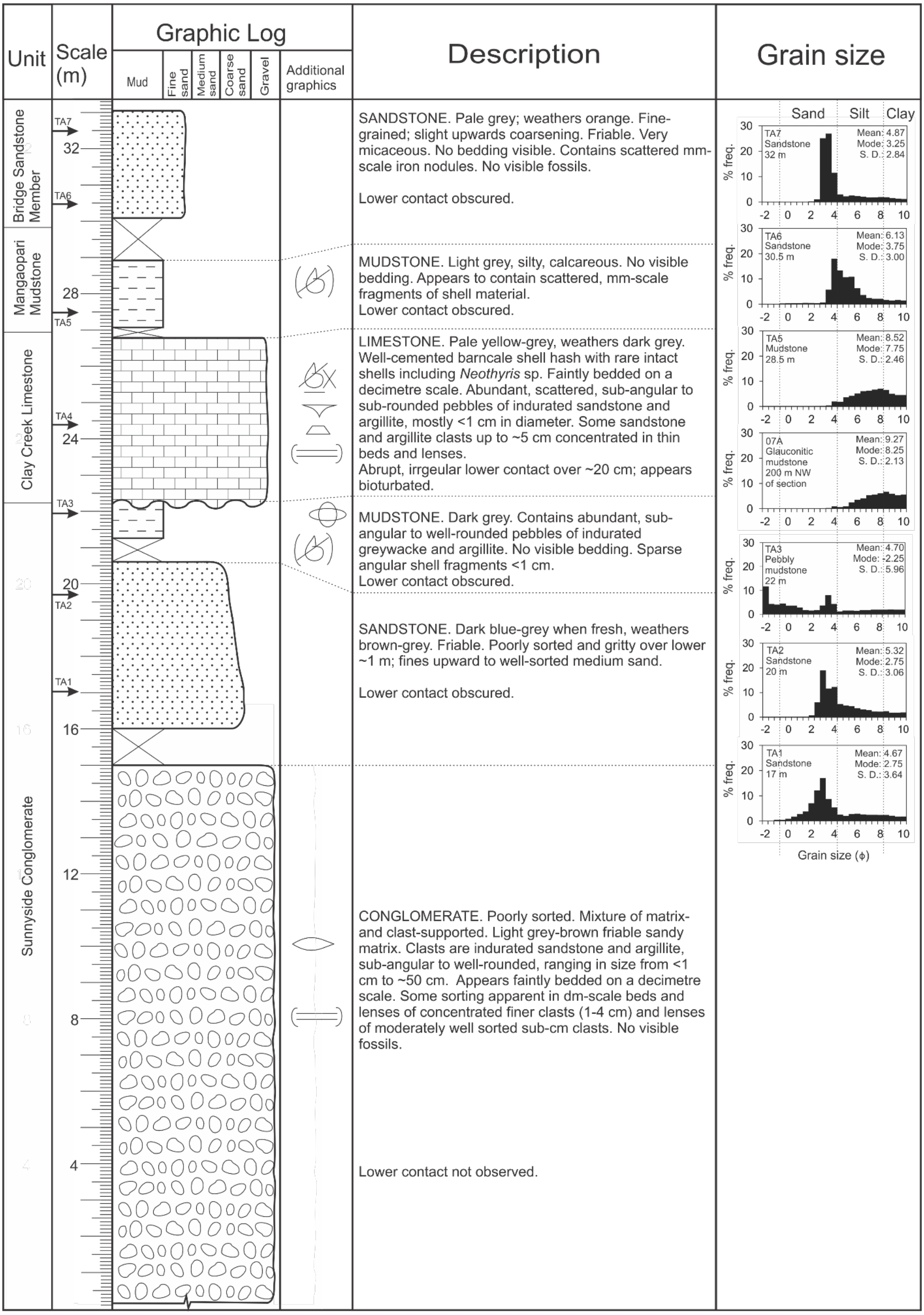

Figure 4.12: Te Ahitaitai measured section. See Fig. 4.1 for location. Arrows denote sample heights. Note that Sample 07A was collected 200 m northwest of the section; it is shown here in its inferred stratigraphic position relative to samples from this section.

The sandstone fines upward to a sandy mudstone which underlies the Clay Creek Limestone. Abundant pebbles and rare shell fragments, which are found in the mudstone up to 30 cm below the limestone contact, are interpreted as having been introduced from the overlying limestone by bioturbation. The mudstone is extremely poorly sorted, and has a bimodal grain size distribution, with modal peaks in the fine gravel and fine sand ranges (Figure 4.12). The fine sand modal peak is similar to those of the underlying sandstone samples.

The Clay Creek Limestone is not well-exposed in this section; it forms the upper row of outcrops in the hillside, which are visible in Figure 4.10. The Clay Creek Limestone is finer-grained here than at many other localities. In contrast to previous sections, the indurated sandstone and argillite clasts in the limestone at this section are mostly sub-centimetre sized.

The Clay Creek Limestone is overlain by a calcareous grey mudstone which is assigned to the Mangaopari Mudstone. The Makara Greensand is therefore absent from this section. The Mangaopari Mudstone in this section is poorly sorted, with a modal peak and mean grain size near the silt-clay boundary. The small sand component of the sample consists almost entirely of foraminifera.

The uppermost unit in the Te Ahitaitai section is a micaceous sandstone which is tentatively assigned to the Bridge Sandstone Member of the Mangaopari Mudstone. Grain size distributions from sandstone samples show a well-sorted fine sand peak with coarse and fine tails. Examination with a binocular microscope shows that the coarse component of these samples consists of iron-cemented aggregates of finer grains. The fine tail is likely to be a diagenetic effect, as, like the sandstones from lower in the section, these samples were collected near the surface of a weathered outcrop. The well-sorted modal peaks to the grain size distributions from these samples closely resemble those of Bridge Sandstone samples analysed by Abbas (1971).

Although absent from the measured section, the Makara Greensand is present on the ridge top 200 m to the northwest, where a sample of greenish-grey glauconitic mudstone was collected. The grain size distribution for this glauconitic mudstone is included in Figure 4.12, in its inferred stratigraphic position relative to the grain size samples from the measured section. The distribution resembles that of the Mangaopari Mudstone sample, and the sample from the ridge top is thought to belong to the top of the Makara Greensand or base of the Mangaopari Mudstone. In addition to foraminifera, the sand component of the glauconitic mudstone also includes glauconite grains and small iron oxide nodules.

4.6 Bells Creek sections

Two sections were measured in Bells Creek. The first, Section A, was measured on the true right of the stream, below White Rock Road (BQ34/073218). This section was measured through the Makara Greensand at its type locality, designated by Vella and Briggs (1971). The measured section is presented in Figure 4.14.

The section starts near the top of the Bells Creek Mudstone, which here contains moderately abundant, scattered shell material and otoliths. Also present in the mudstone are sub-centimetre sized fragments of black carbonaceous matter, and the bulk sample collected from the mudstone was processed for pollen in addition to foraminiferal and grain size analysis. The grain size distribution for this sample is included in Figure 4.14. The Bells Creek Mudstone in this location is poorly sorted, with a modal peak in the silt range and a clay mean.

The Makara Greensand at this locality overlies Bells Creek Mudstone with an irregular, bioturbated contact (Figure 4.13). The greensand is 8 m thick, and can be divided into four distinct sub-units, shown in Figure 4.14. The lowest sub-unit is an 80 cm sandy bed which has a distinct dark green colour when fresh, and weathers brown. This sub-unit contains scattered pebbles and concretions at its base and fines upward to gritty sand.

Figure 4.13: The bioturbated basal contact of the Makara Greensand at Bells Creek section A. Photo: Cliff Atkins. Photo coordinates: BQ34/073218.

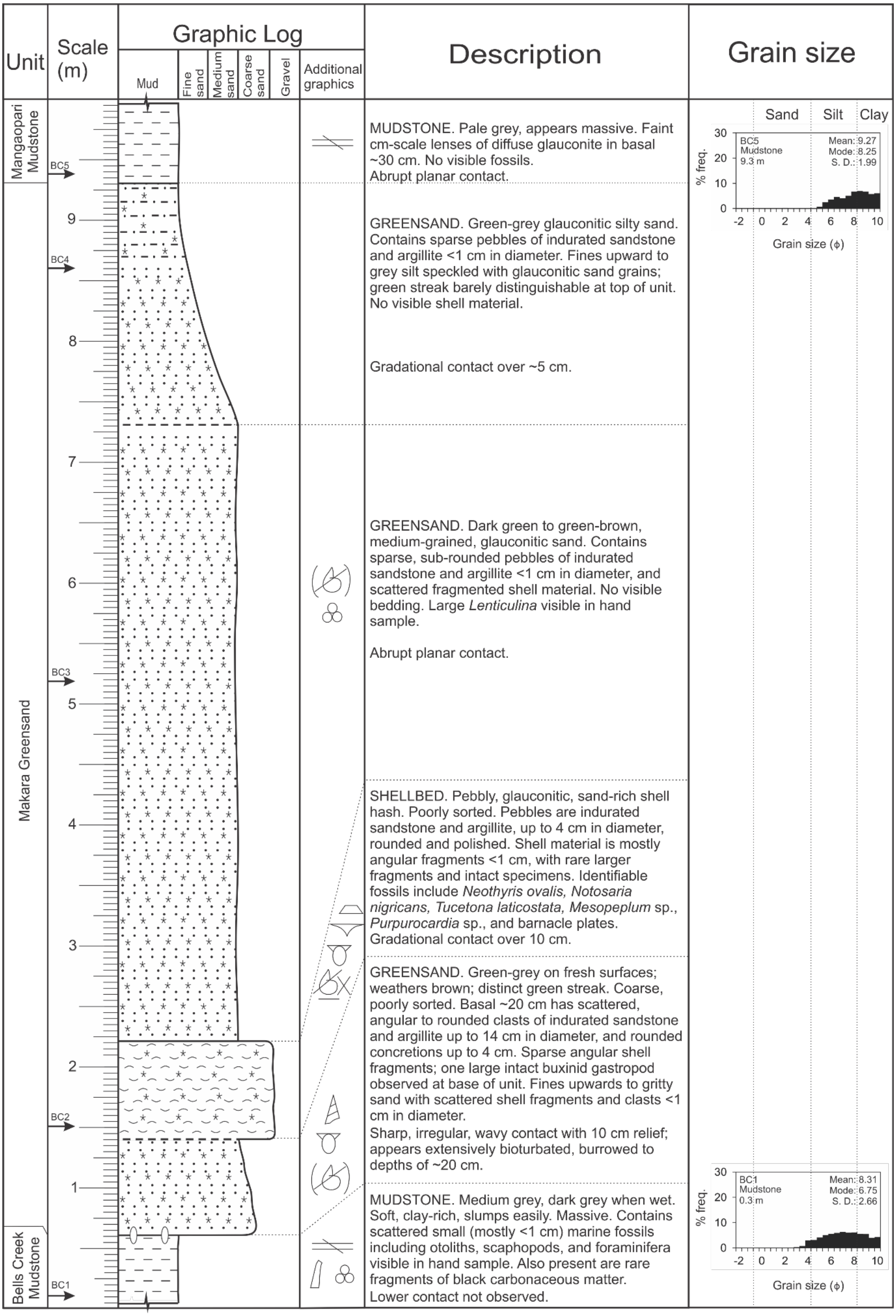

Figure 4.14: Bells Creek measured section A. See Fig. 4.1 for location. Arrows denote sample heights.

The second sub-unit of the greensand is an 80 cm thick, muddy, glauconitic shellbed. Most of the shell material present consists of randomly oriented, angular fragments; in addition, many of the more intact shells are brittle and decalcified. Also present in the shellbed are rounded and polished pebbles of basement-derived sandstone and argillite.

The shellbed is overlain by 4.7 m of medium-grained, friable glauconitic sandstone. This unit is green-brown at its base, and this colour gradually changes to dark green over the lower 3 m as glauconite content increases with stratigraphic height.

The uppermost sub-unit of the Makara Greensand is marked by a change in colour from dark green to greenish grey. This change in colour is taken to indicate an increase in terrigenous sediment content and a decrease in the relative abundance of glauconite in this sub-unit when compared to the other sub-units of the greensand. Terrigenous mud content continues to increase towards the top of the unit, which fines upward to a grey siltstone with only diffuse glauconite grains.

The Makara Greensand is overlain with an abrupt contact by Mangaopari Mudstone. The Mangaopari Mudstone in this section is paler in colour than the Bells Creek Mudstone, and lacks visible fossil material. Its grain size distribution shows better sorting than the Bells Creek Mudstone (although the sample is still poorly sorted) with a mean and mode in the clay range and only a negligible sand component.

A second Bells Creek section, section B, was measured on the true left of Bells Creek (BQ34/071217) by Ben Hines in November 2014, and data from this section are presented in Figure 4.15. A major feature of this section is the presence of a 20 cm interbed of brown, organic-rich siltstone within the Sunnyside Conglomerate. This siltstone bed was sampled for pollen, and its implications for the depositional environment of the Sunnyside Conglomerate are discussed in Chapters 5 and 6. The Sunnyside Conglomerate is at least 18 m thick in this section, considerably thicker than the 10 m estimated by Vella and Briggs. The thickness of the Bells Creek Mudstone in this section cannot exceed 31 m.

The Makara Greensand in section B overlies the Bells Creek Mudstone with a bioturbated contact very similar to its basal contact in section A. The greensand in section B is only 2 m thick. The sub-units identified at Bells Creek section A are not clearly differentiated in section B, and the shellbed from section A is absent in section B.

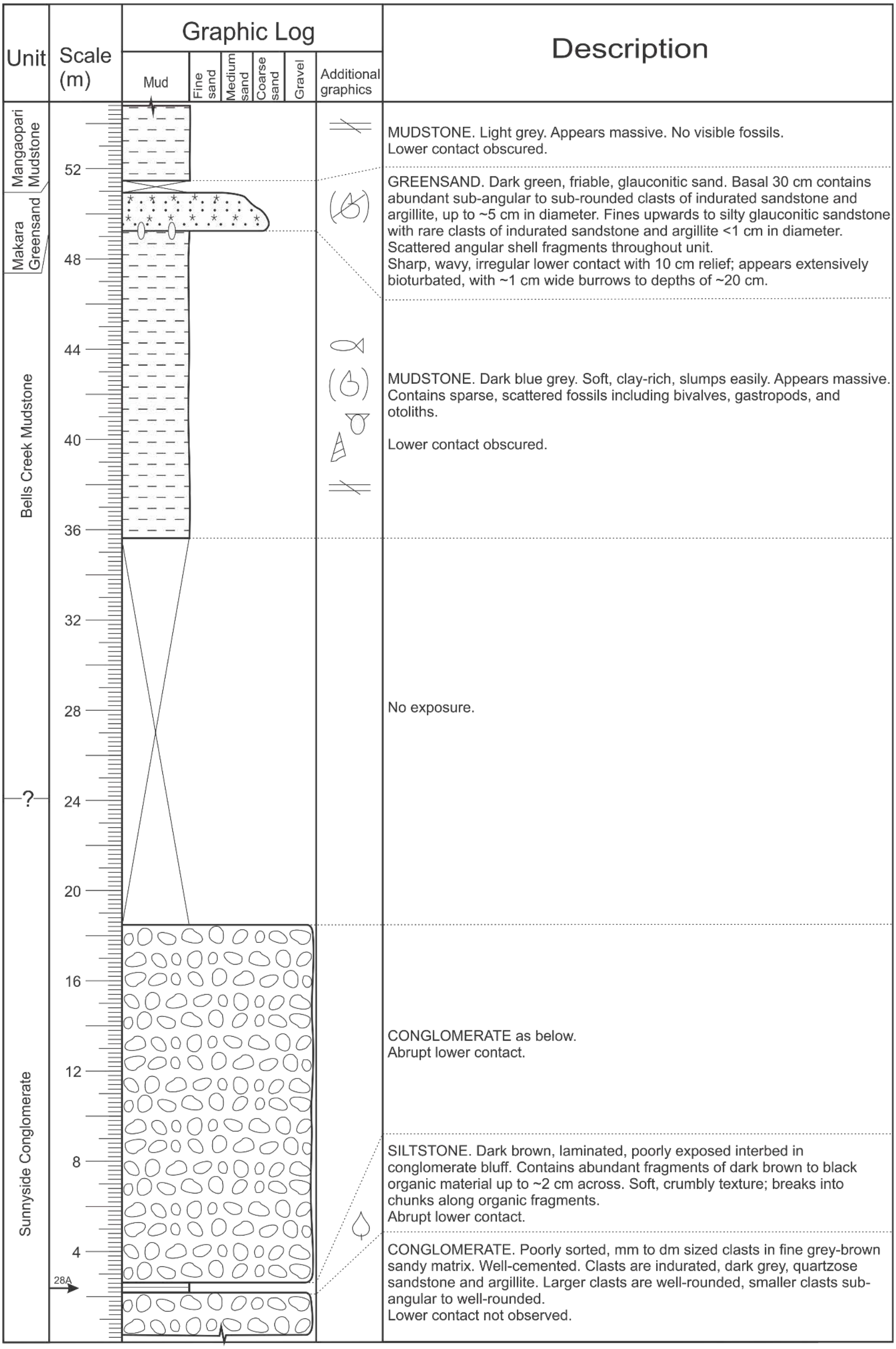

Figure 4.15: Bells Creek measured section B. See Fig. 4.1 for location. Section measured by Ben Hines. Arrows denote sample heights.

4.7 Lower Makara River

The basal contact of the Clay Creek Limestone is exposed in several places in the lower part of Homestead Creek, a small tributary on the true right of the Makara River, 2 km upstream from the Birch Hill homestead (BQ34/057217). At most places where the contact is exposed, the Clay Creek Limestone rests on an irregular, eroded surface of Torlesse sandstone and argillite (Figure 4.16A). However, in one exposure near the mouth of Homestead Creek, the Clay Creek Limestone overlies a fine grey mudstone which resembles the Bells Creek Mudstone (Figure 4.16B). The limestone-mudstone contact appears to be heavily bioturbated.

No section was measured here, but samples were collected from both the mudstone and limestone. The grain size distribution for the mudstone shows poor sorting, with a coarse silt mode and fine silt mean (Figure 4.17). The sand component consists mainly of foraminifera, but also includes grains of glauconite and pyrite. The overall shape of the grain size distribution resembles that of the Bells Creek Mudstone in Bells Creek section A (Figure 4.14), though the Homestead Creek sample has a larger sand component. Due to its stratigraphic position beneath the Clay Creek Limestone, and to other features such as its grain size distribution and the presence of otoliths, this mudstone is correlated with the Bells Creek Mudstone.

The Clay Creek Limestone has an estimated thickness of 4.5 metres in Homestead Creek. Approximately 30 m upstream from the mouth of the creek, a small cave has formed in the limestone, and the creek runs through it for several metres before the valley opens out again. A poorly exposed, weathered glauconitic mudstone found above the cave is correlated with the Makara Greensand.

Across the Makara River from Homestead Creek, the Clay Creek Limestone thins rapidly. In a tributary on the true left of the river (BQ33/055216), the limestone is only 1 m thick, and again rests unconformably on weathered, brecciated Torlesse basement rocks. The limestone in this section is thinner than the overlying greensand, which appears to be at least 2 m thick. The limestone was traced for a further 110 m along the hillside to the south of this tributary. Whether it continues along the western side of the valley, or whether it pinches out, is unknown.

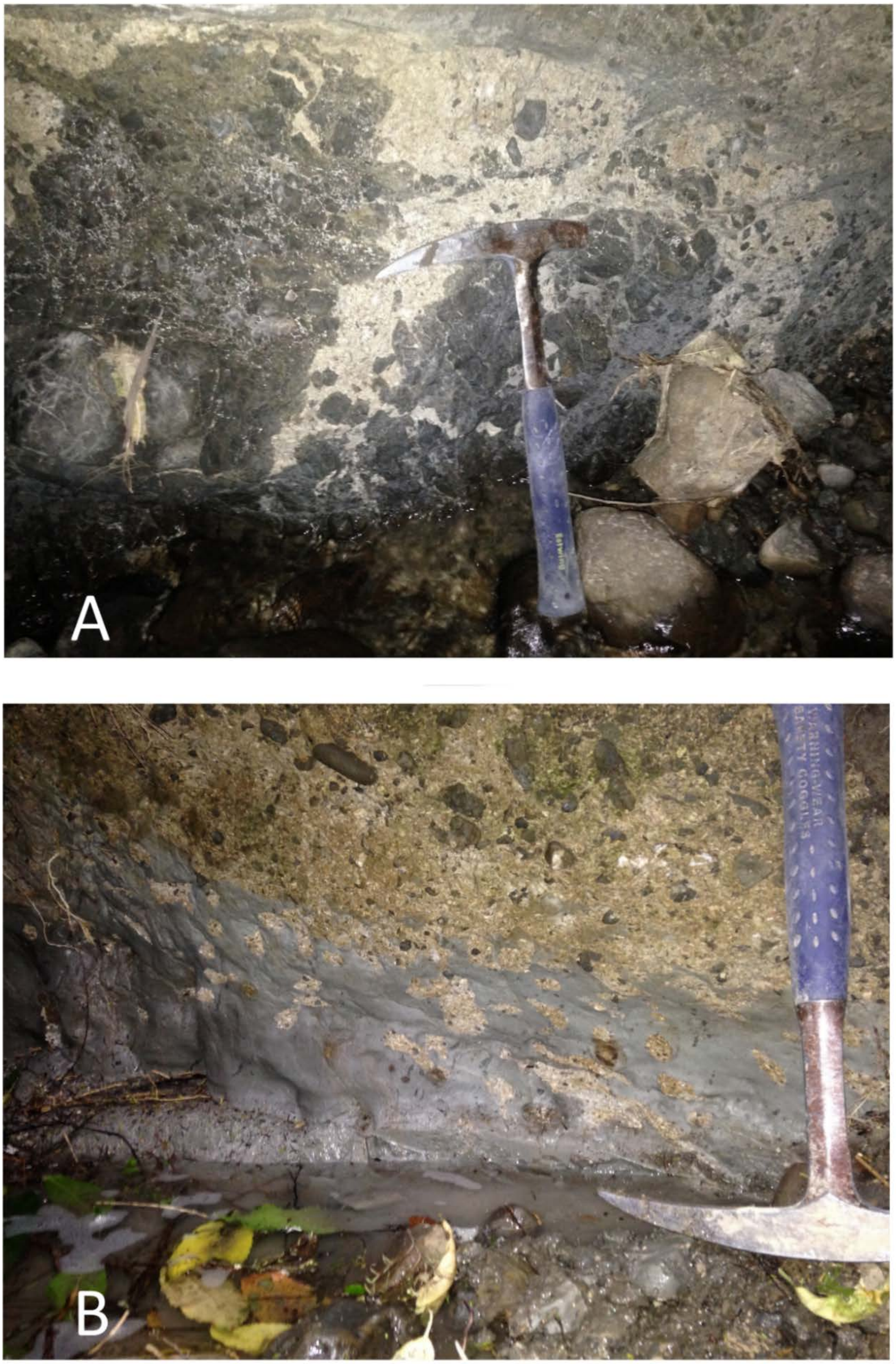

Figure 4.16: Two exposures of the basal contact of the Clay Creek Limestone in Homestead Creek. Photos: Cliff Atkins. Photo coordinates: BQ34/057217 (A and B).

Approximately 250 m northeast of Homestead Creek is another small creek which runs through Clay Creek Limestone for most of its length. Much of this creek is not traversable, as the limestone forms high, narrow gorges and waterfalls. The Clay Creek Limestone is inferred to be thicker in this creek than it is in Homestead Creek, possibly 10 m or more. Limestone bluffs in the hillside above this creek contain abundant intact scallops, and a picked fossil sample was collected for later identification. Slumped, poorly exposed Makara Greensand was found overlying the limestone near the bottom of this creek (BQ34/059217); its thickness here is unknown but thought to be less than 5 m.

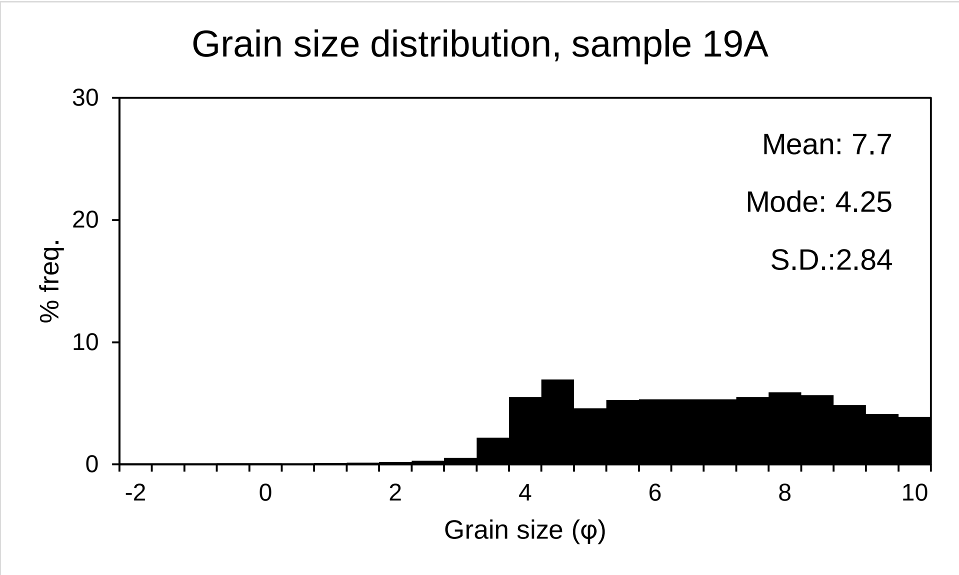

Figure 4.17: Grain size distribution for sample TBG-02-14-19A, mudstone underlying Clay Creek Limestone in Homestead Creek.

4.8 Saw Cut Gorge

The Makara River has cut a narrow, 250 m long gorge through the Clay Creek Limestone at a location called Saw Cut Gorge (BQ34/054190; see Figure 1.1), 3 km south of Homestead Creek. At this location the Clay Creek Limestone unconformably overlies Torlesse basement rocks. Although there is no measured section from this location, field observations show that the Clay Creek Limestone dips 30° to the southeast at the northern end of the gorge. It is inferred from aerial photography to dip to the north or northwest at the gorge's southern end, forming a syncline.

At the northern end of Saw Cut Gorge, the Clay Creek Limestone resembles a calcareous conglomerate, with very abundant sub-angular to rounded clasts of basement-derived sandstone and argillite ranging from 0.5 cm to 10 cm in diameter in a shell hash matrix. Another notable feature of the Clay Creek Limestone at this location is the presence of large sedimentary structures resembling giant cross-beds or channel features, which can be seen from a distance of 50 m in limestone bluffs immediately to the north of the gorge (Figure 4.18). Giant cross-beds are a prominent feature of some Pliocene Te Aute limestones in Hawke's Bay (Kamp et al., 1988), but features such as these have not, to the author's knowledge, been previously recognised in limestones from the Wairarapa region.

Figure 4.18: Bluffs of Clay Creek Limestone north of Saw Cut Gorge in the Makara River valley, showing giant trough cross-bedding or channel structures. Trees are 3-5 m high. Photo: Cliff Atkins. Photo coordinates: BQ34/054190.

The thickness of the Clay Creek Limestone at Saw Cut Gorge is unknown. Couper (1948) estimated it to be approximately 30 m, which is probably a conservative estimate. The Clay Creek Limestone is unconformably overlain by another barnacle plate limestone which dips 10° to the southwest at the gorge's northern end. The upper limestone is yellower in colour and less cemented than the Clay Creek Limestone, and lacks the basement-derived sandstone and argillite clasts which characterise the lower limestone. It consists of coarse, angular barnacle and molluscan fragments and contains moderately abundant intact scallops. This upper limestone was mapped as Bull Creek Limestone by Abbas (1971) and Vella and Briggs (1971).It is here tentatively correlated with the Dyerville Limestone based on its fossil content (see next chapter).

4.9 Paruwai

A second limestone gorge occurs in the Makara River, 1 km south of Saw Cut Gorge, at the Paruwai Farm Settlement (BQ34/501179). On the true right of the gorge, between the two strands of the Mangaopari Fault, the Clay Creek Limestone overlies a fine grey mudstone which is bedded on a cm scale and contains abundant mm-scale shell fragments. The grain size distribution for this mudstone is shown in Figure 4.19. The distribution is bimodal, with peaks near the sand-silt and silt-clay boundaries. The mean grain size is similar to that of samples taken from the Bells Creek and Mangaopari Mudstones. The sand portion of the sample consists mainly of foraminifera, but also includes aggregates of finer grains. This mudstone is likely to be Bells Creek Mudstone based on its foraminifera (see next chapter).

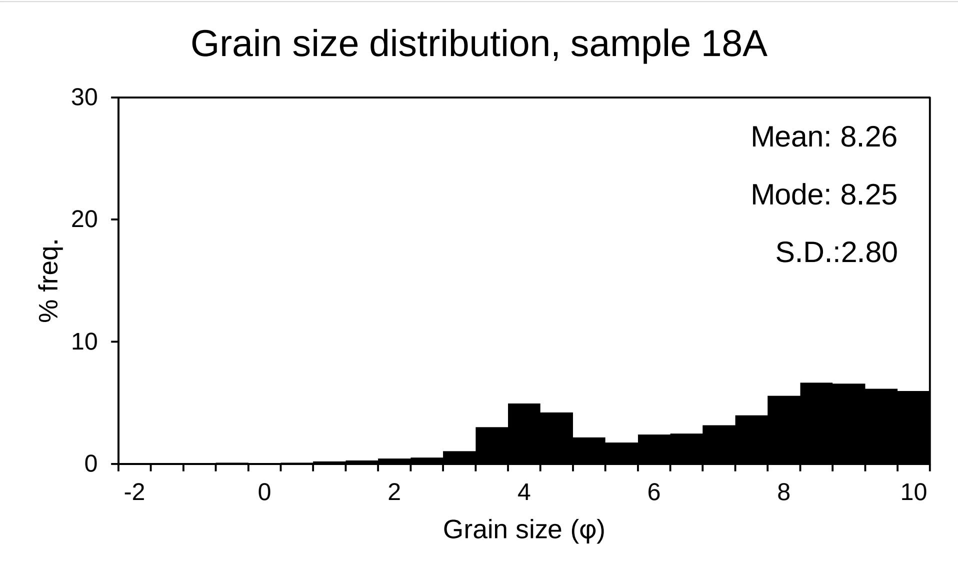

Figure 4.19: Grain size distribution for sample TBG-02-14-18A, mudstone underlying Clay Creek Limestone on the true right of the upper limestone gorge, Makara River.

The Clay Creek Limestone may be locally as thick as 100 m in the vicinity of the gorge at Paruwai (See Figure 4.2). Between Paruwai and Clay Creek is a broad limestone plateau with numerous large sinkholes and other karst features. Observations from caves in the plateau (G. Holden, pers. comm.) indicate a thick (at least 30 m) unit of cemented, pebbly limestone unconformably overlying Torlesse sandstone and argillite, which is likely to be Clay Creek Limestone.

In the Makara River valley to the south of the upper limestone gorge, the Clay Creek Limestone is overlain by greensand (Green, 1981). Overlying the greensand is a unit of grey mudstone interbedded with cemented pebbly shellbeds on a decimetre scale (Figure 4.20). These shellbeds have sharp basal contacts and grade upwards into mudstone in repeating packages; the shellbeds resemble the Clay Creek Limestone in lithology. This shellbed and mudstone unit is considered to be a facies within the Mangaopari Mudstone.

Figure 4.20: Cemented pebbly shellbeds interbedded with mudstone at the Paruwai Farm Settlement. Photo: Cliff Atkins. Photo coordinates: BQ34/051175.

Chapter 5 Biostratigraphy and Paleontology

5.1 Introduction

This chapter summarises biostratigraphic and paleontological data from the study area. Sections 5.2-5.4 outline the biostratigraphy and paleontology of key sections from southwest to northeast. The Clay Creek section is omitted, as foraminiferal censuses were not conducted for Clay Creek Limestone samples collected at this section, and no foraminifera or other fossils were found in the Mangaopari Mudstone sample collected at this location. Sections 5.5-5.7 outline the biostratigraphy and paleontology of samples collected from key locations in the Makara River, from north to south. A table showing sample numbers, locations, and VUW locality numbers is presented in Appendix 1. Full faunal lists are presented in Appendix 4.

Some foraminiferal species are referred to in the literature by multiple taxonomic names. For example, one key index species is referred to as *Globorotalia miotumida* in the World Foraminifera Database (Hayward et al., 2015), as *Globorotalia (Globoconella) miotumida* by Kennett and Srinivasan (1983), and as *Globoconella miotumida* in the New Zealand Geological Timescale (Cooper, 2004, Raine et al., 2015). As this study uses the stages of the New Zealand Geological Timescale (Raine et al., 2015; see Appendix 3) for correlating biostratigraphic ages, taxonomic names used in the timescale and associated literature are given priority here.

Paleoenvironmental assessments for foraminiferal samples are made using the paleodepth and oceanicity zones defined in Hayward et al. (2010). These are shown in Figure 5.1. It should be noted that the oceanicity of the water mass, which is indicated by the percentage of planktic specimens in an assemblage, does not always correspond to paleodepth, which is indicated by the depth ranges of benthic taxa. Planktic specimens can be abundant in shallow, inshore locations if they are transported by currents (e.g. Hayward et al., 1994), and deep nearshore basins may be sheltered by land and isolated from the open ocean, resulting in low planktic percentages even at bathyal depths (e.g. Hayward et al., 1986). However, in general, planktic percentages increase with increasing water depth and distance from land (Hayward et al., 2010).

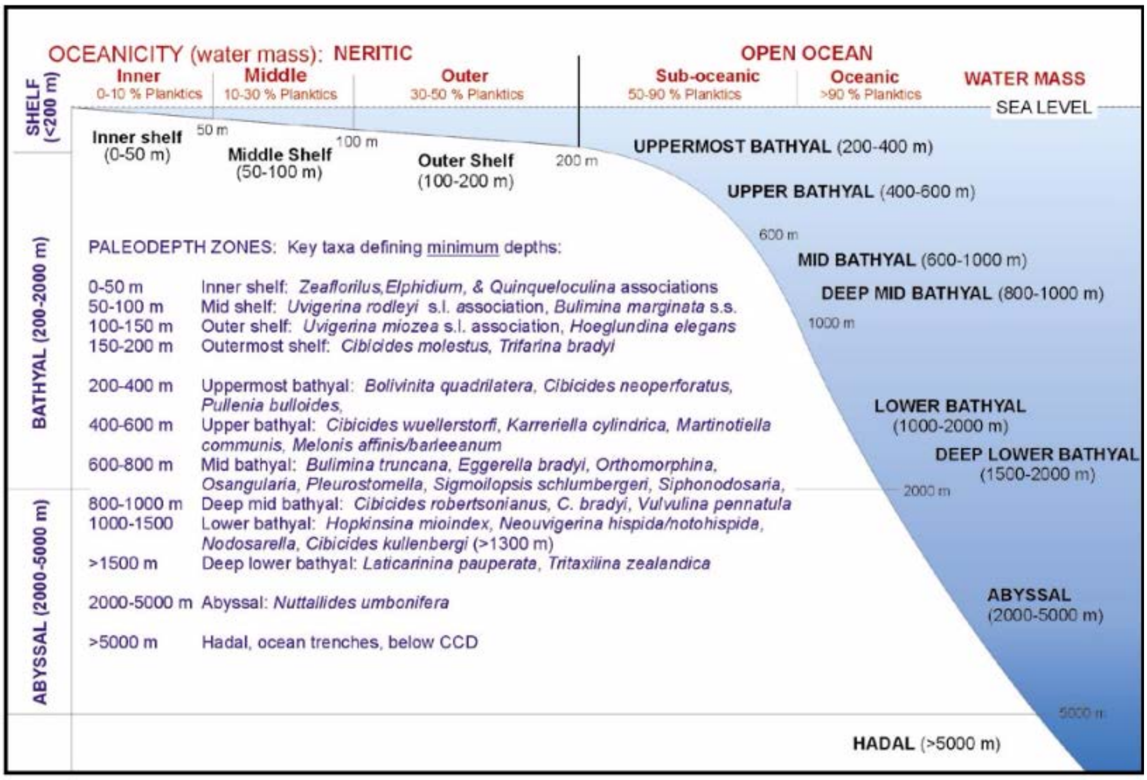

Figure 5.1: Diagram summarising divisions of the continental shelf and ocean, and key foraminiferal depth indicators for New Zealand Cenozoic faunas. From Hayward et al. (2010), after Morgans and Strong (unpublished).

5.2 Haurangi Hairpin section

Foraminiferal censuses were conducted for three samples collected at the Haurangi Hairpin: one from the Clay Creek Limestone (sample HH1) and one from each sub-unit of the Makara Greensand (samples HH2 and HH3). Sample heights are shown in Figure 4.7. Some macrofossils were identified in outcrop, and additional specimens were extracted from the HH1 and HH3 bulk samples.

5.2.1 Clay Creek Limestone

Foraminifera are abundant in the Clay Creek Limestone at this location. Preservation is somewhat poor, with many specimens showing signs of abrasion. The assemblage consists mostly of benthic species, with only a 5% planktic component. Agglutinated foraminifera are especially abundant: 141 of the 300 specimens picked in the census for this sample were agglutinated. Of the 141 agglutinated specimens, 87 belonged to the species *Gaudryina convexa* (Figure 5.2), accounting for close to 30% of the total benthic fauna. Other significant agglutinated species include *Spiroplectinella proxispira, Textularia barnwelli,* and *Textularia* cf. *kapitea*.

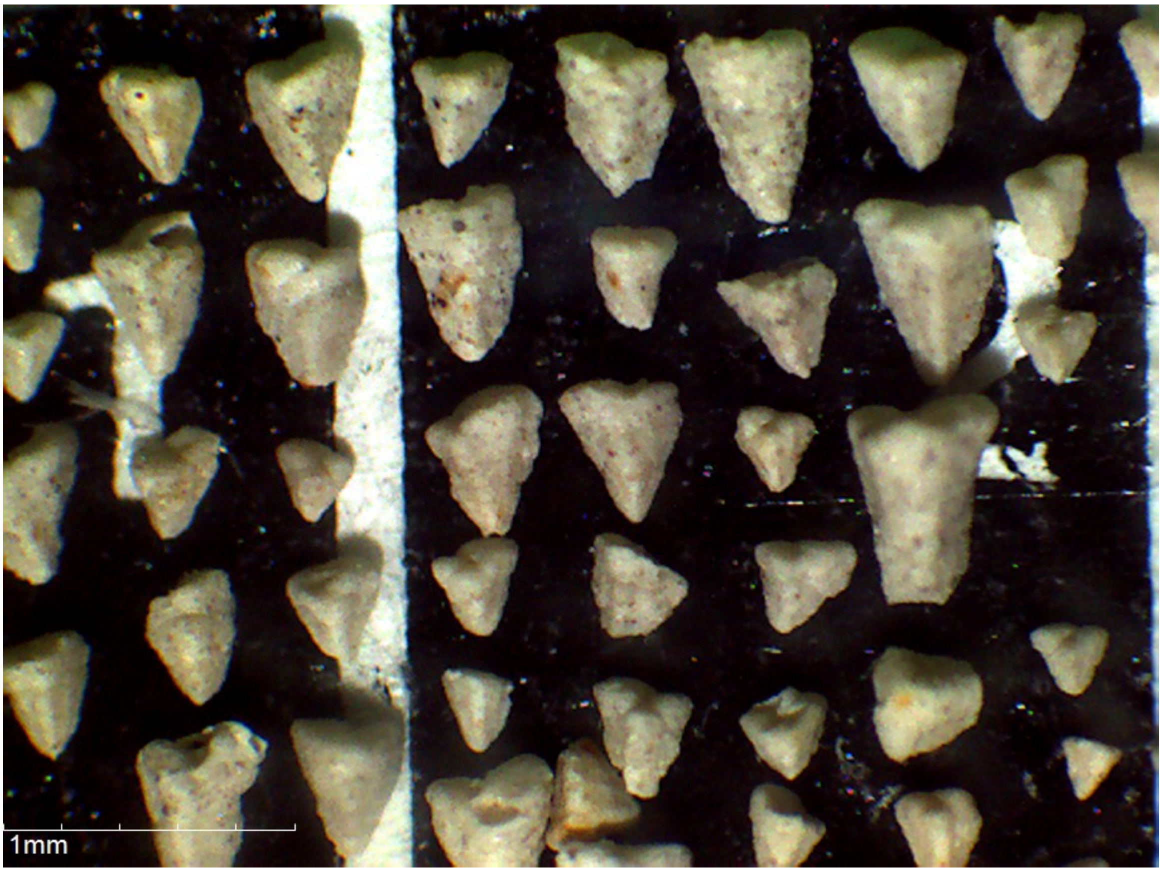

Figure 5.2: Abundant specimens of *Gaudryina convexa* from the Clay Creek Limestone at the Haurangi Hairpin section (sample HH1).

The remainder of the benthic fauna consists mainly of buliminids and rotaliids, including *Trifarina bradyi, Cibicides molestus,* and *Melonis* sp. A small number of lagenids, mostly unilocular species, were also found. The planktic component of the assemblage includes *Globigerina bulloides, Orbulina universa, Neogloboquadrina pachyderma,* and both *Globoconella miotumida* and *Globoconella conomiozea.* In addition to foraminifera, micro-brachiopods and several species of ostracod were found in the Clay Creek Limestone (Figure 5.3). Most ostracod shells are disarticulated, but some remain articulated.

Few macrofossils could be identified from the Clay Creek Limestone, as the vast majority of shell material in the limestone consists of angular fragments. However, some intact fossils were extracted from the disaggregated bulk limestone sample. These included the brachiopods *Notosaria nigricans* and *Neothyris* sp., spheroidal bryoliths up to 1 cm in diameter, and moderately abundant, disarticulated juvenile ostreid valves (Figure 5.4). A partial valve of a mature ostreid was identified as *Crassostrea ingens,* and a cast of an unidentified pectinid was also found.

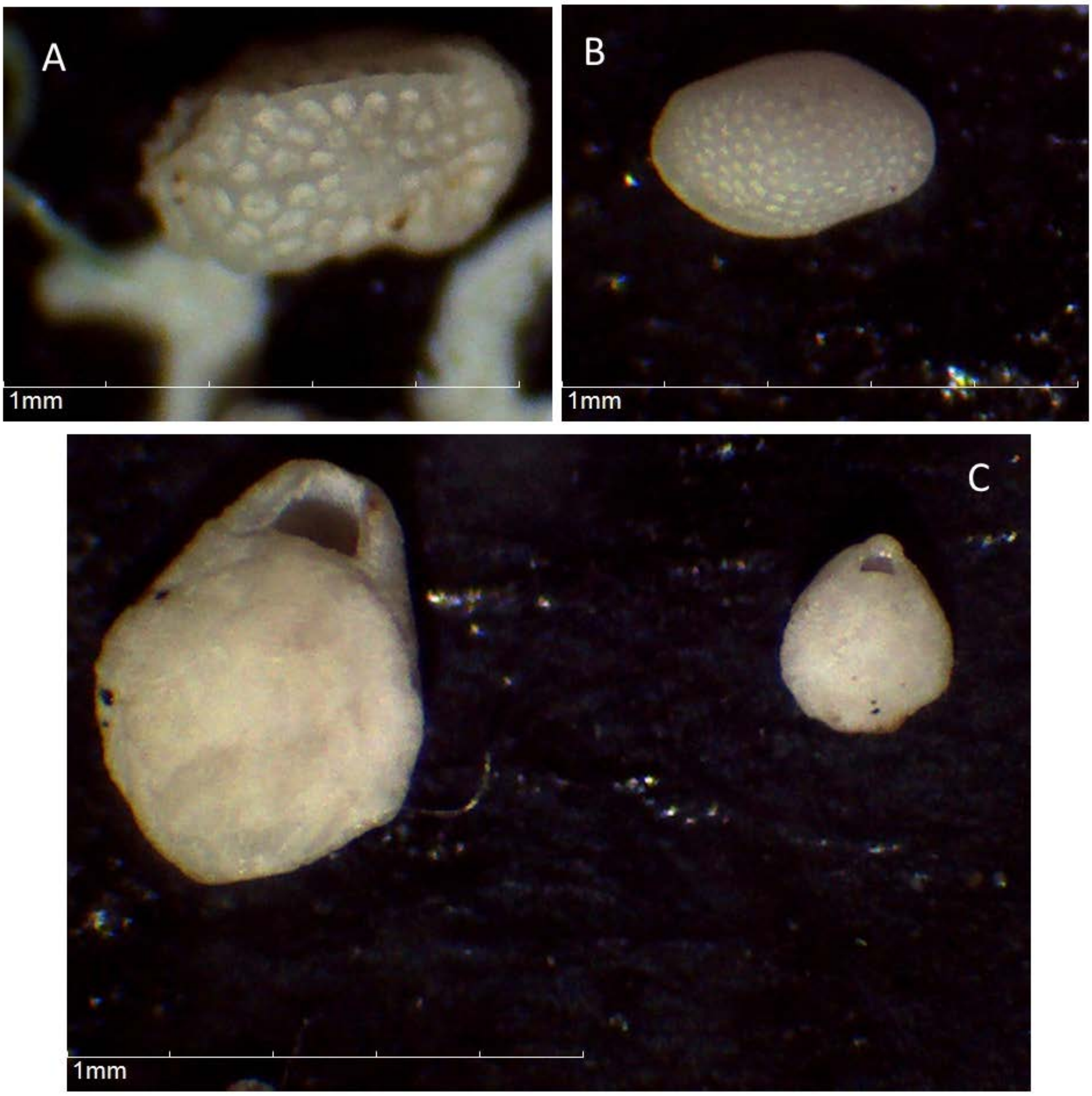

Figure 5.3: Articulated ostracods (A and B) and micro-brachiopods (C) from the Clay Creek Limestone at the Haurangi Hairpin section (sample HH1).

Gaudryina convexa is most abundant in exposed, high-energy, inner- to mid-shelf environments, forming up to 25% of benthic assemblages in such environments around New Zealand in recent times (Hayward et al., 2010). The low planktic percentage in the sample is consistent with an inner shelf depositional environment. However, *Cibicides molestus* and *Trifarina bradyi* both have upper depth limits of approximately 150 m, and *Melonis* is restricted to outer shelf and bathyal depths (Hayward et al., 2010). This combination of species suggests that some mixing of benthic faunas has occurred, possibly by transportation of shallow-water sediment and deposition on the outer shelf.

Figure 5.4: Examples of macrofossils collected from the Clay Creek Limestone at the Haurangi Hairpin section (sample HH1). Pictured are (a) bryoliths, (b) barnacle plates, (c) juvenile oyster valves, (d) brachiopods.

The presence of both the Tongaporutuan index species *Globoconella miotumida* and the Kapitean *Globoconella conomiozea* suggests that the Clay Creek Limestone at this location has a lower Kapitean or possibly upper Tongaporutuan age, as *Gc. miotumida* grades into *Gc. conomiozea* at the base of the Kapitean stage (Cooper, 2004, Crundwell and Nelson, 2007).

5.2.2 Makara Greensand

Sample HH2, collected from the lower, muddy sub-unit of the Makara Greensand (see Figure 4.6) yielded no macrofossils, but abundant foraminifera. The benthic assemblage is dominated by buliminids and rotaliids. The most abundant species in the sample are *Cassidulina carinata, Bulimina aculeata,* and *Trifarina bradyi*. Agglutinated species are far less abundant than in the underlying limestone, and include *Martinottiella communis* and *Karreriella ?cylindrica* (Figure 5.5), and *Sigmoilopsis schlumbergi.* Lagenids in the sample are relatively rare but diverse, including *Lenticulina calcar,* elongate species such as *Laevidentalina communis,* and unilocular species such as *Favulina hexagona.*

The sample has a 17 % planktic component. This includes *Globoconella puncticulata* and *Globoconella pliozea, Globigerina bulloides* and *Globigerina falconensis,* and other species such as *Neogloboquadrina pachyderma, Turborotalita quinqueloba,* and *Orbulina suturalis.* In addition to foraminifera, rare ostracods fish scales, and possible bryozoan fragments were found.

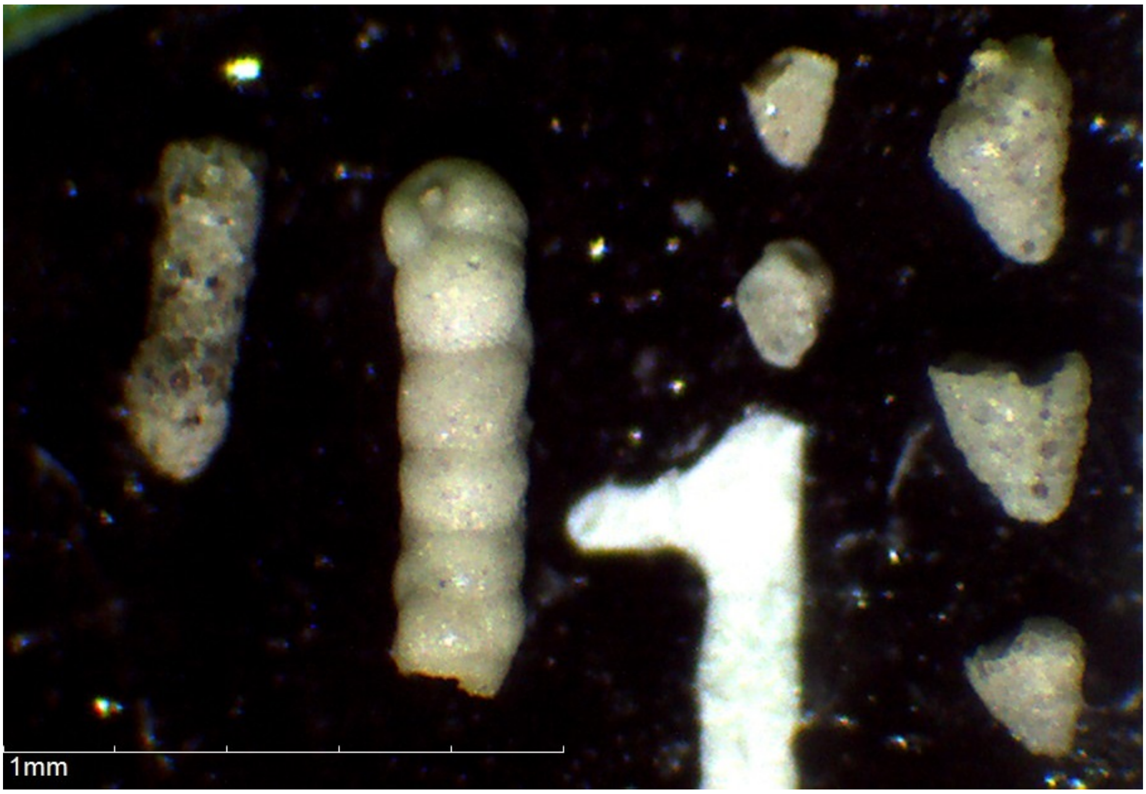

Figure 5.5: Textulariids from the lower part of the Makara Greensand (sample HH2) at the Haurangi Hairpin section, including (L-R) *Martinottiella communis*, *Karreriella ?cylindrica*, *Siphotextularia wairoana,* and *Textularia* sp.

Sample HH3 was collected 1.3 m above the base of the Makara Greensand, in the sandy, calcareous upper sub-unit (see Figure 4.6). Like sample HH2, it contains abundant foraminifera, with a benthic assemblage dominated by buliminids and rotaliids, with abundant specimens of *Globocassidulina cuneata, Globocassidulina subglobosa,* and *Cibicides deliquatus.* Other notable buliminids and rotaliids in this sample include *Patellinella inconspicua, Cibicides molestus, Gyroidina soldanii,* and *Notorotalia taranakia.* Rare specimens of *Gaudryina convexa* are the only agglutinated foraminifera identified from this sample, and the only lagenids to be found are *Sigmoidella (Sigmoidina) pacifica, Amphicoryna hirsuta,* and *Bifarilaminella advena.* The foraminiferal assemblage has a 30% planktic component, which includes many of the same species as sample HH2, including *Globoconella puncticulata* and *Globoconella pliozea*.

In addition to foraminifera, disarticulated ostracod valves are abundant and varied in sample HH3 (Figure 5.6). Macrofossils extracted from the bulk sample from the upper greensand include *Neothyris* sp., which is the dominant species in the brachiopod-dominated shell beds within this unit (see section 4.3). A single, bored specimen of *Talochlamys gemmulata* was also found.

The overall assemblage from sample HH2 resembles a typical Mangaopari Mudstone fauna (J. Collen, pers. comm.). The low planktic percentage in this sample indicates low oceanicity, but several benthic species indicate a bathyal depositional environment. *Martinottiella communis* has a minimum depth of 500 ±100 m, and *Sigmoilopsis schlumbergi* has a minimum depth of 600 ±150 m (Hayward et al., 2010). Collectively, these suggest deposition at mid-bathyal depths in a coastal basin which was close to land and sheltered from the open ocean.

Sample HH3 lacks the mid-bathyal index species which are present in HH2, and instead contains a mixture of shelf and upper bathyal species. *Globocassidulina subglobosa* has an upper depth limit of 250 ±80 m, and several other species present in the sample, such as *Cibicides molestus, Gyroidina soldanii,* and *Amphicoryna hirsuta,* suggest an outermost shelf or upper bathyal depositional environment. Species which are most abundant on the inner to mid-shelf, such as *Gaudryina convexa* and *Patellinella inconspicua*, are assumed to have been transported. The planktic percentage indicates a more oceanic water mass at the time when HH3 was deposited, compared to HH2, suggesting a more exposed, but still coastal, depositional setting for HH3.

Samples HH2 and HH3 are assigned to the lower Opoitian stage, based on the presence of *Globoconella puncticulata* and *Globoconella pliozea*. It appears that the later part of the Kapitean stage is not recorded at this location, missing in a disconformity between the Clay Creek Limestone and Makara Greensand.

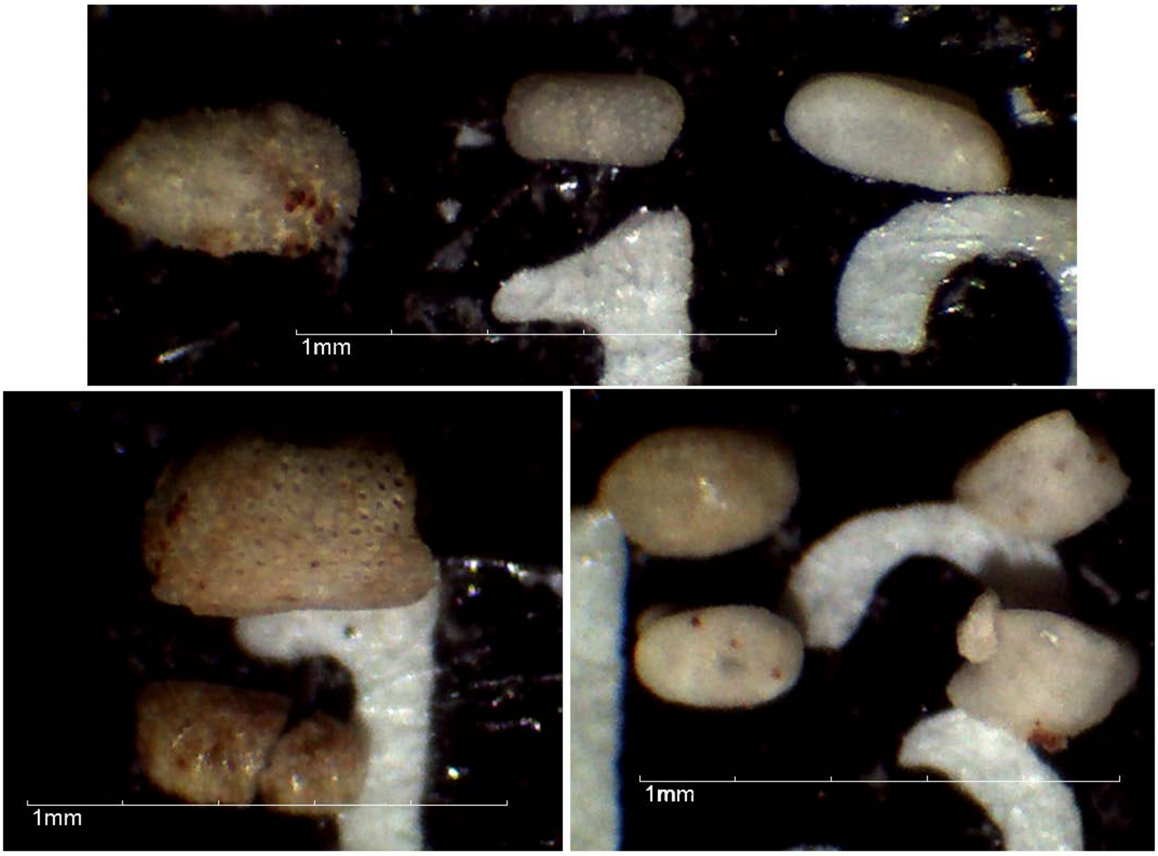

Figure 5.6: Disarticulated ostracod valves from the upper part of the Makara Greensand (sample HH3), Haurangi Hairpin section.

A sample held in the GNS collection (sample GS14873, S28/f215), collected at the Haurangi Hairpin from the same calcareous greensand interval as sample HH3, provides some additional biostratigraphic information. Two scallop species were identified from this sample by Dr. Alan Beu as *Phialopecten* aff. *tolagaensis* and *Mesopeplum waikohuense*. *Mesopeplum waikohuense* has a first appearance in the Opoitian, while *Phialopecten tolagaensis* is restricted to the Kapitean.

5.3 Te Ahitaitai section

Seven bulk rock samples were collected from the Te Ahitaitai section, but fossil material was only recovered from samples TA3, TA4, and TA5 (see Figure 4.12). Foraminifera were also found in sample 07A, collected from the ridge top 200 m northeast of the measured section. Foraminiferal censuses were conducted for samples TA4 and TA5, while insufficient specimens were found for censuses from samples TA3 and 07A.

5.3.1 Sunnyside Conglomerate

No macrofossils were observed in outcrop in the Sunnyside Conglomerate, and no foraminifera or other microfossils were found in samples TA1 or TA2. Sample TA3, collected from the pebbly, sandy mudstone overlying the conglomerate and sandstone facies and immediately underlying the Clay Creek Limestone, is the lowest sample in this section to contain fossil material. Foraminifera in sample TA3 are very rare and are poorly preserved, showing signs of dissolution. A foraminiferal census could not be conducted, but 13 species were identified, mostly buliminids and rotaliids. These include *Cassidulina carinata, Globocassidulina cuneata, Trifarina bradyi,* and *Cibicides molestus.* No agglutinated species or lagenids were found. Planktic species include *Globoconella* cf. *miotumida* and *Neogloboquadrina pachyderma.* Also present are sponge spicules, bryozoan fragments, and sharks' teeth.

Trifarina bradyi and *Cibicides molestus* both have upper depth limits on the outer shelf. The age of the fossils in sample TA3 is not well constrained, although the presence of *Globoconella* cf. *miotumida* suggests a possibly Tongaporutuan age. Given the rarity of fossil material in sample TA3, and the complete absence of fossils in samples from lower in the Sunnyside Conglomerate, it is likely that the fossils in sample TA3 were introduced from the overlying Clay Creek Limestone by bioturbation (see Section 4.5).

5.3.2 Clay Creek Limestone

Foraminifera are abundant in sample TA4, collected from the Clay Creek Limestone. Many specimens show signs of wear and abrasion. Unlike sample HH1, sample TA4 has a benthic foraminiferal assemblage dominated by buliminids and rotaliids, with abundant *Cassidulina* *carinata* and *Cibicides deliquatus.* Other notable buliminids include *Trifarina bradyi* (Figure 5.7D), *Patellinella inconspicua,* and *Uvigerina ?delicatula*; notable rotaliids include *Cibicides molestus, Elphidium novozelandicum, Pileolina sp.,* and *Notorotalia ?hurupiensis.* Agglutinated species make up 14% of the benthic assemblage, and include *Gaudryina convexa* and *Textularia kapitea* (Figure 5.7C).Rare lagenids include *?Nodosaria vertebralis*, *Lenticulina calcar, Saracenaria latifrons,* and unilocular species. One miliolid, *Cornuspira* sp., was also found.

The foraminiferal assemblage from sample TA4 is 12% planktic. The planktic assemblage includes *Globoconella miotumida* (Figure 5.7A) and *Globoconella conomiozea* (Figure5.7B), in addition to *Globigerina bulloides, Zeaglobigerina woodi,* and *Neogloboquadrina pachyderma*. Like sample HH1, sample TA4 includes moderately abundant ostracods, some of which are articulated. Bryozoan and sponge fragments were also found. The only macrofossil identified from the Te Ahitaitai section is *Neothyris* sp., which was identified in the Clay Creek Limestone outcrop but not collected.

The overall benthic foraminiferal assemblage from sample TA4 resembles those associated with upper bathyal depths (M. Crundwell, pers. comm.). Depth index species for the outermost shelf are present, including *Trifarina bradyi* and *Cibicides molestus*. Specimens of shallow water species, such as *Gaudryina convexa, Pileolina* sp., and *Elphidium novozealandicum* are generally somewhat abraded, and are likely to have been transported. The presence of *Globoconella miotumida, Globoconella conomiozea,* and *Textularia kapitea* indicate that, like sample HH1, sample TA4 has a lower Kapitean or possibly upper Tongaporutuan age.

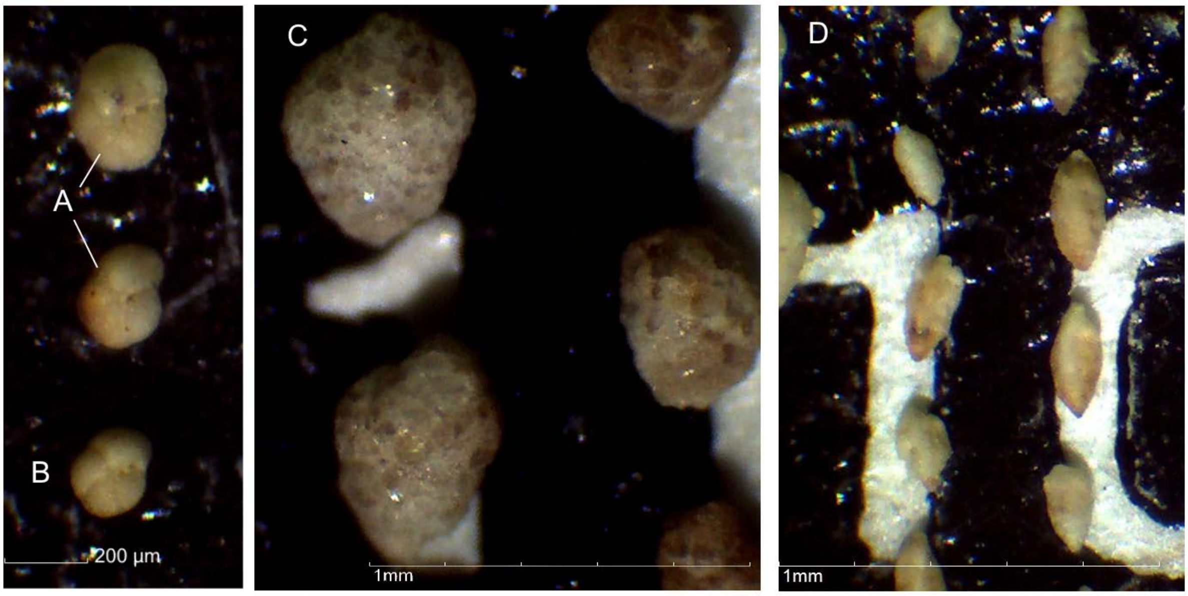

Figure 5.7: Key foraminifera from the Clay Creek Limestone at the Te Ahitaitai section, sample TA4. A: *Globoconella miotumida,* B: *Globoconella conomiozea,* C: *Textularia kapitea,* D: *Trifarina bradyi.*

5.3.3 Mangaopari Mudstone

Sample TA5, from the Mangaopari Mudstone in the Te Ahitaitai section, contains foraminifera which are abundant and well-preserved. The benthic component of the assemblage is dominated by buliminids, including abundant *Uvigerina* and *Neouvigerina* spp., *Bulimina striata, Bulimina aculeata, Globocassidulina cuneata, Globocassidulina subglobosa,* and *Trifarina bradyi.* Rotaliids are moderately abundant, and include *Gyroidina soldanii, Cibicides molestus,* and *Pullenia bulloides.* Only two agglutinated species were found, *Gaudryina convexa* and *?Siphotextularia* sp. Seven species of lagenid were found, predominantly elongate species such as *Neugeborina longiscata, ?Nodosaria vertebralis, Amphicoryna hirsuta,* and *Stilostomella* sp. Planktic species make up 35% of the foraminiferal sample. These include *Globoconella puncticulata, Truncorotalia crassaformis, Globigerina bulloides, Zeaglobigerina woodi,* and *Neogloboquadrina pachyderma.*

The presence of *Pullenia bulloides, Amphicoryna hirsuta, Gyroidina soldanii,* and *Globocassidulina subglobosa* indicate deposition in water depths of at least 200 m. Abundant buliminids also support a bathyal depositional environment. The sample is inferred to represent an upper bathyal environment due to the absence of deeper water index species such as *Karreriella cylindrica, Martinottiella communis* and *Sigmoilopsis schlumbergi.* Despite the bathyal depositional environment, the relatively low planktic percentage suggests deposition close to land in neritic waters. The sample belongs to the Opoitian stage, as indicated by the presence of *Globoconella puncticulata* and *Truncorotalia crassaformis.*

No macro- or microfossils were found in samples TA6 and TA7, which were collected from the Bridge Sandstone Member of the Mangaopari Mudstone at the Te Ahitaitai section.

5.3.4 Makara Greensand

Rare and poorly preserved foraminifera were found in the glauconitic mudstone sample 07A, collected on the ridge top 200 m northwest of the Te Ahitaitai section. This sample is assigned to the upper Makara Greensand or possibly the base of the Mangaopari Mudstone. In many cases only internal casts of foraminifera are present, and where tests are preserved, the original calcium carbonate has been diagenetically replaced by iron oxide minerals (Figure 5.8). No census was conducted, but 22 species were identified. The benthic component of the sample consists mostly of buliminids and rotaliids, including *?Uvigerina* sp., *Sphaeroidina bulloides, Chilostomella ovoidea, Nonionella* sp., and *Pullenia quinqueloba.* Like sample TA5, the planktic component of sample 07A includes *Zeaglobigerina woodi, Globoconella puncticulata* and *Truncorotalia crassaformis.*

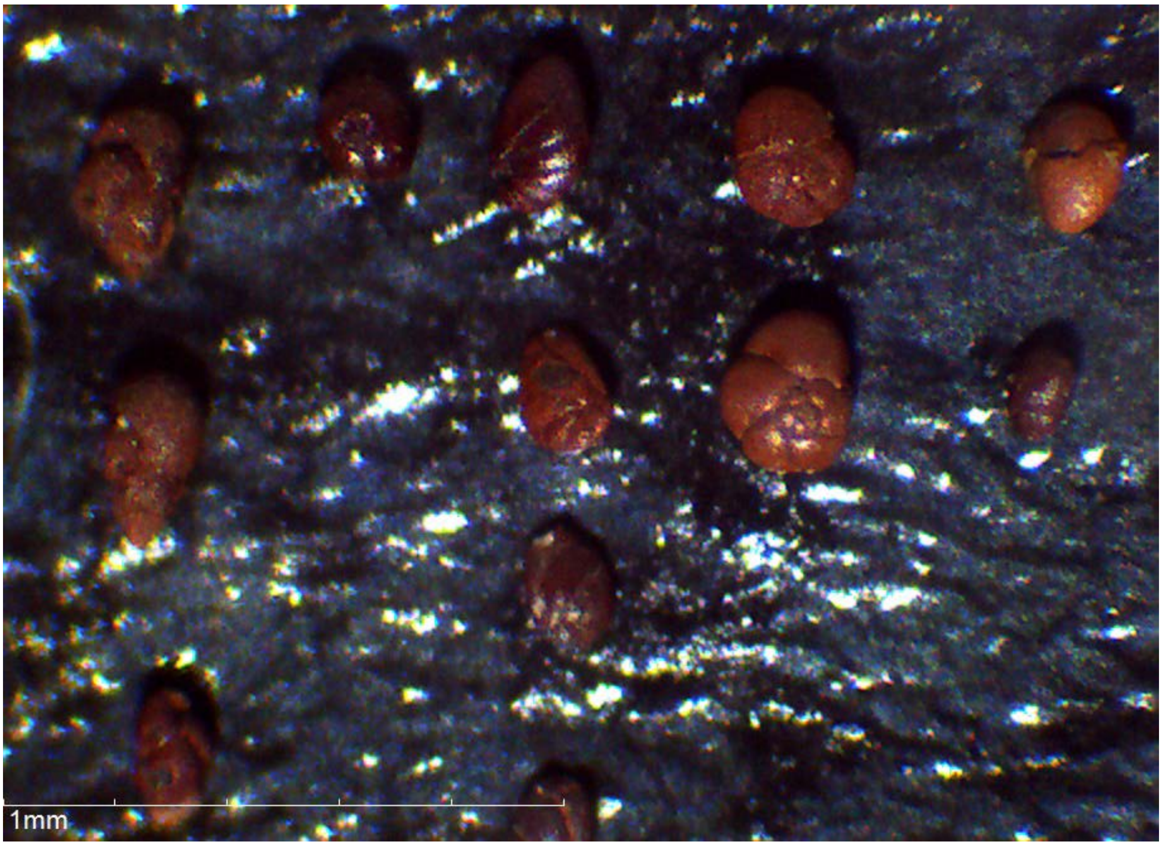

Figure 5.8: Foraminifera from the Makara Greensand on Te Ahitaitai Ridge, showing poor preservation and diagenetic replacement of calcium carbonate by iron oxide.

The benthic component of sample 07A resembles an outer shelf or upper bathyal assemblage (J. Collen, pers. comm.), although this depositional environment is not well constrained due to the poor preservation of the sample and the likelihood that some species may have been preferentially weathered or preserved. The presence of *Globoconella puncticulata* and *Truncorotalia crassaformis* indicates an Opoitian age for this sample.

5.4 Bells Creek sections

Bells Creek section A yielded the most detailed biostratigraphic record of the sections measured in this study. One sample was collected near the top of the Bells Creek Mudstone, three were taken from different sub-units of the Makara Greensand, and a sample was taken from the base of the overlying Mangaopari Mudstone (See Figure 4.14). Foraminiferal censuses were conducted for all five samples, and sample BC1 was also found to contain spores and pollen. Spores and pollen were also found in sample 28A, the only sample collected from Bells Creek section B.

5.4.1 Bells Creek Mudstone

Sample BC1 was collected from the Bells Creek Mudstone 60 cm below the base of the Makara Greensand. It contains abundant foraminifera which are generally well preserved. The benthic component of the sample consists mainly of buliminids and rotaliids, and includes extremely abundant *Uvigerina* spp. (Figure 5.9), which make up 33% of the total foraminiferal assemblage. *Bolivinita pohana* is also abundant in the sample. Key rotaliids include *Pullenia bulloides, Gyroidina soldanii,* and *Gyroidinoides zelandica.* Agglutinated species are rare, and lagenids moderately abundant, including elongate species such as *Stilostomella* sp. and *Mucronina subtregonata.* Planktic foraminifera account for only 8% of the sample, and only five planktic species were identified. These were *Globigerina bulloides, Zeaglobigerina woodi, Globigerinita glutinata, Globigerinita uvula,* and a single specimen of *Globoconella miotumida.*

The presence of *Pullenia bulloides* indicates deposition at a depth of at least 200 m. The relative abundance of *Uvigerina* may indicate a mid-bathyal or deeper depositional environment, and additionally suggests high carbon flux and low oxygen levels (Hayward et al., 2010). The very low planktic percentage suggests that the sample was deposited in a deep coastal basin which was sheltered from oceanic waters. The presence of *Globoconella miotumida* indicates a probable Tongaporutuan age, and the absence of *Globoquadrina dehiscens* suggests that the sample belongs to the upper Tongaporutuan (Cooper, 2004, Crundwell and Nelson, 2007). However, being based on a single specimen, this age estimate should be treated with caution.

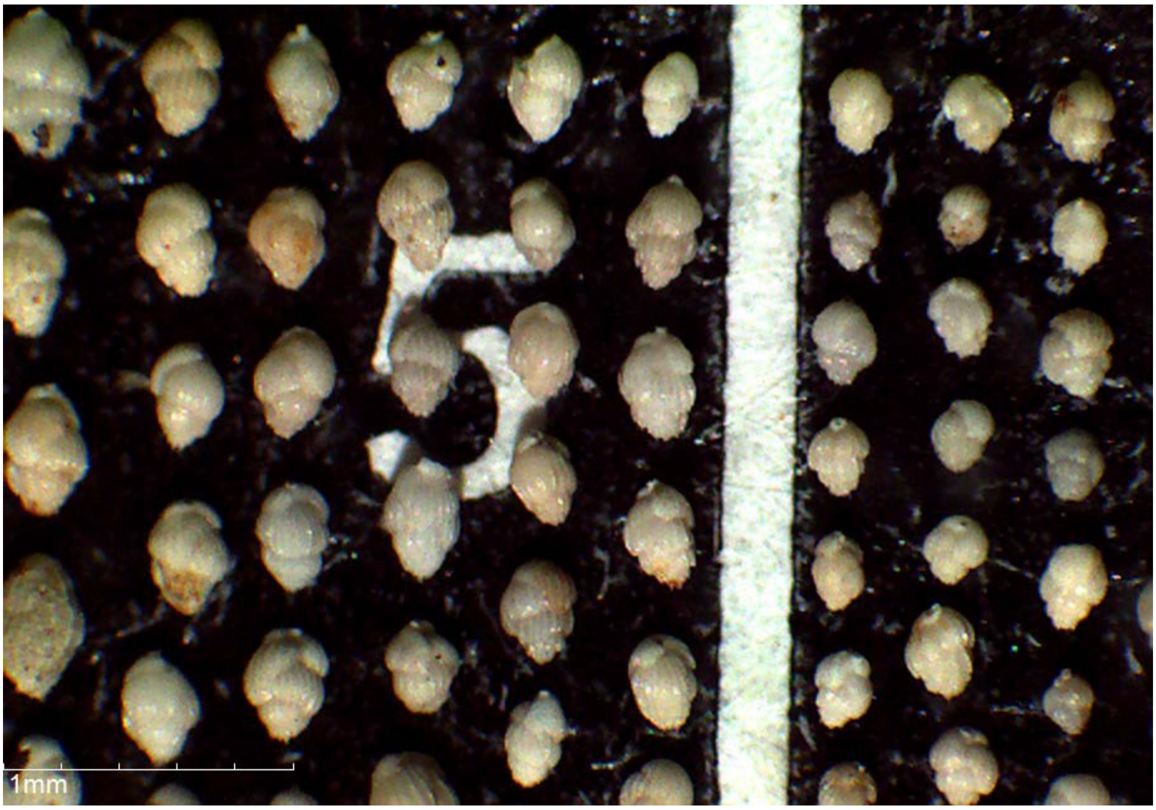

Figure 5.9: Abundant *Uvigerina* spp. in sample BC1, collected from the Bells Creek Mudstone, Bells Creek section A.

Sample BC1 was sampled for pollen in addition to foraminifera, due to the significant amount of black, carbonaceous matter visible in hand sample. It was found to contain spores, pollen and plant debris. Pollens extracted from the sample include *Nothofagidites* type and *Lateropora* type.

5.4.2 Makara Greensand

Sample BC2, the lowest of the three samples collected from the Makara Greensand, was collected from the shellbed sub-unit (see Figure 4.14). Foraminiferal preservation in this sample is variable, with some well-preserved specimens and some that are fractured or abraded. The benthic assemblage is dominated by buliminids and rotaliids; the most abundant species are *Cassidulina laevigata* (Figure 5.10A), *Cassidulina carinata, Cibicides deliquatus,* and *Gyroidina soldanii*. *Pullenia bulloides* is also present. Agglutinated species are rare, though more abundant and varied than in sample BC1, and include *Textularia* cf. *kapitea, Martinottiella communis,* and *Haeuslerella morgani.* Six species of lagenid were found: *Nodosaria* sp., *Stilostomella* sp., *Plectofrondicularia pohana, Lenticulina calcar, Lenticulina loculosa,* and *Lenticulina orbicularis* (Figure 5.10B). Also present was one species of robertinid, *Hoeglundina elegans.* Planktic foraminifera make up 12% of the assemblage. Both *Globoconella miotumida* and *Globoconella conomiozea* are present (Figure 5.10B), along with dominantly sinistral *Neogloboquadrina pachyderma.* Macrofossils present in the shellbed are generally poorly preserved, fragile and decalcified. Taxa identified in the outcrop include *Tucetona laticostata, Purpurocardia* sp., *Mesopeplum* sp., *Neothyris ovalis,* and *Notosaria nigricans.*

Sample BC3 was collected 3.5 m above sample BC2, in the dark green, sandy sub-unit of the Makara Greensand. Foraminifera from this sample are generally poorly preserved: many show signs of abrasion and minor dissolution, and almost all are stained orange-brown (Figure 5.10C-D). The benthic assemblage contains abundant buliminids, with *Uvigerina* spp. accounting for 36% of the total benthic assemblage. Rotaliids are moderately abundant, including *Cibicides molestus* and *Laticarinina pauperata.* Agglutinated species are also moderately abundant, including *Karreriella cylindrica, Karreriella cushmani,* and *Martinottiella communis.* Lagenids include large *Lenticulina* specimens >1 mm in diameter (Figure5.10C). Sample BC3 is 48% planktic, with abundant *Globoconella puncticulata* specimens and less common *Globoconella pliozea* and *Globoconella* cf. *conomiozea* (Figure 5.10D).

The third sample from the Makara Greensand at this locality, sample BC4, was collected from the greensand's uppermost, silty sub-unit. It contains a diverse and well-preserved foraminiferal fauna. The benthic assemblage includes abundant buliminids and rotaliids, and moderately abundant agglutinated species and lagenids. Key benthic species include *Pleurostomella alternans, Laticarinina pauperata* (Figure 5.10E)*, Karreriella cylindrica,* and *Karreriella bradyi,* along with *Sigmoilopsis schlumbergi* and elongate nodosariids such as *Laevidentalina communis* (Figure 5.10F). The assemblage is 35% planktic. The planktic component includes *Globoconella puncticulata, Globoconella* cf. *sphericomiozea,* and *Truncorotalia crassaformis.*

The three foraminiferal samples from the greensand show a gradual increase in water depth. The presence of *Martinottiella communis* in sample BC2 indicates a paleodepth of at least 400 m, and deposition at upper bathyal depths is supported by the presence of *Gyroidina soldanii* and *Pullenia bulloides,* and the absence of deeper index species. Shallower water species are assumed to have been transported, and this is supported by the degree of abrasion and fragmentation of many foraminiferal tests and macrofossils. The low planktic percentage indicates deposition in a deep coastal basin sheltered from the open ocean, and dominantly sinistral *Neogloboquadrina pachyderma* may indicate a cold climate, although a more detailed census of *N. pachyderma* specimens would be needed to confirm this.

Sample BC3 was also deposited at a depth of at least 400 m, as indicated by the presence of *Martinottiella communis* and *Karreriella cylindrica.* The abundance of *Uvigerina* spp. and the presence of *Laticarinina pauperata* in this sample may indicate a deeper depositional environment, as recent New Zealand benthic assemblages with more than 25% *Uvigerina* are restricted to mid-bathyal and deeper environments, and *Laticarinina pauperata* has a modern minimum depth of 1500 ± 500 m (Hayward et al., 2010). The planktic percentage in this sample indicates a significant increase in oceanic influence, from a middle neritic water mass in sample BC2 to an outer neritic water mass in sample BC3.

Sample BC4 contains more bathyal index species than sample BC3. The presence of *Karreriella bradyi, Sigmoilopsis schlumbergi,* and *Pleurostomella alternans* in sample BC4 indicates a paleodepth of at least 600 m for this sample. In addition, the presence of *Laticarinina pauperata* suggests that the sample may have been deposited in a lower bathyal (>1000 m) environment, though other lower bathyal index species were not found. The planktic percentage in sample BC4 is consistent with an outer neritic water mass, with limited oceanic influence.

The presence of *Globoconella miotumida, Globoconella conomiozea,* and *Textularia* cf. *kapitea* in sample BC2 indicates a Kapitean or possibly upper Tongaporutuan age for this sample, while the presence of *Globoconella puncticulata* in samples BC3 and BC4 places these samples in the Opoitian. The Miocene-Pliocene boundary is therefore probably located within the Makara Greensand in this section, between samples BC2 and BC3.

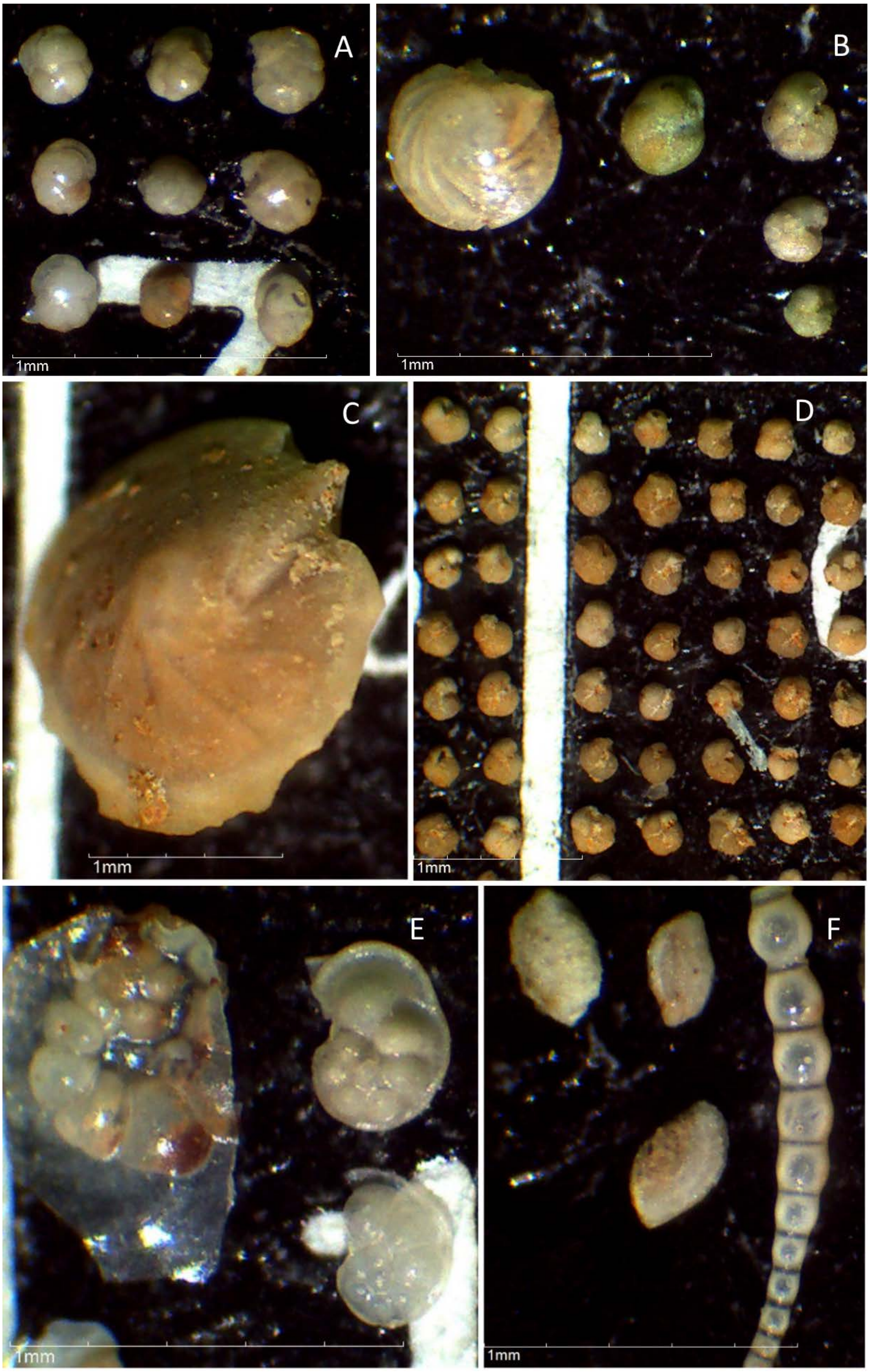

Figure 5.10: Key foraminifera from the Makara Greensand in Bells Creek section A. Top row from sample BC2, A: *Cassidulina laevigata*, B: *Lenticulina orbicularis, Globoconella conomiozea, Globoconella miotumida*. Middle row from sample BC3. Note poor preservation and orange-brown discolouration. C: *Lenticulina* sp., D: abundant *Globoconella* spp., mostly *Gc. puncticulata*. Bottom row from sample BC4. E: *Laticarinina pauperata, Laticarinina altocamerata*, F: *Sigmoilopsis schlumbergi, Laevidentalina communis*.

5.4.3 Mangaopari Mudstone

Foraminifera from sample BC5, from the base of the Mangaopari Mudstone, are smaller and less abundant than the foraminifera from samples BC1-BC4. The benthic assemblage from sample BC5 is dominated by buliminids and rotaliids, including *Cassidulina carinata, Uvigerina* spp., *Trifarina bradyi, Laticarinina altocamerata, Pullenia bulloides,* and *Cibicides molestus.* Rare agglutinated species include *Martinottiella communis, Karreriella cylindrica,* and *Sigmoilopsis schlumbergi.* Lagenids are also rare, and include *Mucronina hasta, Amphicoryna hirsuta,* and *Parafrondicularia antonina.* One robertinid species, *Hoeglundina elegans,* was also found. Planktic species make up 64% of sample BC5, the highest percentage of planktic foraminifera to be found in any sample in this study. The planktic assemblage includes *Globoconella puncticulata, Hirsutella* cf. *scitula, Neogloboquadrina pachyderma,* and *Globigerina bulloides.* Additional fossil material found in this sample includes sponge spicules and shark's teeth.

The presence of *Sigmoilopsis schlumbergi* indicates that sample BC5 was deposited at a depth of at least 600 m. The planktic percentage indicates that the basin was more exposed to oceanic water at the time of deposition of sample BC5 than it was when samples BC1-BC4 were deposited, with sample BC5 deposited in a sub-oceanic environment. The presence of *Globoconella puncticulata* indicates an Opoitian age for sample BC5.

5.4.4 Sunnyside Conglomerate (Bells Creek section B)

Foraminiferal samples were not collected from Bells Creek section B, but a bulk sample (sample 28A) was collected from the organic-rich siltstone interbedded in the Sunnyside Conglomerate (see Figure 4.15) and processed for pollen. This sample was found to contain very abundant plant debris, pollen, and spores. Pollen grains identified from the sample include *Nothofagidites* type, abundant swamp types, *Myrtaceae* type, *Podocarpaceae* type, *Proteacidites* type, *Haloragacidites* type, and *Asteraceae* type (Figure 5.11). The pollen assemblage indicates the presence of nearby shrubland and forest. The abundance of plant material in this sample, combined with the absence of marine fossils in the Sunnyside Conglomerate, strongly implies that this unit may have been deposited in a terrestrial rather than a marine environment, as has previously been suggested (Vella and Briggs, 1971).

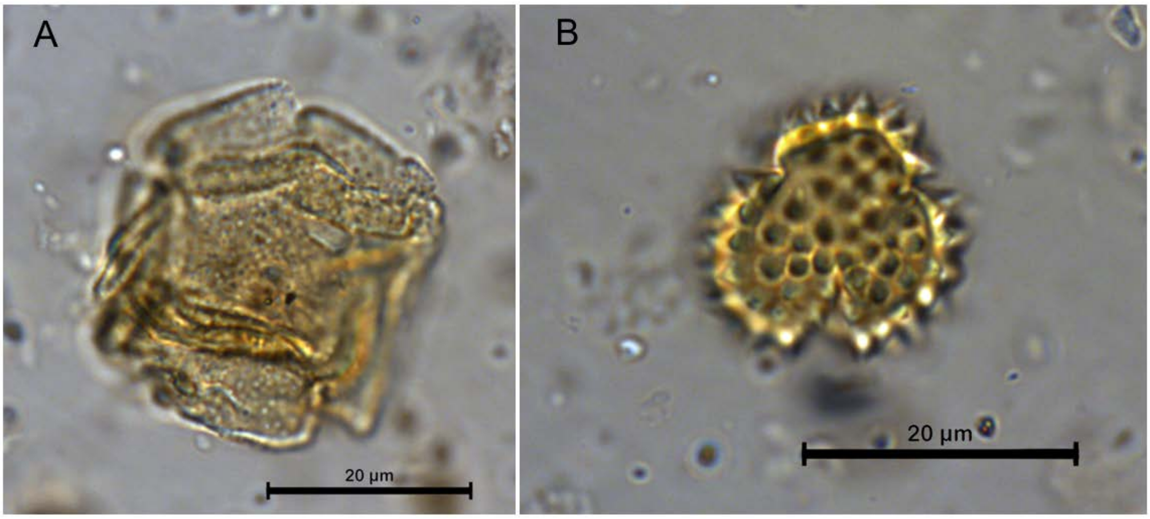

Figure 5.11: Examples of *Nothofagidites* type (A), and *Asteraceae* type (B) pollen grains from the Sunnyside Conglomerate.

5.5 Lower Makara River

Although no section was measured, several samples were collected in the lower Makara River area. Foraminiferal censuses were conducted for three samples from Homestead Creek (map ref. BQ34/057217): one from the Bells Creek Mudstone (sample 19A) and two from the Clay Creek Limestone (samples 23A and 24A). In addition, spores and pollen were found in sample 19A, and some macrofossils were identified from sample 23A. Additional macrofossils were identified from sample 25A, a picked fossil sample collected from the Clay Creek Limestone on the hillside north of Homestead Creek (BQ34/059216). Bulk samples were also collected from the Makara Greensand at both Homestead Creek and the creek 200 m to the northeast (see section 4.7); however, no foraminifera or other fossil material was found in these samples.

5.5.1 Bells Creek Mudstone

Abundant, diverse, and well-preserved foraminifera were found in sample 19A, collected from the grey mudstone underlying the Clay Creek Limestone near the mouth of Homestead Creek. The benthic foraminifera from this sample are predominantly buliminids and rotaliids, including several species of *Bolivina, Bolivinita quadrilatera* (Figure 5.12A)*, Cibicides deliquatus* and *Cibicides molestus,* and abundant *Gyroidinoides zelandica* (Figure 5.12B). Agglutinated species are relatively rare, but diverse, including *Textularia miozea, Karreriella cylindrica, Martinottiella communis,* and several species of *Siphotextularia.* Rare lagenids include elongate species such as *?Nodosaria vertebralis,* unilocular species such as *Favulina melo,* and three species of *Lenticulina.* Two miliolids, *Spiroloculina* sp. and *Biloculina* sp., and one robertinid, *Hoeglundina elegans,* were also found.

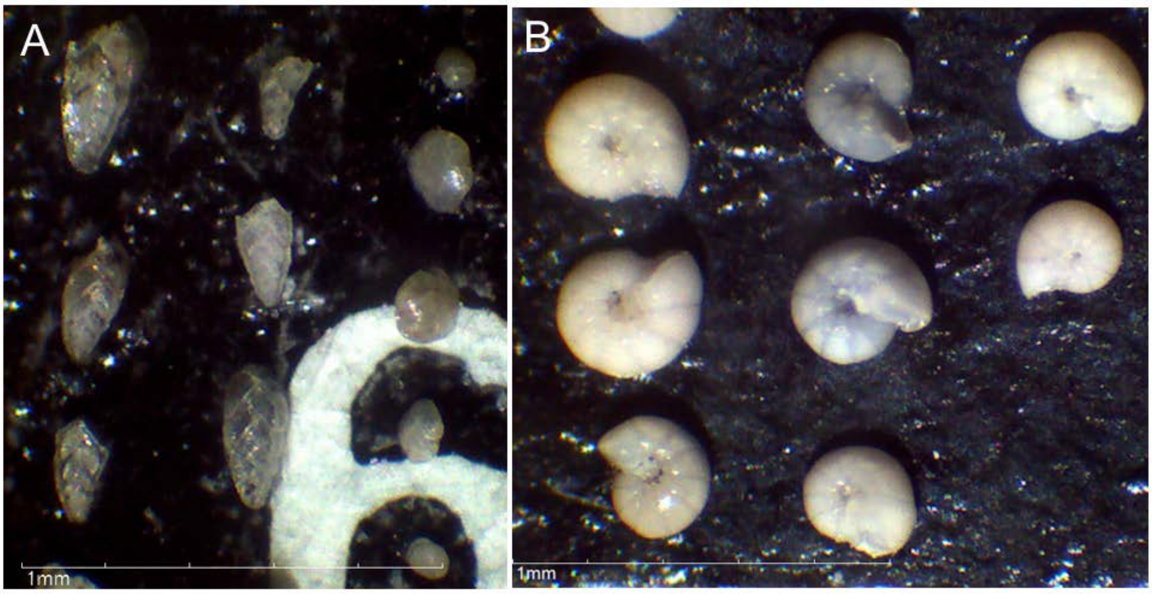

Figure 5.12: Well-preserved benthic foraminifera from sample 19A, collected from the Bells Creek Mudstone at Homestead Creek. A: *Bolivinita quadrilatera, Cassidulina carinata,* B: *Gyroidinoides zelandica.*

The foraminiferal assemblage from sample 19A is 38% planktic. *Globoconella miotumida* specimens from this sample are predominantly dextrally coiled, and a few, mostly sinistrally coiled, specimens of *Globoconella* cf. *conomiozea* are also present. Other notable planktic species include *Zeaglobigerina nepenthes, Hirsutella scitula, Neogloboquadrina pachyderma,* and rare specimens of *Globoquadrina dehiscens.* In addition to foraminifera, sample 19A includes otoliths, a small unidentified gastropod, and ostracods, including *Bradleya* sp. The carbonaceous matter in this mudstone includes spores, pollen, and plant debris. *Cyathea* type and monolete fern spores were identified, as well as *Pimelea* type, *Centrolepis* type, and *Nothofagidites* type pollen grains.

The presence of *Karreriella cylindrica* and *Martinottiella communis* in sample 19A indicate that the sample was deposited at a depth of at least 400 m. The planktic percentage is consistent with an outer neritic water mass, and the presence of pollen and plant matter also suggest that the sample was deposited in coastal waters. The sample is interpreted as having been deposited at upper or mid-bathyal depths in a sheltered coastal basin with limited oceanic influence.

The presence of both *Globoquadrina dehiscens* (Figure 5.13A) and *Globoconella miotumida* (Figure 5.13 D) places the sample in the lower Tongaporutuan substage, as the regional extinction of *Globoquadrina dehiscens,* at 8.96 Ma, defines the base of the upper Tongaporutuan substage (Raine et al., 2015). Four-chambered *Globoconella* cf. *conomiozea* specimens are also known to occur in New Zealand during the lower Tongaporutuan (Raine et al., 2015) (Figure 5.13B), and the presence of *Textularia miozea* (Figure 5.13C) further supports a Tongaporutuan age for the sample. The high percentage of dextrally coiled *Globoconella miotumida* specimens means that the age of the sample can be further constrained to one of three dextral coiling zones recognised in the lower Tongaporutuan: the Kaiti, Mapiri, and Tukemokihi Coiling Zones. Finally, the presence of *Neogloboquadrina pachyderma* constrains the sample to the Tukemokihi Coiling Zone, as the lowest occurrence of this species occurs above the Kaiti and Mapiri Coiling Zones (Cooper, 2004).

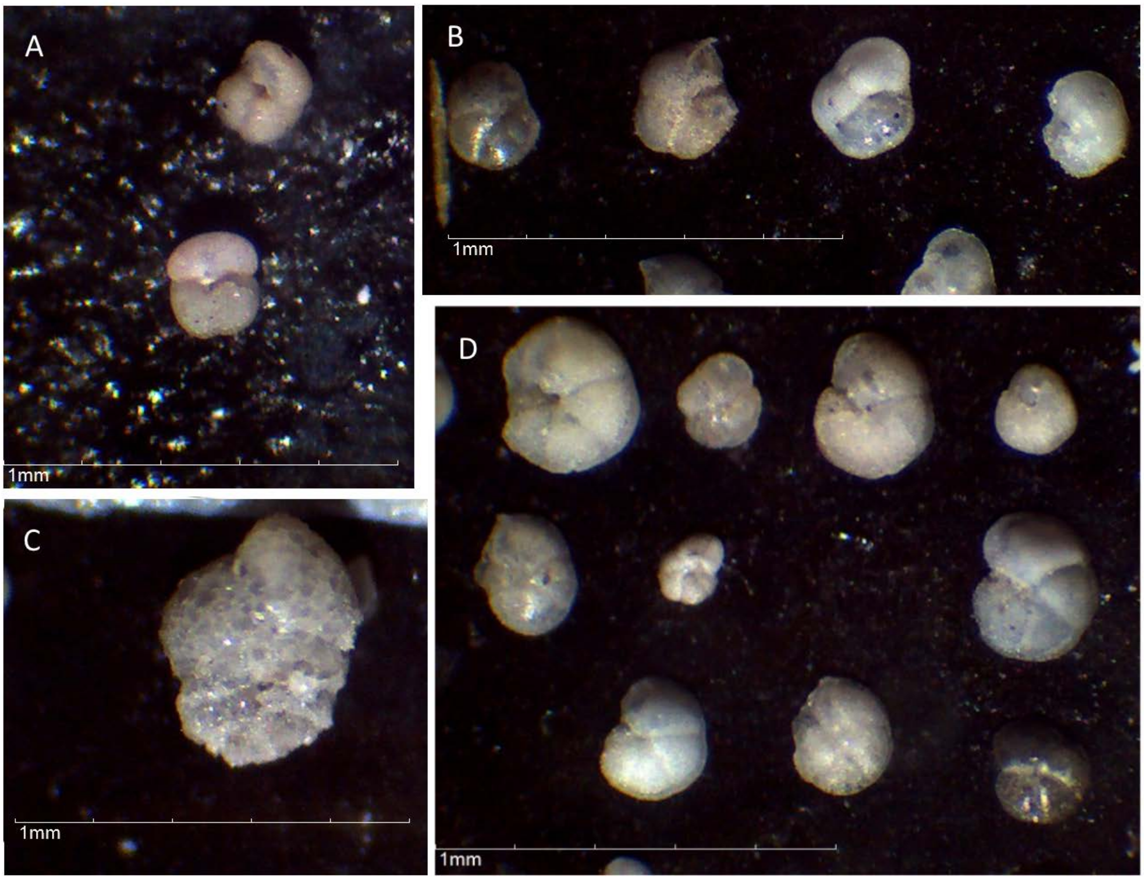

Figure 5.13: Age-indicative foraminifera from the Bells Creek Mudstone at Homestead Creek. A: *Globoquadrina dehiscens,* B: *Globoconella* cf. *conomiozea,* C: *Textularia miozea,* D: *Globoconella miotumida*, mostly dextral forms.

5.5.2 Clay Creek Limestone

Two foraminiferal samples were collected from the Clay Creek Limestone in Homestead Creek. The lower sample, sample 24A, was collected from a discontinuous, 10 cm thick layer of shelly mudstone and angular Torlesse fragments at the contact between the Clay Creek Limestone and Torlesse basement. The benthic foraminiferal assemblage from sample 24A is dominated by rotaliids, including *Cibicides deliquatus, Cibicides molestus*, and *Cibicides* cf. *novozelandicus.* Buliminids are also abundant, including *Cassidulina carinata* and *Trifarina bradyi.* Agglutinated species are moderately rare, and include *Gaudryina convexa* and *Spiroplectinella proxispira.* Rare unilocular lagenids are also present, along with one miliolid, *Cornuspira* sp. Sample 24A has an

8% planktic component, which includes *Globigerina falconensis, Globigerinita uvula,* and *Globigerinita glutinata.*

The second foraminiferal sample collected from the Clay Creek Limestone at this location, sample 23A, was taken from 1.5 m above the basal contact. Agglutinated species make up 41% of the benthic assemblage in this sample, including abundant *Gaudryina convexa.* Other agglutinated species include *Spiroplectinella proxispira* and several species of *Textularia,* including one specimen of *Textularia kapitea.* Rotaliids are also very abundant, and include *Cibicides molestus, Cibicides deliquatus, Pileolina* spp., and *Laticarinina altocamerata.* The only buliminid species found in the sample was *Cassidulina laevigata,* although this is moderately abundant. Rare lagenids include *Lenticulina calcar, Lenticulina orbicularis,* and *Fissurina* spp. Sample 23A contains only one identified planktic species, *Globigerina falconensis,* which accounts for just 1% of the sample. In addition to foraminifera, micro-brachiopods (Figure 5.14) and ostracods were found in the sample. Microfossil specimens from sample 23A are larger than those from other samples, with the average size in the coarse sand range.

An almost intact scallop valve was found in sample 23A, and was identified as *Mesopeplum (Borehamia) crawfordi* (Figure 5.15A). A large fragment of *Crassostrea ingens* was also found at this location, and the scaphopod *Fissidentalium solidum* was noted in the outcrop but not collected. The scallops in sample 25A, collected from the hillside 200 m northeast of Homestead Creek, were identified as *Mesopeplum burnetti* (Figure 5.15B).

Figure 5.14: Micro-brachiopods from sample 23A, collected from the Clay Creek Limestone at Homestead Creek.

The foraminiferal assemblage collected from sample 24A resembles the assemblage found in sample TA4 from the Te Ahitaitai section, while the assemblage from sample 23A resembles that of sample HH1 from the Haurangi Hairpin section. The presence of *Cibicides molestus* in samples 24A and 23A suggests that both samples were deposited at outer shelf depths; shallow water species such as *Gaudryina convexa* and *Pileolina* spp. are assumed to have been transported. The relatively low diversity of the assemblage in sample 23A, along with the large average size of specimens and the anomalously low planktic percentage, may be attributed to current action winnowing away finer grains (Hayward et al., 2010).

The foraminiferal samples from the Clay Creek Limestone in Homestead Creek do not have well-constrained ages. The presence of *Textularia kapitea* in sample 23A suggests a Kapitean age, but *T. kapitea* is also found in the upper Tongaporutuan and lower Opoitian (Hornibrook et al., 1989). *Mesopeplum burnetti* has a probable last appearance in the Kapitean (Beu, 1995), while *Crassostrea ingens* has its first appearance in the Tongaporutuan (Beu and Maxwell, 1990). *Mesopeplum crawfordi*, once thought to be a Waipipian index species, has now been found in samples dating back to the Waiauan stage (A. Beu, pers. comm.). Based on correlations with the Clay Creek Limestone at other locations, samples 23A, 24A, and 25A are all assumed to belong to the Kapitean stage.

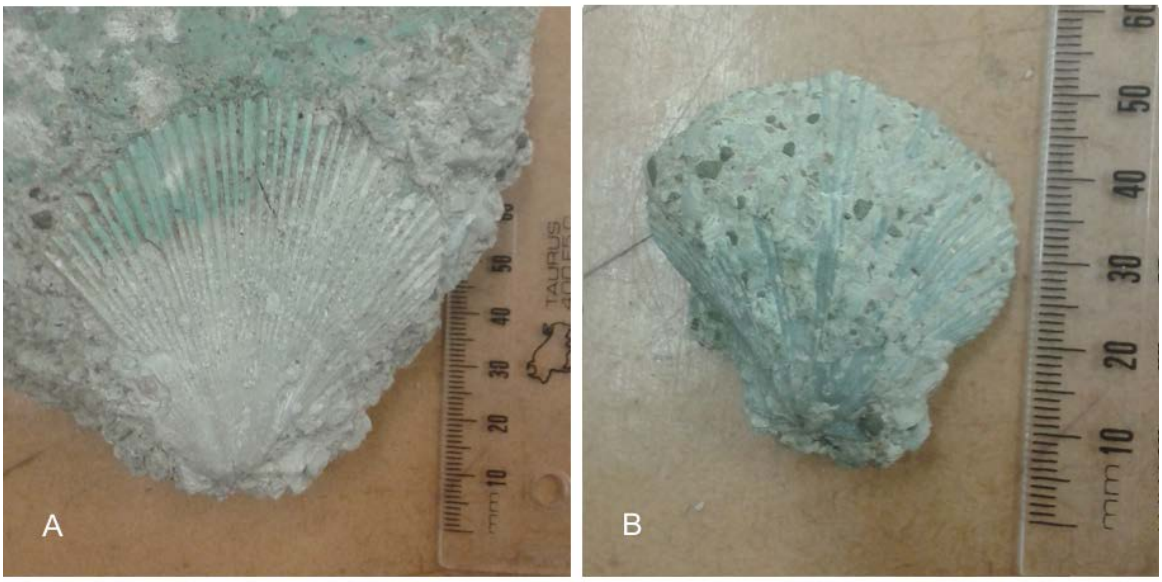

Figure 5.15: Pectinid fossils from the Clay Creek Limestone, lower Makara River valley. A: *Mesopeplum (Borehamia) crawfordi* from sample 24A, B: *Mesopeplum burnetti* from sample 25A.

5.6 Saw Cut Gorge

Two samples were collected at Saw Cut Gorge (BQ34/054190), one from each of the limestones present. A foraminiferal census was carried out for the Clay Creek Limestone sample, sample 35B. The sample collected from the upper limestone (probable Dyerville Limestone) did not contain sufficient foraminifera for a census to be conducted.

5.6.1 Clay Creek Limestone

Sample 35B, collected from the Clay Creek Limestone at Saw Cut Gorge, contains abundant foraminifera, but preservation is poor. Many specimens are fractured and abraded, and most show signs of partial dissolution and recrystallization. The benthic assemblage is dominated by buliminids and rotaliids, and the most abundant species are *Cassidulina carinata, Cassidulina laevigata,* and *Cibicides deliquatus*. Other notable buliminids and rotaliids from this sample include *Trifarina bradyi, Cibicides molestus* and *Elphidium novozealandicum*. Agglutinated species make up 8% of the sample, and include *Gaudryina convexa* and *Spiroplectinella proxispira*. Rare lagenids include *Lenticulina* sp. and *Fissurina* cf. *submarginata.* The sample is 12% planktic. The planktic component includes *Truncorotalia juanai, Turborotalita quinqueloba, Neogloboquadrina pachyderma, Globoconella miotumida,* and one specimen of *Globoconella* cf. *conomiozea.*

Like other samples from the Clay Creek Limestone, sample 35B includes both shallow water species such as *Elphidium novozealandicum* and outer shelf species such as *Trifarina bradyi* and *Cibicides molestus.* It is interpreted as having been deposited on the outer shelf, but containing specimens transported from shallower depths. The presence of *Globoconella miotumida, Truncorotalia juanai,* and *Globoconella* cf. *conomiozea* indicate that sample 35B has an upper Tongaporutuan or possibly lower Kapitean age.

5.6.2 Dyerville Limestone

Sample 35A, collected from the upper limestone at Saw Cut Gorge, contained only one identifiable foraminifer, a single, battered *Lenticulina* sp. An intact scallop valve from this sample was identified as *Phialopecten marwicki* (Figure 5.16)*,* which is a characteristic species of the Dyerville Limestone (Beu, 1995). The Dyerville Limestone is thought to be Opoitian in age, but the scallop collected resembles the Waipipian form of *P. marwicki* more closely than the Opoitian form (A. Beu, pers. comm.).

Figure 5.16: ***Phialopecten marwicki*** **from sample 35A, collected from the Dyerville Limestone at Saw Cut Gorge.**

5.7 Paruwai

One foraminiferal sample, sample 18A was collected in the Paruwai area. The sample was collected from the calcareous mudstone which underlies the Clay Creek Limestone on the true right of the upper limestone gorge (map ref. BQ34/052178; see section 4.9). The benthic component of the sample is dominated by buliminids and rotaliids, including very abundant *Uvigerina* spp. Only three agglutinated species were found to be present: *Karreriella cylindrica, Haeuslerella morgani,* and *Sigmoilopsis schlumbergi.* Lagenids are also relatively rare in the sample, but include large specimens of *Lenticulina calcar* and *Saracenaria italica.* The foraminiferal assemblage from sample 18A is 14% planktic, and many of the planktic specimens appear to have been compressed and sheared after deposition (Figure 5.17A). The planktic assemblage includes *Globigerina bulloides, Truncorotalia* cf. *juanai, Globoconella conomiozea* (Figure 5.17B), and a single specimen of *Globoconella* cf. *miotumida.*

The presence of *Sigmoilopsis schlumbergi* indicates that sample 18A was deposited at a depth of at least 600 m. The abundance of *Uvigerina* spp. also supports a bathyal depositional environment, probably with low oxygen and high carbon flux to the seafloor. The low planktic percentage indicates deposition in a sheltered coastal basin, with a neritic water mass despite the sample's bathyal depth. The presence of *Globoconella conomiozea* indicates that the sample belongs to the lower Kapitean stage. On the basis of its Kapitean age, and stratigraphic position below the Clay Creek Limestone, Sample 18A is correlated with the Bells Creek Mudstone.

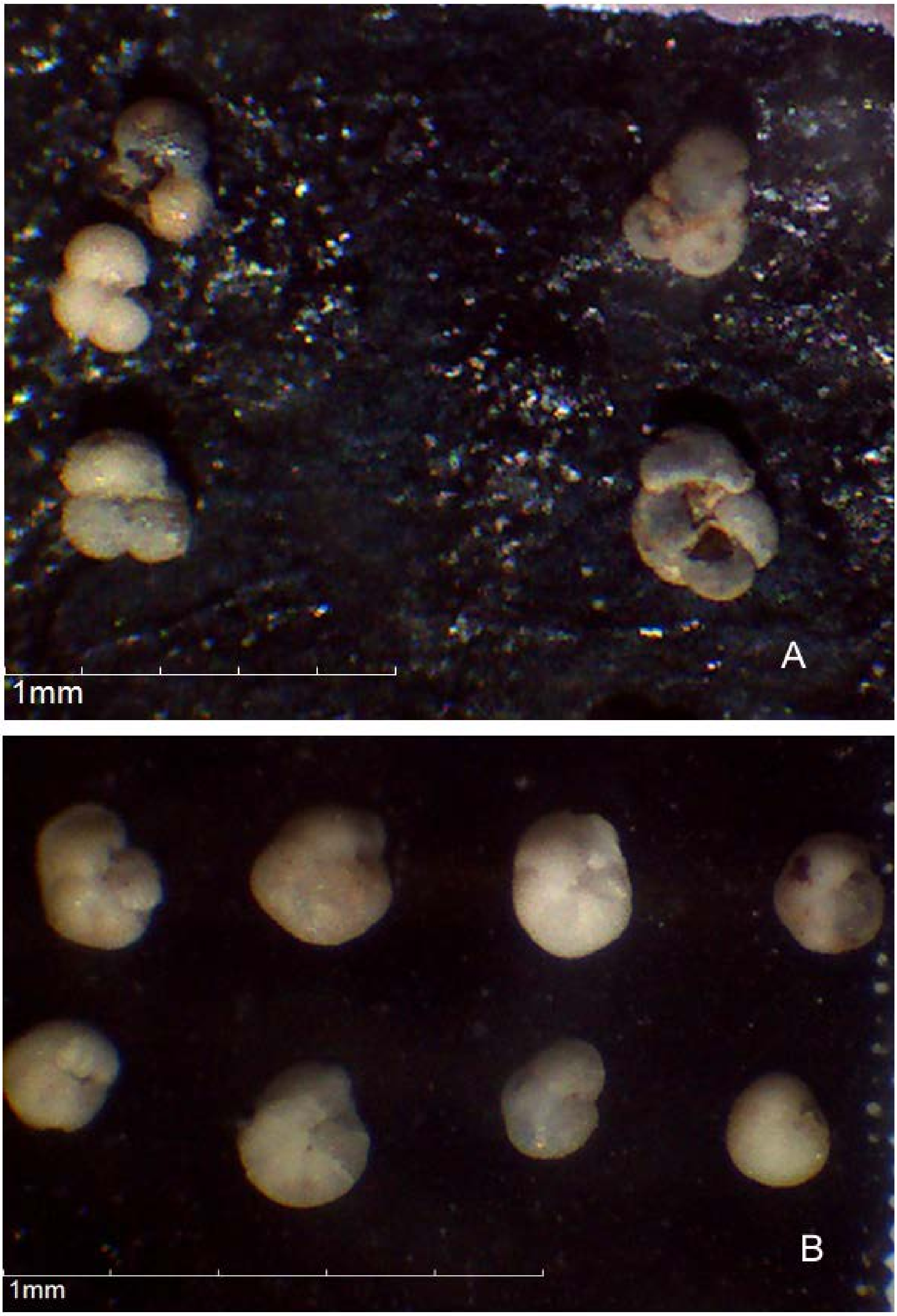

Figure 5.17: Planktic foraminifera from sample 18A, collected from the Makara River's upper limestone gorge at Paruwai. A: Poorly preserved, squashed, and sheared specimens of *Globigerina* and *Zeaglobigerina* spp., B: *Globoconella conomiozea.*

Chapter 6 Correlations and geological history

6.1 Introduction

The chapter presents an interpretation of the late Miocene-early Pliocene stratigraphy and geological history of the study area, based on the data presented in Chapters 4 and 5. Section 6.2 discusses stratigraphic correlations between late-Miocene-early Pliocene formations across the field area. Section 6.3 presents an interpretation of the area's geological history through the late Miocene and early Pliocene. Section 6.4 discusses the larger context of this study and its results, including correlations outside the study area, time constraints on episodes of accelerated deformation, and comparisons between the Clay Creek Limestone and key Hawke's Bay Te Aute Lithofacies limestones.

6.2 Unit correlations

6.2.1 Key features of regional stratigraphy

The fence diagram (Figure 6.1) shows lateral relationships between units across the study area. Eight stratigraphic columns are presented and correlated. Stratigraphic columns are compiled from measured sections and other key locations presented in Chapter 4, with additional unit thickness data from Vella and Briggs (1971) for the Haurangi Hairpin column, Green (1981) for the upper limestone gorge column, and Couper (1948) for the Saw Cut Gorge column. Unit thicknesses in the Homestead Creek column are estimates.

The fence diagram shows changes in late Miocene-early Pliocene stratigraphy from the southwest to the northeast of the study area. Aside from the Torlesse basement, the most persistent units across the study area are the Clay Creek Limestone, Makara Greensand, and Mangaopari Mudstone. The fence diagram illustrates the lateral transition discussed in Section 4.2, from limestone-dominated stratigraphy at the Haurangi Hairpin, to limestone overlain by mudstone in central parts of the study area, and then to mudstone-dominated stratigraphy overlying the Sunnyside Conglomerate in the Bells Creek sections.

The fence diagram shows significant lateral variations in the thicknesses of both the Clay Creek Limestone and Bells Creek Mudstone. The Clay Creek Limestone is shown to be a wedge- or lens-shaped unit, varying in thickness between 1 m and as much as 100 m over distances of only a few kilometres. It reaches its maximum thickness at the upper limestone gorge at Paruwai, and thins rapidly to the northeast and to the west. The Bells Creek Mudstone shows a similarly rapid change in thickness across the Te Ahitaitai area. In Bells Creek Section B, the thickness of the Bells Creek Mudstone cannot exceed 31 m (see Figure 4.15), but it has an estimated thickness of

Figure 6.1: Stratigraphic columns and correlations between geological units in the study area

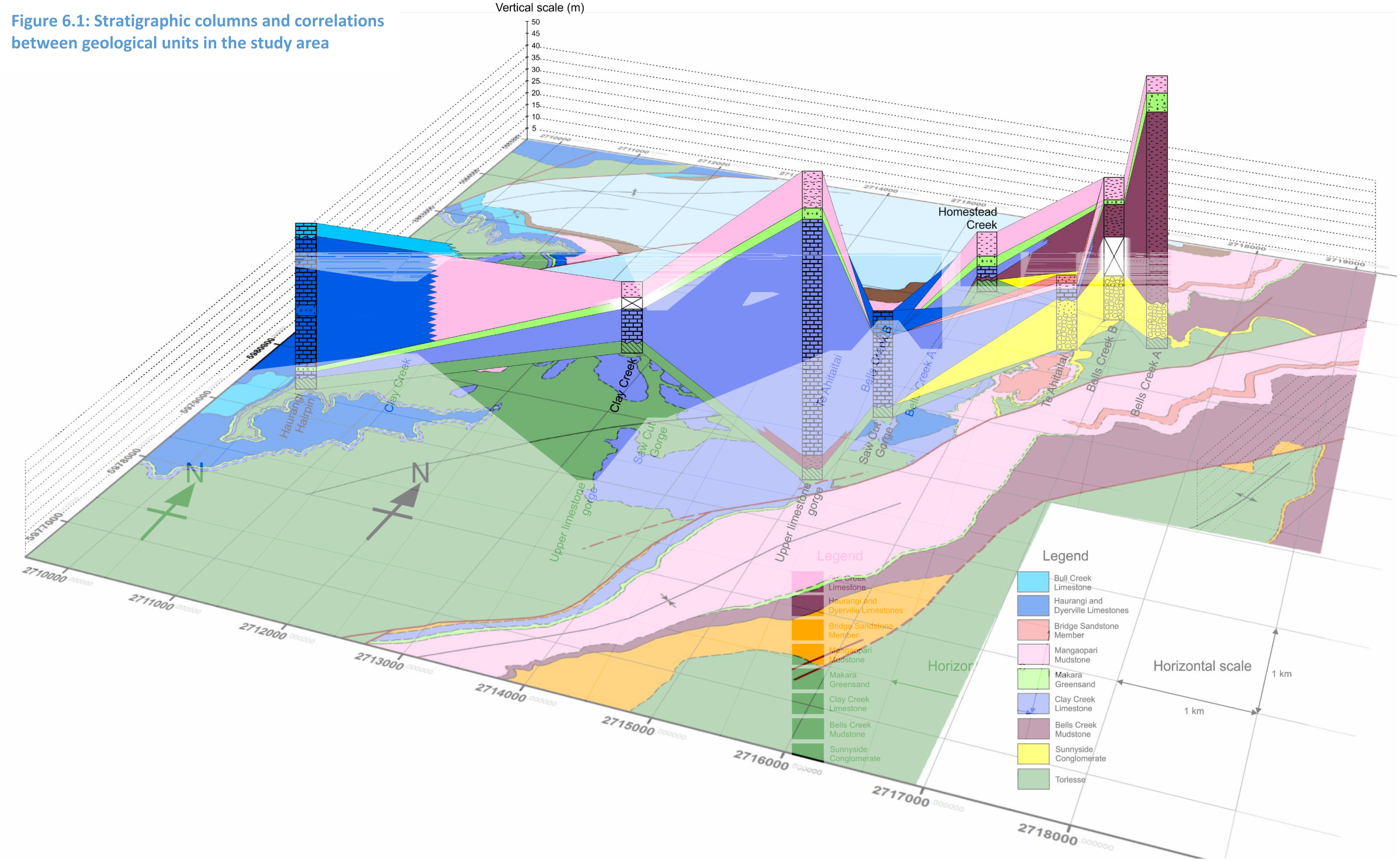

80 m below Bells Creek section A, only 200 m away. In the Mangaopari Stream section (not shown on the fence diagram) the thickness of the Bells Creek Mudstone has been measured as 290 m (Vella and Briggs, 1971).

Another key feature of the late Miocene-early Pliocene stratigraphy in the study area is the presence of rapid lateral transitions between fine-grained bathyal mudstone and coarse-grained limestone, which can be seen in both the Bells Creek Mudstone-Clay Creek Limestone transition in the Te Ahitaitai area, and the Mangaopari Mudstone-Haurangi and Dyerville Limestones transition in the Ruakokoputuna Valley.

Inferred spatial and temporal relationships between late Miocene-early Pliocene lithostratigraphic units are summarised in Figure 6.2. These relationships between units are discussed in greater detail below. Significant differences in stratigraphy are apparent on either side of the Mangaopari Fault. The Hurupi Formation is present on the eastern (downthrown) side of the fault but absent on the upthrown side, suggesting that it may have been removed from the upthrown block by erosion. The Makara Greensand differs in age across the fault, indicating that greensand formed at different times on the upthrown and downthrown blocks. The implications of these differences in stratigraphy across the Mangaopari Fault are discussed in Sections 6.3 and 6.4.

6.2.2 Sunnyside Conglomerate

The age of the Sunnyside Conglomerate in the study area is not well constrained. In the mapped area, the Bells Creek Mudstone overlies the Sunnyside Conglomerate unconformably. To the south of the area mapped in this study, Hatfield (1981) mapped Sunnyside Conglomerate underlying the Hurupi Formation with a gradational contact. Based on this stratigraphic relationship, the age of the Sunnyside Conglomerate is considered to be early Tongaporutuan and possibly partly Waiauan.

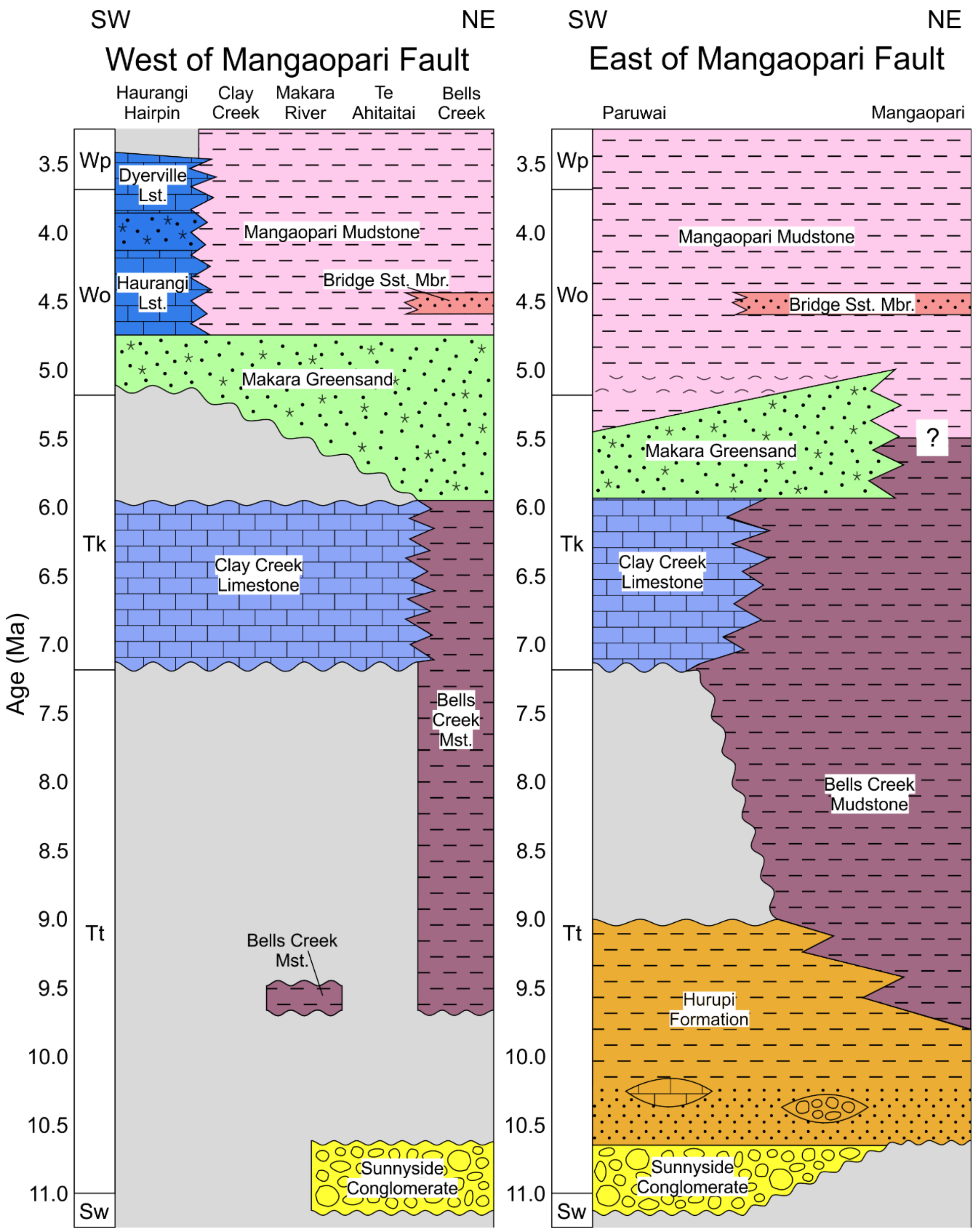

Figure 6.2: Late Miocene-early Pliocene lithostratigraphy, showing approximate ages of units and lateral changes in stratigraphy in two parallel sections from southwest to northeast of the study area, separated by the Mangaopari Fault. Grey areas indicate intervals of erosion or non-deposition.

6.2.3 Hurupi Formation

Although it was not sampled or examined in detail in this study, the Hurupi Formation has been studied extensively by others, and its early Tongaporutuan age and shallow marine depositional environment are well established (e.g. King, 1933, Vella, 1954, Beu and Maxwell, 1990). In the Paruwai area, Green (1981) and Hatfield (1981) described the Hurupi Formation as fining upward from basal sandstone to grey mudstone, and also becoming finer-grained and muddier to the northeast. At Paruwai, the Bells Creek Mudstone overlies the Hurupi Formation disconformably, but northeast of Paruwai, the upper, muddy part of the Hurupi Formation is interpreted to grade laterally into the lower Bells Creek Mudstone; in the southern part of Mangaopari Stream, the Hurupi Formation is represented only by a thin sandstone unit which underlies Bells Creek Mudstone and overlies Torlesse (see Figures 4.2 and 4.3).

6.2.4 Bells Creek Mudstone

Vella and Briggs (1971) considered the relationship between the Sunnyside Conglomerate and Bells Creek Mudstone to be conformable. However, results from this study show that the two units are separated by an angular unconformity. The clearest evidence for this can be found on the western side of Te Ahitaitai Ridge and in Homestead Creek. The Sunnyside Conglomerate is present on the downthrown side of the Makara Fault, but absent on the upthrown side, where a lens of Bells Creek Mudstone rests unconformably on Torlesse basement. Additional evidence comes from the marked difference in strike between the Sunnyside Conglomerate and Makara Greensand in Bells Creek, noted in Section 4.2.

The Bells Creek Mudstone ranges from early Tongaporutuan (sample 19A) to Kapitean (sample 18A) in age; the lower part of the 'Paruwai Formation', informally named by Hatfield (1981) and Green (1981), is here considered to be a part of the Bells Creek Mudstone. The upper part of the Bells Creek Mudstone is therefore a deep-water lateral equivalent of the Clay Creek Limestone. Lateral equivalence between the two units is most obvious in the Paruwai area, where Clay Creek Limestone in the western side of the Makara Syncline passes into Bells Creek Mudstone on the eastern side of the syncline (see Figures 4.2 and 4.3). A similar relationship between the units is inferred in Bells Creek, with Clay Creek Limestone passing laterally into Bells Creek Mudstone on the eastern side of Te Ahitaitai Ridge. The age of the uppermost Bells Creek Mudstone in this area is poorly constrained (see Section 5.3) but is inferred to be latest Tongaporutuan to early Kapitean, equivalent to the Clay Creek Limestone in the Te Ahitaitai section (see section 5.2).

6.2.5 Clay Creek Limestone

Vella and Briggs (1971) considered the Clay Creek Limestone to be separated from the Bells Creek Mudstone by a regional unconformity. While an angular unconformity is indeed present between the two units in Homestead Creek, results from this study show that the Clay Creek Limestone and Bells Creek Mudstone are conformable and partly laterally equivalent in other locations. Foraminiferal assemblages show that the Clay Creek Limestone belongs to the early

Kapitean stage, and may extend back to the latest Tongaporutuan at some locations where *Globoconella miotumida* is present.

The glauconitic shellbed in Bells Creek section A (see Figure 4.13) has previously been considered to be part of the Clay Creek Limestone (Vella and Briggs, 1971, Dobbie, 1976, Beu, 1995), which was thought to grade laterally from cemented pebbly limestone on Te Ahitaitai Ridge to poorly cemented pebbly shell bed in Bells Creek. The absence of limestone or a shellbed in Bells Creek section B is here considered to be evidence against this interpretation.

The limestone on the Makara River-Clay Creek interfluve was mapped as undifferentiated by Vella and Briggs (1971) and Abbas (1971), although Vella and Briggs recognised the presence of Clay Creek Limestone at the upper limestone gorge, and described the karst plateau between Paruwai and Clay Creek as including large areas of Clay Creek Limestone. In this study, all the limestone in the upper gorge and on the plateau is assigned to the Clay Creek Limestone, following the stratigraphy of Green (1981).

6.2.6 Makara Greensand

Foraminiferal abundance and preservation in the Makara Greensand vary greatly, which can make correlations difficult. Crundwell (1997) inferred the Makara Greensand to be Kapitean in age, and a separate unit from the Opoitian greensand that overlies the Clay Creek Limestone. Results from this study show that the Makara Greensand is partly Opoitian in age at its type locality (Bells Creek section A), and that it can be correlated with the greensand which overlies the Clay Creek Limestone at the Haurangi Hairpin section. However, the presence of Tongaporutuan and Kapitean species in the shellbed at Bells Creek section A indicates that the base of the greensand is older at this section than at the Haurangi Hairpin. The greensand mapped in the Paruwai area by Green (1981) and Hatfield (1981) is inferred to be entirely Kapitean in age, as the Kapitean index scallop *Sectipecten wollastoni* was recorded from shellbeds in the overlying mudstone. The Makara Greensand is therefore interpreted as a diachronous unit which ranges in age from Kapitean to early Opoitian.

6.2.7 Mangaopari Mudstone

The lower part of the Mangaopari Mudstone is Opoitian in age on the western (upthrown) side of the Mangaopari Fault. However, on the eastern (downthrown) side of the fault, the basal Mangaopari Mudstone is of Kapitean age. Both Green (1981) and Hatfield (1981) reported the presence of *Sectipecten wollastoni* in the pebbly shellbeds which are interbedded in the Mangaopari Mudstone at Paruwai. The Opoitian foraminifer *Globoconella puncticulata* was reported as first occurring in the massive mudstone which overlies the shellbed facies (Green, 1981, Hatfield, 1981). The Bridge Sandstone Member is also of early Opoitian age, and is interpreted as a sequence of turbidites, following Vella and Briggs (1971). The Mangaopari Mudstone extends through to the Mangapanian stage (Vella and Briggs, 1971).

6.2.8 Haurangi Limestone and Dyerville Limestone

The Haurangi Limestone and the Dyerville Limestone are known to be shallow-water equivalents of the Mangaopari Mudstone (Vella and Briggs, 1971); both limestones have previously been assigned to the Opoitian stage (Beu, 1995). However, this study shows that the limestone mapped as Dyerville Limestone is probably of Waipipian age at Saw Cut Gorge. The upper limestone at Saw Cut Gorge may therefore be younger than the Dyerville Limestone recognised at other locations, or the Dyerville Limestone may by Waipipian in other locations too.

6.3 Late Miocene-early Pliocene geological history

The general tectonic and paleoenvironmental trend in the northern Aorangi Range throughout late Miocene and early Pliocene times was one of subsidence (Wells, 1989a) and increasing oceanicity. However, episodes of accelerated shortening across the plate boundary were accommodated by reverse faulting and folding and the growth of contractional structures (Nicol et al., 2002), creating local uplift episodes which are superimposed on the regional subsidence trend. Although Antarctic ice sheets were present during the late Miocene and early Pliocene, glacio-eustatic fluctuations in sea level at this time were relatively small (<50 m) in amplitude (Miller et al., 2005) and are not considered to have played a major role in the changes in water depth that occurred in the study area during this time.

At the end of the Waiauan and beginning of the Tongaporutuan stage, the Aorangi Range was emergent as a hilly, forested island, ‘Aorangi Island’ (previously referred to as Haurangi Island by Beu, 1995), separated from the westerly mainland by a proto-Ruataniwha Strait. The island was gradually subsiding at this time, and the hills were being eroded by rivers. The Sunnyside Conglomerate was deposited in a river and lake system. Early in the Tongaporutuan, the sea transgressed across the study area, and the Hurupi Formation was deposited in a shallow marine environment as subsidence continued. Subsidence was more rapid in the east of the study area, with bathyal Bells Creek Mudstone being deposited in the Mangaopari area while shallower facies associated with the Hurupi Formation continued to be deposited at Paruwai.

An episode of local uplift occurred in the early Tongaporutuan, and is superimposed on the trend of regional subsidence. This uplift is associated with movement on the Makara Fault, and is correlated with the rapid uplift event identified by Wells (1989a) as occurring at around 10.5-10 Ma. The uplift event caused a hiatus in deposition across much of the study area, and the

Sunnyside Conglomerate and Hurupi Formation were eroded from the upthrown side of the Makara Fault. As activity ceased on the Makara Fault and regional subsidence continued, Bells Creek Mudstone was deposited continuously across the Makara Fault in the later part of the early Tongaporutuan substage. The Aorangi Island remained emergent during this time, possibly as a low-lying, swampy and forested island surrounded by relatively deep sea, including some deep, sheltered coastal basins or embayments. Pollen and organic matter, washed out to sea from the island, were deposited into a coastal basin along with terrigenous mud. The lack of exposure to oceanic water and sheltering from currents created a stratified water column in these coastal basins, with foraminiferal assemblages indicating low oxygen levels at depth. Low-oxygen conditions allowed for the preservation of carbonaceous matter.

A second episode of tectonic shortening and uplift occurred in late Tongaporutuan time. The Mangaopari Fault became active at this time, along with the Huangarua and Martinborough Faults (Nicol et al., 2002), and possibly also the Ruakokoputuna, Blue Rock, and Nikorima Faults. The western and central parts of the study area were raised above sea level by folding and reverse movement on the Mangaopari Fault. In the uplifted area, the Bells Creek Mudstone was eroded back to basement level, with the exception of a few localised patches from the base of the unit preserved in depressions in the Torlesse surface. Uplift was less pronounced in the northeast of the study area, where the Mangaopari Fault passed laterally into an anticline, and deposition of Bells Creek Mudstone continued on the anticline's eastern limb. On the downthrown side of the Mangaopari Fault, a basin formed, which subsequently allowed for the accumulation of over 100 m of Kapitean limestone and mudstone in the Paruwai area.

This uplift episode ended near the Tongaporutuan-Kapitean boundary, and regional subsidence continued. In the early Kapitean, the Aorangi Island was fringed by shoals and reefs created by basement antiforms which had been uplifted in the late Tongaporutuan. These shoals, reefs, and tide-swept, rocky coasts became carbonate factories for the Clay Creek Limestone. Tidal currents and storm events periodically transported shell material and basement-derived gravel from these coastal environments, across a narrow inner shelf, to the outer shelf, where the Clay Creek Limestone was deposited. Finer-grained terrigenous sediment bypassed the shelf, and was deposited at bathyal depths further offshore to the east, forming the uppermost Bells Creek Mudstone. This depositional model for the Clay Creek Limestone is discussed further in Section 6.4.4.

An acceleration of subsidence in the middle of the Kapitean reduced terrigenous sediment supply to much of the study area. The Makara Greensand began to form at bathyal depths on the downthrown side of the Mangaopari Fault and eastern limb of the proto-Mangaopari Anticline at this time, as bottom currents winnowed away terrigenous mud and left behind a lag deposit of glauconite, pebbles, and foraminifera. This interval of greensand formation was relatively brief at Paruwai, but extended into the early Opoitian in Bells Creek and Mangaopari Stream. In the western and central parts of the study area, greensand did not begin to form until early Opoitian times, when the upthrown side of the Mangaopari Fault eventually subsided to bathyal depths.

In the late Kapitean, deposition of mudstone resumed at Paruwai. The south-western corner of the study area remained at shelf depths during this time, and carbonate sediments resembling the Clay Creek Limestone were deposited on this shelf. This was the source area for the shellbeds which are interbedded in the lower Mangaopari Mudstone at Paruwai; following Hatfield (1981) and Green (1981) these alternating shellbeds and mudstones are interpreted as turbidites. Also during the latter part of the Kapitean, the shellbed in Bells Creek section A (see Figure 4.13) was deposited as a debris flow from the shelf, accounting for the abundant angular shell fragments and basement-derived pebbles in this sub-unit.

Throughout the late Kapitean and early Opoitian, the subsidence of Aorangi Island and the surrounding shelf and reefs reduced barriers to oceanic water. Increasing oceanicity in the study area at this time is recorded by the increased abundance of planktic foraminifera in successively younger Opoitian samples from both the Haurangi Hairpin and Bells Creek sections. In early Opoitian times, the study area was tilted, uplifting the far west of the area to shelf depths while the rest of the area continued to subside. The Haurangi Limestone was deposited in the far west of the study area, probably at shallower depths than the Clay Creek Limestone, as the better preservation of shell material in the Haurangi Limestone indicates a shorter transport distance. Across the central and eastern parts of the study area, the Mangaopari Mudstone was deposited as a deep-water lateral equivalent to the Haurangi Limestone. Regional subsidence continued, and by the beginning of the Late Pliocene, the Aorangi Island was mostly or entirely submerged (Beu, 1995, Trewick and Bland, 2011) (see Figure 1.3).

6.4 Discussion

6.4.1 Lateral correlations

The Sunnyside Conglomerate can be correlated with the Putangirua Conglomerate in Palliser Bay, which would have been located on the western margin of the Aorangi Island in Tongaporutuan times. Another likely correlative for the Sunnyside Conglomerate is the basal conglomerate of the Mangaoranga Formation (sm1 conglomerate of Neef, 1974) in the western

Wairarapa and Tararua districts. Both of these suggested correlatives are terrestrial, fluvial conglomerates which rest unconformably on Torlesse basement, and are conformably overlain by shallow marine sandstone and mudstone of the Hurupi and Mangaoranga Formations (e.g. Bates, 1967, Wells, 1989b, Begg and Johnston, 2000, Neef, 1974).

In the Eketahuna district, the Mangaoranga Formation is overlain by the Kaiparoro Formation (Neef, 1974) which includes the Kaiparoro Limestone Member, a Kapitean limestone of the Te Aute Lithofacies. Beu (1995) suggested that the Kaiparoro and Clay Creek Limestones may be equivalent units, which were laterally adjacent before being separated by dextral strike-slip faulting after the formation of the Wairarapa Fault zone at 2.5 Ma. Subsequent studies have shown that the Aorangi and Eketahuna districts would not have been adjacent at this time, and that strike-slip motion has not played a major role in the Neogene tectonic history of the East Coast Basin (e.g. Nicol et al., 2007). However, the similarity of facies present in these areas indicates that Eketahuna and the Aorangi Range have similar late Miocene-early Pliocene tectonic and paleoenvironmental histories. Other Te Aute Limestones of Kapitean or partly Kapitean age include the Waikopiro Limestone Member of the Mangatoro Formation, which outcrops in the Dannevirke-Ormondville area, and the Owhaoko Limestone, a cemented, pebbly unit of Tongaporutuan to Kapitean age which has been found along the Napier-Taihape Road (Beu, 1995).

The lateral extent on the Clay Creek Limestone beyond the study area is unknown. It is likely to be present adjacent to the Dry River Fault in the upper Tauanui River, west of the Haurangi Hairpin (approx. NZTopo50 coordinates BQ33/932161 to BQ33/947175). In this area, Bates (1967) described a coarse-grained, cemented limestone unconformably overlying Torlesse basement and containing abundant basement-derived pebbles, which was overlain by greensand and by a finer-grained limestone believed to be Haurangi Limestone. Fittall (1979) mapped isolated outcrops of loosely consolidated Kapitean calc-arenite between Mangaopari and Whakapuni Streams, which he assigned to the Clay Creek Limestone. An isolated outcrop of Clay Creek Limestone unconformably overlying Torlesse is present at the crest of the Harris Ridge Anticline, 4 km southeast of Martinborough (Collen and Vella, unpublished, Nicol et al., 2002), and the presence of Clay Creek Limestone has been interpreted in a seismic section between the Huangarua and Martinborough Faults (Nicol et al., 2002) (see Figure 6.3). The Clay Creek Limestone is absent at Hinakura Road (Vella and Collen, 1984) and in Palliser Bay (Bates, 1967, Vella and Briggs, 1971), where the lower Kapitean is represented by Bells Creek Mudstone.

Despite being a thin unit, the Makara Greensand is present across much of the Wairarapa, and is thought to represent a regional disconformity (Cape et al., 1990, Crundwell, 1997). In Crundwell's (1997) stratigraphic interpretation, the base of the Makara Greensand is treated as the contact between the Palliser and Onoke Groups; in sections where the greensand is absent, the contact is marked by the first appearance of Kapitean fossils. However, this study has shown the Makara Greensand to be diachronous and partly Opoitian in age; in the study area, the Makara Greensand is found stratigraphically above the Kapitean Clay Creek Limestone and laterally equivalent mudstone. As the Clay Creek Limestone is also part of the Onoke Group (Vella and Briggs, 1971, Crundwell, 1997) this creates a discrepancy. In light of these findings, it may be necessary to re-evaluate the classification of the Palliser and Onoke Groups.

6.4.2 Constraints on late Miocene-early Pliocene deformation

The findings from this study can provide some constraints for the episode of accelerated shortening identified by Cape et al. (1990) and Nicol et al. (2002, 2007) as occurring in latest Miocene or earliest Pliocene time. The partly conformable and partly unconformable relationship between the Bells Creek Mudstone and Clay Creek Limestone, described in this study, was also noted by Nicol et al. (2002), who interpreted the Clay Creek Limestone as overlying Torlesse basement and Bells Creek Mudstone with an angular unconformity on the upthrown side of the Huangarua Fault, but showed the Clay Creek Limestone conformably overlying Bells Creek Mudstone further west, on the downthrown side of the Martinborough Fault (Figure 6.3). This relationship indicates that deformation immediately preceded the deposition of the Clay Creek Limestone, and that erosion in uplifted areas coincided with near-continuous sedimentation in other areas.

Foraminiferal biostratigraphy from this study shows that the base of the Clay Creek Limestone is of early Kapitean to possibly latest Tongaporutuan age. The base of the Kapitean stage has a calibrated age of 7.2 Ma (Raine et al., 2015), so the deformational event is inferred to have occurred prior to 7.2 Ma, and deformation is constrained to the older end of the 8 Ma-6 Ma possible age range identified by Nicol et al. (2002).

In addition to movement on the Martinborough, Huangarua, and Mangaopari faults, this deformational episode caused the growth of folds throughout the Wairarapa, such as the Chester and Gladstone anticlines (Wells, 1989a, Cape et al., 1990, Nicol et al., 2002) (Figure 6.4). Deformation was associated with an erosional event which affected most of the Wairarapa, and removed up to a kilometre of sediment from the crests of anticlines (Wells, 1989a). It should be noted that Nicol et al. (2002) also correlated this shortening event with movement on the

Makara Fault; however, this study shows that the Makara Fault was associated with a separate, earlier deformational event.

A comparison between the stratigraphy described in this study and the stratigraphy described by Wells (1989b) in the Carrington area, 45 km north of the present study area, suggests that the latest Miocene deformation event, while regionally widespread, was not isochronous. At Carrington, the Mangaoranga Formation records a history of subsidence throughout the late Miocene, from Tongaporutuan fluvial conglomerate and shallow marine sandstone to bathyal mudstone of Kapitean age. The Mangaoranga Formation is unconformably overlain by Hurunui Limestone, a poorly sorted sandy limestone containing pebbles and cobbles of basement-derived, indurated sandstone and argillite, which is lower Opoitian in age (Wells, 1989b, Beu, 1995). This indicates that uplift in the Carrington area took place during Kapitean rather than latest Tongaporutuan times. It is here suggested that crustal shortening in latest Miocene time progressed from south to north, or from southeast to northwest, across the Wairarapa, although more detailed study in other areas is needed in order to confirm this.

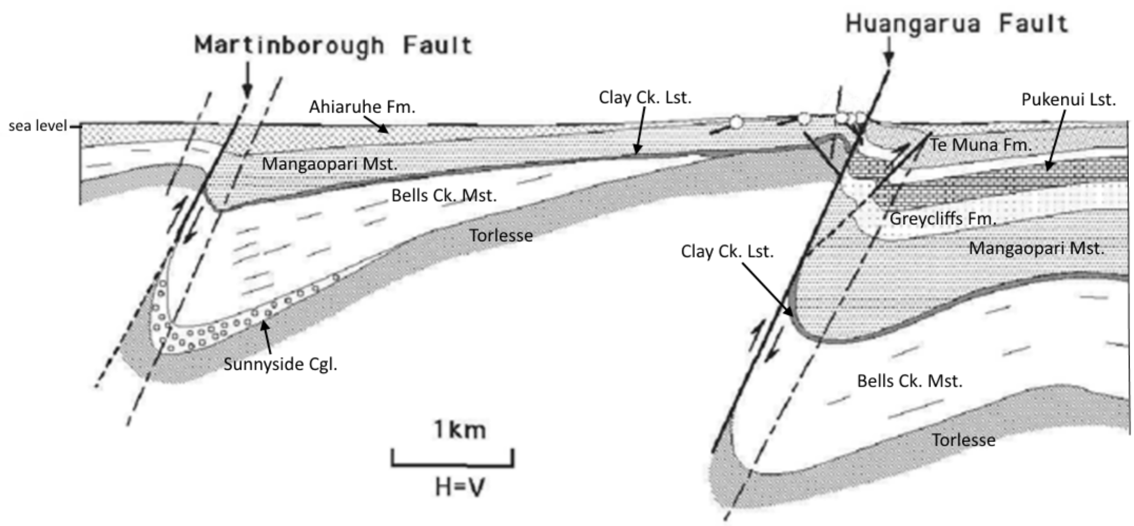

Figure 6.3: Cross-section based on seismic data interpreted by Nicol et al. (2002), showing partly conformable and partly unconformable relationship between the Bells Creek Mudstone and Clay Creek Limestone. Modified from Nicol et al. (2002).

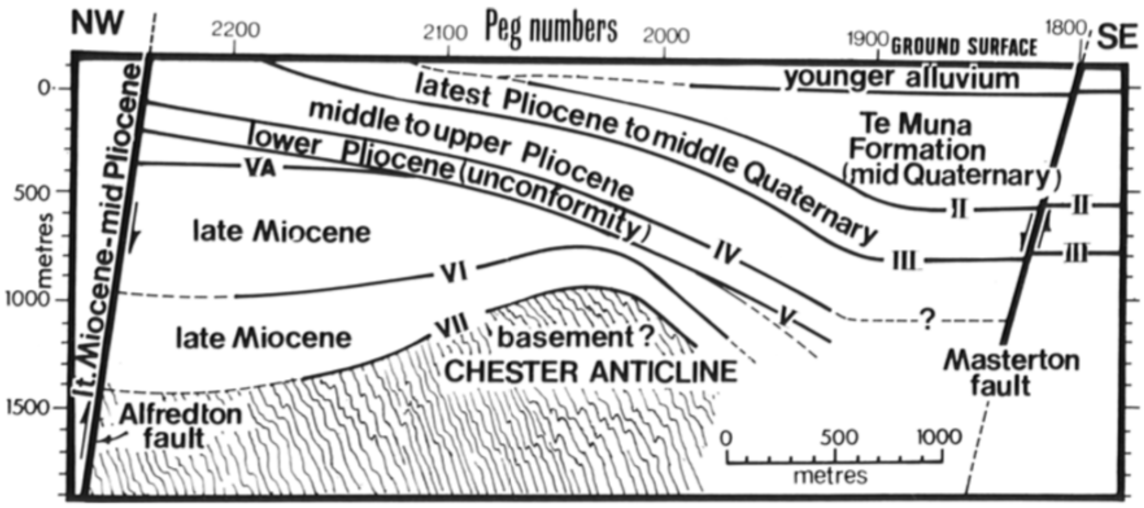

Figure 6.4: Cross-section showing the Chester Anticline, a buried fold in the western Wairarapa which was formed in late Miocene sediments during the latest Miocene episode of crustal shortening. From Cape et al. (1990).

6.4.3 Deformation after the early Opoitian

Regional subsidence in the Wairarapa continued through most of the Pliocene, but was punctuated by further episodes of crustal shortening which caused localised uplift. The presence of Waipipian Dyerville Limestone unconformably overlying Clay Creek Limestone at Saw Cut Gorge suggests that one such episode of localised uplift took place in the mid-Pliocene. This uplift event would have led to the removal of the Makara Greensand and Mangaopari Mudstone from above the Clay Creek Limestone at Saw Cut Gorge, and the deposition of shallow water limestone. The presence of a 6 m muddy greensand between the Haurangi and Dyerville Limestones in the Haurangi Hairpin section provides additional evidence for an episode of subsidence followed by uplift in late Opoitian or basal Waipipian times.

An unconformity of this age is also present at Carrington, where the Waipipian Tea Creek Limestone Member of the Carrington Formation overlies bathyal Mangatarere Mudstone of Opoitian age (Wells, 1989b). The base of the Waipipian has a calibrated age of 3.7 Ma (Raine et al., 2015), so this deformational event predates the episode of deformation identified by Vella and Collen (1998) and Nicol et al. (2002) as occurring between 3.4 and 2.4 Ma, in mid-Waipipian to Mangapanian times. It is therefore likely that two episodes of deformation and localised uplift occurred in the Wairarapa area during mid- to Late Pliocene times. The earlier episode probably occurred in the late Opoitian or earliest Waipipian (ca. 4.3-3.6 Ma), prior to the deposition of the Dyerville and Tea Creek Limestones. Further investigation will be needed in order to identify faults and folds involved in this contractional episode.

The later Pliocene deformational episode occurred after the deposition of the Spooner Tuff, which has an age of 3.44 Ma (Shane et al., 1995). This episode included movement on the

McLeod Fault and development of the McLeod Monocline (Vella and Collen, 1998), as well as renewed activity on the Mangaopari Fault and growth of the Mangaopari Anticline, creating the angular discordance between the Dyerville and Bull Creek Limestones (Nicol et al., 2002). The monocline in the Clay Creek Limestone at Paruwai (see Figure 4.4) may also have formed during this late Pliocene deformational episode.

6.4.4 A depositional model for the Clay Creek Limestone

Results from this study show that the Clay Creek Limestone has more characteristics in common with the Pliocene Te Aute limestones of Hawke's Bay than previously thought, including an extremely variable stratigraphic thickness, and the presence of possible giant cross-beds at Saw Cut Gorge. However, other characteristics of the Clay Creek Limestone, such as its high degree of cementation, micritic cement, and inferred outer shelf depositional environment, set it apart from many younger Te Aute limestones.

A conceptual model for the deposition of giant cross-bedded facies in the Te Onepu and Whakapunake Limestones of Hawke's Bay was proposed by Kamp et al. (1988), and is illustrated in Figure 6.5. In this model, the giant cross-beds are interpreted as showing the basinward migration of a series of large bodies of coarse-grained carbonate sediment, which formed submarine deltas or fans on the flanks of basement antiforms. The crests of these antiforms acted as carbonate factories, supporting an assemblage of epifaunal bivalves, barnacles, and bryozoa. Saddles in the antiform ridges acted to focus strong tidal currents, which periodically entrained sand- and gravel-sized carbonate particles and transported them to deeper water.

The giant cross-bedded facies of the Te Onepu and Whakapunake Limestones often overlies, or is contained within, limestone exhibiting smaller-scale cross-bedding, including bipolar cross-beds. These are seen as evidence that carbonate fans were deposited in relatively shallow water, where they continued to be influenced by strong, bidirectional tidal currents (Kamp et al., 1988). Smaller-scale cross-bedding of this sort has not been observed in the Clay Creek Limestone, and, throughout the study area, the Clay Creek Limestone has been found to contain benthic foraminifera which are depth index species for the outermost shelf. In order to account for these key differences, a modified version of Kamp et al.'s (1988) depositional model is proposed for the Clay Creek Limestone.

Like the Te Onepu and Whakapunake Limestones, much of the carbonate material in the Clay Creek Limestone was probably derived from exposed, tide-swept antiforms at inner to mid-shelf depths. This is supported by the abundance of *Gaudryina convexa* in the Clay Creek Limestone, as *G. convexa* is most abundant in shallow, exposed, current-swept marine environments

(Hayward et al., 2010). Material from these antiforms was entrained by tidal currents funnelled through saddles in the antiform crests, as proposed by Kamp et al (1988). However, the transport distance for carbonate sediment in the Clay Creek Limestone was greater than that for the Te Onepu and Whakapunake Limestones, and carbonate deltas and fans were deposited on the outer shelf, in lower-energy conditions than the Hawke's Bay limestones. A greater transport distance accounts for the fragmentation and general poor preservation of shell material in the Clay Creek Limestone, when compared with many younger limestones of the Te Aute Lithofacies.

Unlike the Hawke's Bay limestones, the antiforms that acted as carbonate sources for the Clay Creek Limestone were part of a network of shoals and reefs around the fringes of an uplifted island of Torlesse basement. The abundant basement-derived pebbles and cobbles in the limestone are considered to have been eroded from this island and surrounding rocky reefs, and transported by the same mechanisms as the shell material, while finer-grained terrigenous sediment was transported further offshore and deposited in a bathyal environment. Reefs and shoals would also have sheltered parts of the island's coast from powerful waves and currents. These sheltered bays on the margins of the Aorangi Island provided a secondary source of carbonate material, and are considered to be the source for the brachiopods, juvenile oysters, and bryoliths that are present in the Clay Creek Limestone. Shell material from these calmer-water environments would have been transported to the outer shelf in storm events.

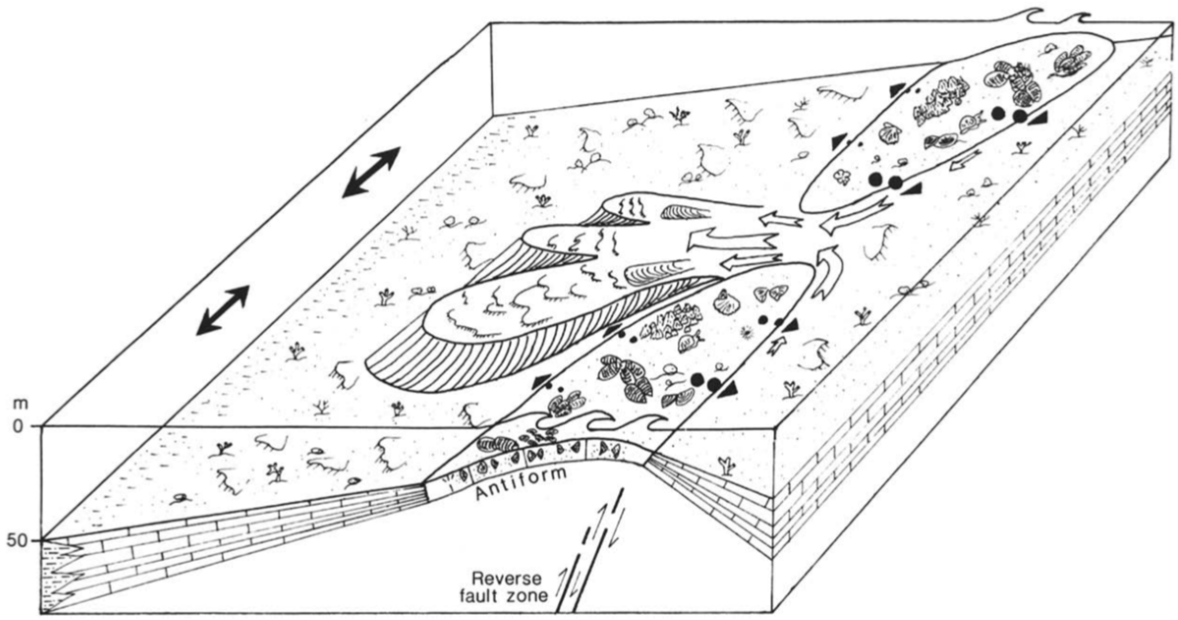

Figure 6.5: Conceptual model for the deposition of giant cross-beds in the Te Onepu and Whakapunake Limestones of Hawke's Bay. Black arrows show the direction of tidal currents in the seaway, while open arrows show tidal flow through saddles and channels in antiform crests. From Kamp et al. (1988).

The Clay Creek Limestone is interpreted as having been deposited at water depths of between 150 and 250 m. Coarse-grained skeletal carbonate platform deposits have been observed at depths of up to 250 m around New Zealand in the present day (Nelson et al., 1988). The Clay Creek Limestone in the Te Ahitaitai section, which is finer-grained than at other locations visited in this study, may represent a transitional facies between the coarse-grained, pebbly limestone found at localities to the west, and laterally equivalent finer-grained, deeper-water mudstone to the east. Rapid lateral and down-dip transitions from coarse-grained limestone to fine-grained terrigenous sediment are commonly observed in Te Aute Lithofacies limestones (Kamp et al., 1988, Beu, 1995, Nelson et al., 2003), and similarly rapid transitions from carbonate to terrigenous sediment are frequently observed in modern shelf carbonates around New Zealand (Nelson et al., 1988, Beu, 1995).

Chapter 7 Conclusions

7.1 Summary of work

This project set out to reconstruct late Miocene-early Pliocene geological history in the northern Aorangi Range, and to place this in the wider context of the Neogene evolution of the southern Hikurangi Margin. In order to achieve this aim, sections were measured at four key localities, and detailed field mapping was carried out around Te Ahitaitai Ridge. Grain size and paleontological data, including macrofossils, foraminifera, and pollen, were used to interpret depositional environments for samples collected in the field. Foraminiferal biostratigraphy was used to constrain the age of samples. Data from this study were combined with previous authors' work to produce a synthesis map and geological cross-sections for the Makara and Ruakokoputuna Valleys. An interpretation of late Miocene-early Pliocene stratigraphy and geological history has been presented, the timing and style of latest Miocene deformation have been constrained, and episodes of tectonic activity have been correlated with those previously recognised in other studies.

7.2 Key findings

The key findings of this study can be summarised as follows:

- The late Miocene-early Pliocene succession in the study area records a history of subsidence on the margins of an island of uplifted basement rock, showing a progression from terrestrial to increasingly deep marine environments. Regional subsidence was punctuated by episodes of crustal shortening which led to localised uplift and erosion in parts of the study area.
- Two deformational episodes are identified in the late Miocene. The first, in the early Tongaporutuan, is associated with movement on the Makara Fault. A second episode of uplift is correlated with a regional deformation event which led to the growth of contractional structures across the Wairarapa region (Wells, 1989a, Cape et al., 1990, Nicol et al., 2002).
- Despite their contrasting lithologies, the Clay Creek Limestone and Bells Creek Mudstone are partially laterally equivalent, and the overlying Makara Greensand is a diachronous unit which ranges in age from Kapitean to early Opoitian.
- The partly conformable and partly unconformable relationship between the Clay Creek Limestone and Bells Creek Mudstone indicates that deformation took place immediately prior to the deposition of the Clay Creek Limestone at the beginning of the Kapitean

stage. Deformation in the study area is therefore inferred to have taken place before 7.2 Ma.

- Major differences in stratigraphy have been identified between the upthrown and downthrown sides of the Mangaopari Fault, which confirm that this fault was active during the latest Miocene deformational episode.
- Carbonate content and basement-derived pebbles in the Clay Creek Limestone were transported from high-energy coastal environments and deposited on the outer shelf. A depositional model modified after Kamp et al. (1988) is proposed to explain the presence of giant cross-beds in the Clay Creek Limestone.
- Lateral correlations can be made between the stratigraphy of this study area and other locations with similar Neogene tectonic and paleoenvironmental histories in the Wairarapa and broader East Coast Basin.

7.3 Suggestions for further study

This study has highlighted several possible avenues for future work towards reconstructing the Neogene history of the East Coast Basin. These include:

- Constraining the ages of the Makara Greensand, Bells Creek Mudstone, and Mangaopari Mudstone at other localities in the Wairarapa, and re-evaluating the classification of the Palliser and Onoke Groups, as results from this study have raised significant questions regarding the current classification of these units.
- Searching for evidence of latest Miocene deformation in other parts of the Wairarapa and wider East Coast Basin; constraining the age of deformation in different areas; and determining whether deformation progressed from south to north, as proposed here.
- Determining whether the mid-Pliocene deformational episode identified in this study, associated with the Dyerville Limestone, can be correlated in other locationss, and whether it represents a localised or basin-wide event.
- Determining the extent to which the depositional model proposed here for the Clay Creek Limestone can be applied to other limestones of the Te Aute Lithofacies, especially to pebbly limestones such as the Owhaoko and Hururua Limestones, and to cemented limestones with a significant mud component, such as the Haurangi and Bull Creek Limestones.

References

ABBAS, S. H. 1971. *Some aspects of the sedimentology of Pliocene and Miocene rocks north of Aorangi Range, Wairarapa.* Unpublished MSc thesis, Victoria University of Wellington.

ANDERSON, J. M. 1976. *A Diagenetic and Environmental Interpretation of a Limestone Sequence at Haurangi Hairpin, Northern Aorangi Range, Southern Wairarapa.* Unpublished BSc (Honours) thesis, Victoria University of Wellington.

ANDREWS, P. B. 1982. Revised guide to recording field observations in sedimentary sequences. *New Zealand Geological Survey Report.* Lower Hutt: Department of Scientific and Industrial Research.

BATES, T. E. 1967. *The Geology of the Northern Aorangi Range and part of Palliser Bay, Sheet N165.* Unpublished MSc thesis, Victoria University of Wellington.

BEANLAND, S., MELHUISH, A., NICOL, A. & RAVENS, J. 1998. Structure and deformational history of the inner forearc region, Hikurangi subduction margin, New Zealand. *New Zealand Journal of Geology and Geophysics,* 41**,** 325-342.

BEGG, J. G. & JOHNSTON, M. R. 2000. *Geology of the Wellington Area: Scale 1: 250 000,* Lower Hutt: Institute of Geological & Nuclear Sciences.

BEU, A. G. 1995. *Pliocene Limestones and their Scallops: Lithostratigraphy, Pectinid Biostratigraphy and Paleogeography of Eastern North Island Late Neogene Limestone,* Lower Hutt, Institute of Geological and Nuclear Sciences.

BEU, A. G. & EDWARDS, A. R. 1984. New Zealand Pleistocene and late Pliocene glacio-eustatic cycles. *Palaeogeography, Palaeoclimatology, Palaeoecology,* 46**,** 119-142.

BEU, A. G. & MAXWELL, P. A. 1990. *Cenozoic Mollusca of New Zealand*, Lower Hutt: New Zealand Geological Survey, DSIR.

CAPE, C. D., LAMB, S. H., VELLA, P., WELLS, P. E. & WOODWARD, D. J. 1990. Geological structure of Wairarapa Valley, New Zealand, from seismic reflection profiling. *Journal of the Royal Society of New Zealand,* 20**,** 85-105.

CLARK, D. 1998. *A biostratigraphic investigation of the Pukenui Limestone formation, South Wairarapa, New Zealand.* Unpublished MSc thesis, Victoria University of Wellington.

COLE, J. W. & LEWIS, K. B. 1981. Evolution of the Taupo-Hikurangi subduction system. *Tectonophysics,* 72**,** 1-21.

COLLEN, J. & VELLA, P. unpublished. Geological map of New Zealand 1:50,000 Sheet S27, Martinborough.

COOPER, R. A. (ed.) 2004. *The New Zealand Geological Timescale,* Lower Hutt: Institute of Geological and Nuclear Sciences.

COUPER, R. A. 1948. *The Geology of the Makara and Ruakokopatuna Valleys, East Wairarapa.* Unpublished MSc thesis, Victoria University of Wellington.

CRUNDWELL, M. P. 1979. *The Occurrence of Glauconite in Late Miocene to Early Pliocene Sediments of the Northern Aorangi Range, Wairarapa.* Unpublished BSc (Honours) thesis, Victoria University of Wellington.

CRUNDWELL, M. P. 1987. *Neogene Stratigraphy and Geological History of the Wainuioru Valley, Eastern Wairarapa, New Zealand.* Unpublished MSc thesis, Victoria University of Wellington.

CRUNDWELL, M. P. 1997. Neogene lithostratigraphy of southern Wairarapa. *Institute of Geological & Nuclear Sciences Science Report 97/36*. Lower Hutt: Institute of Geological & Nuclear Sciences.

CRUNDWELL, M. P. & NELSON, C. S. 2007. A magnetostratigraphically-constrained chronology for late Miocene bolboformids and planktic foraminifers in the temperate Southwest Pacific. *Stratigraphy 4 (1)***,** 1-34.

DEVEREUX, I., HENDY, C. H. & VELLA, P. 1970. Pliocene and early pleistocene sea temperature fluctuations, Mangaopari Stream, New Zealand. *Earth and Planetary Science Letters,* 8**,** 163-168.

DOBBIE, W. A. 1976. *A Study of the Clay Creek Limestone, Makara Greensand, and Lower Haurangi Limestone Formations of the Northern Aorangi Range, Wairarapa.* Unpublished BSc (Honours) thesis, Victoria University of Wellington.

DUNBAR, G. B. & BARRETT, P. J. 2005. Estimating palaeobathymetry of wave-graded continental shelves from sediment texture. *Sedimentology,* 52**,** 253-269.

EGGO, A. J. 1979. *Biostratigraphic Zonation within Late Cenozoic Mudstone, Mangaopari Stream, Wairarapa.* Unpublished BSc (Honours) thesis, Victoria University of Wellington.

FIELD, B. D., URUSKI, C. & OTHERS 1997. *Cretaceous-Cenozoic geology and petroleum systems of the East Coast region, New Zealand*, Lower Hutt: Institute of Geological & Nuclear Sciences.

FINLAY, H. J. & MARWICK, J. The division of the Upper Cretaceous and Tertiary in New Zealand. 1940. Royal Society of New Zealand.

FINLAY, H. J. & MARWICK, J. 1947. New divisions of the New Zealand upper Cretaceous and Tertiary. *New Zealand Journal of Science and Technology B,* 28, 228-236.

FITTALL, M. E. 1979. *The Geology of an Area North of Mangaopari Stream, South-east Wairarapa.* Unpublished BSc (Honours) thesis, Victoria University of Wellington.

GAMMON, P. R. 1997. *Sequence stratigraphy of the Mangaopari Basin, southeastern North Island, New Zealand.* Unpublished PhD thesis, James Cook University.

GREEN, D. R. 1981. *The Stratigraphy, Structure, and Geological History of Late Tertiary Strata, Makara River, S. E. Wairarapa.* Unpublished BSc (Honours) thesis, Victoria University of Wellington.

HATFIELD, D. I. 1981. *The Geology of Upper Makara Valley, S. E. Wairarapa.* Unpublished BSc (Honours) thesis, Victoria University of Wellington.

HAYWARD, B. W., CEDHAGEN, T., KAMINSKI, M. & GROSS, O. 2015. World Foraminifera Database.

HAYWARD, B. W., GRENFELL, H., SABAA, A., NEIL, H. & BUZAS, M. 2010. *Recent New Zealand deep-water benthic foraminifera: taxonomy, ecologic distribution, biogeography, and use in paleoenvironmental assessment,* Lower Hutt, GNS Science.

HAYWARD, B. W., HOLLIS, C. J. & GRENELL, H. 1994. Foraminiferal associations in Port Pegasus.Stewart Island, New Zealand. *New Zealand Journal of Marine and Freshwater Research,* 28**,** 69-95.

HAYWARD, B. W., MILDENHALL, D. & WILSON, G. 1986. *Biostratigraphy of Te Kiri-1 onshore well, west Taranaki*, Paleontology Group, New Zealand Geological Survey, Department of Scientific and Industrial Research.

HENRY, A. A. 1996. *Upper Cenozoic Sedimentary Sequence from Birch Hill in South-eastern Wairarapa.* Unpublished BSc (Honours) thesis, Victoria University of Wellington.

HORNIBROOK, N. D. B., BRAZIER, R. C. & STRONG, C. P. 1989. *Manual of New Zealand Permian to Pleistocene foraminiferal biostratigraphy*.

KAMP, P. J. J., HARMSEN, F. J., NELSON, C. S. & BOYLE, S. F. 1988. Barnacle-dominated limestone with giant cross-beds in a non-tropical, tide-swept, Pliocene forearc seaway, Hawke's Bay, New Zealand. *Sedimentary geology,* 60**,** 173-195.

KENNETT, J. P. & SRINIVASAN, M. S. 1983. *Neogene planktonic foraminifera: a phylogenetic atlas*, Hutchinson Ross.

KENNETT, J. P., WATKINS, N. D. & VELLA, P. 1971. Paleomagnetic Chronology of Pliocene-Early Pleistocene Climates and the Plio-Pleistocene Boundary in New Zealand. *Science,* 171**,** 276-279.

KING, L. C. Tertiary molluscan faunas from the southern Wairarapa. Transactions of the New Zealand Institute, 1933. 334-354.

LAMB, S. H. & VELLA, P. 1987. The last million years of deformation in part of the New Zealand plate-boundary zone. *Journal of Structural Geology,* 9**,** 877-891.

MCKAY, A. 1878. Report on east Wairarapa district. *New Zealand Geological Survey report of geological explorations during 1877-1878,* 11**,** 14-24.

MCLEAN, D. B. G. 1953. *The Geology of the Haurangi-Stoney Creek Area, South-East Wairarapa.* Unpublished MSc thesis, Victoria Univesity of Wellington.

MILLER, K. G., KOMINZ, M. A., BROWNING, J. V., WRIGHT, J. D., MOUNTAIN, G. S., KATZ, M. E., SUGARMAN, P. J., CRAMER, B. S., CHRISTIE-BLICK, N. & PEKAR, S. F. 2005. The Phanerozoic record of global sea-level change. *science,* 310**,** 1293-1298.

MOORE, P. & SPEDEN, I. G. 1984. *The Early Cretaceous (Albian) sequence of eastern Wairarapa, New Zealand*, Published for New Zealand Geological Survey by Science Information Pub. Centre.

NEEF, G. 1974. *Sheet N153, Eketahuna*. Geological map of New Zealand 1:63,360. DSIR, Wellington.

NELSON, C. S., KEANE, S. L. & HEAD, P. S. 1988. Non-tropical carbonate deposits on the modern New Zealand shelf. *Sedimentary geology,* 60**,** 71-94.

NELSON, C. S., WINEFIELD, P. R., HOOD, S. D., CARON, V., PALLENTIN, A. & KAMP, P. J. J. 2003. Pliocene Te Aute limestones, New Zealand: Expanding concepts for cool-water shelf carbonates. *New Zealand Journal of Geology and Geophysics,* 46**,** 407-424.

NICOL, A., MAZENGARB, C., CHANIER, F., RAIT, G., URUSKI, C. & WALLACE, L. 2007. Tectonic evolution of the active Hikurangi subduction margin, New Zealand, since the Oligocene. *Tectonics,* 26**,** TC4002.

NICOL, A., VANDISSEN, R., VELLA, P., ALLOWAY, B. & MELHUISH, A. 2002. Growth of contractional structures during the last 10 my at the southern end of the emergent Hikurangi forearc basin, New Zealand. *New Zealand Journal of Geology and Geophysics,* 45**,** 365-385.

RAINE, J. I., BEU, A. G., BOYES, A. F., CAMPBELL, H. J., COOPER, R. A., CRAMPTON, J. S., CRUNDWELL, M. P., HOLLIS, C. J. & MORGANS, H. E. G. 2015. Revised calibration of the New Zealand Geological Timescale: NZGT2015/1. *GNS Science Report.* GNS Science.

RODLEY, D. R. 1961. *The geology and paleoecology of Nukumaruan strata near the junction of Ruakokopatuna and Makara Rivers.* Unpublished MSc thesis, Victoria University of Wellington.

SHANE, P., FROGGATT, P., BLACK, T. & WESTGATE, J. 1995. Chronology of Pliocene and Quaternary bioevents and climatic events from fission-track ages on tephra beds, Wairarapa, New Zealand. *Earth and Planetary Science Letters,* 130**,** 141-154.

TREWICK, S. A. & BLAND, K. J. 2011. Fire and slice: palaeogeography for biogeography at New Zealand's North Island/South Island juncture. *Journal of the Royal Society of New Zealand,* 42**,** 153-183.

VELLA, P. Tertiary Mollusca from south-east Wairarapa. Transactions of the Royal Society of New Zealand, 1954. 539-555.

VELLA, P. & BRIGGS, W. 1971. Lithostratigraphic names, upper Miocene to lower Pleistocene, northern Aorangi range, Wairarapa. *New Zealand journal of geology and geophysics,* 14**,** 253-274.

VELLA, P. & COLLEN, J. D. 1984. Four rhyolitic tuff marker beds, lower Pliocene, Wairarapa, New Zealand. *Journal of the Royal Society of New Zealand,* 14**,** 133-138.

VELLA, P. & COLLEN, J. D. 1998. McLeod Fault: associated monocline and Pliocene angular unconformity, Point Range and Mangaopari Stream, Wairarapa, New Zealand. *Journal of the Royal Society of New Zealand,* 28**,** 157-164.

WAGHORN, R. J. The geology of the Ruakokopatuna Valley, southern Wairarapa. 1926.

WELLS, P. E. 1989a. Burial history of Late Neogene sedimentary basins on part of the New Zealand convergent plate margin. *Basin Research,* 2**,** 145-160.

WELLS, P. E. 1989b. Late Neogene stratigraphy of the Carrington area, western Wairarapa, North Island, New Zealand. *Journal of the Royal Society of New Zealand,* 19**,** 283-303.

Appendix 1: Table of samples

VUW locality number	Sample number	Location	Coordinates	Stratigraphic unit	Date collected
100903	HH1	Haurangi Hairpin, 20 cm above base of Clay Creek Limestone	BQ33/001178	Clay Creek Limestone	Feb-14
100907	HH2	Haurangi Hairpin, middle of glauconitic mudstone	BQ33/001178	Makara Greensand	Feb-14
100908	HH3	Haurangi Hairpin, middle of lower shelly greensand	BQ33/001178	Makara Greensand	Feb-14
100913	07A	Te Ahitaitai Ridge, bank next to farm track	BQ34/064208	Makara Greensand	Feb-14
100914	TA1	Gully on eastern side of Te Ahitaitai Ridge, 2 m above conglomerate outcrops	BQ34/066207	Sunnyside Conglomerate	Feb-14
100915	TA2	Gully on eastern side of Te Ahitaitai Ridge, 3 m below limestone outcrops	BQ34/066207	Sunnyside Conglomerate	Feb-14
100916	18A	True right of upper limestone gorge, Makara River, 5 cm below base of limestone	BQ34/052178	Bells Creek Mudstone	Feb-14
100917	19A	Homestead Creek, 10 m downstream from cave, 10 cm below base of limestone	BQ34/057217	Bells Creek Mudstone	Feb-14
100918	23A	Homestead Creek, 5 m upsteram from 19A	BQ34/057217	Clay Creek Limestone	May-14
100919	24A	Homestead Creek cave, limestone-basement contact	BQ34/057217	Clay Creek Limestone	May-14
100920	25A	Western side of Te Ahitaitai Ridge, 200 m north of Homestead Creek	BQ34/059216	Clay Creek Limestone	May-14
100921	BC1	Bells Creek near White Rock Road, 60 cm below base of greensand	BQ34/073218	Bells Creek Mudstone	Nov-14
100922	BC2	Bells Creek near White Rock Road, shellbed 80 cm above base of greensand	BQ34/073218	Makara Greensand	Nov-14
100923	BC3	Bells Creek near White Rock Road, 3 m above shellbed	BQ34/073218	Makara Greensand	Nov-14
100924	BC4	Bells Creek near White Rock Road, 40 cm below top of greensand	BQ34/073218	Makara Greensand	Nov-14
100925	BC5	Bells Creek near White Rock Road, base of mudstone overlying greensand	BQ34/073218	Mangaopari Mudstone	Nov-14
100926	28A	Trributary on true left of Bells Creek, 20 cm siltstone interbed in conglomerate	BQ34/071217	Sunnyside Conglomerate	Nov-14
100927	TA3	Gully on eastern side of Te Ahitaitai Ridge, 30 cm below limestone	BQ34/066207	Sunnyside Conglomerate	Nov-14
100928	TA5	Gully on eastern side of Te Ahitaitai Ridge, 10 cm above top of limestone	BQ34/066207	Mangaopari Mudstone	Nov-14
100929	TA4	Gully on eastern side of Te Ahitaitai Ridge, 1 mabove base of limestone	BQ34/066207	Clay Creek Limestone	Nov-14
100931	CC1	QEII creek, Greycliffs station, 6.8 m above base of limestone	BQ33/026195	Clay Creek Limestone	Nov-14
100932	CC2	QEII creek, Greycliffs station, 8.3 m above base of limstone	BQ33/026195	Clay Creek Limestone	Nov-14
100933	CC3	QEII creek, Greycliffs station, 9.8 m above base of limestone	BQ33/026195	Clay Creek Limestone	Nov-14
100934	CC4	QEII creek, Greycliffs station, 11.2 m above base of limestone	BQ33/026195	Clay Creek Limestone	Nov-14
100935	CC5	QEII creek, Greycliffs station, 12.7 m above base of limestone	BQ33/026195	Clay Creek Limestone	Nov-14
100936	CC6	QEII creek, Greycliffs station, 10 m above top of limestone	BQ33/026195	Mangaopari Mudstone	Nov-14
100939	35A	Saw Cut Gorge, 2 m above base of upper limestone	BQ34/054190	?Dyerville Limestone	Feb-15
100940	35B	Saw Cut Gorge, 2 m below base of upper limestone	BQ34/054190	Clay Creek Limestone	Feb-15
100946	TA6	Gully on eastern side of Te Ahitaitai Ridge, 1 m above top of limestone	BQ34/066207	Bridge Sandstone Member	Feb-15
100947	TA7	Gully on eastern side of Te Ahitaitai Ridge, 3 m above top of limestone	BQ34/066207	Bridge Sandstone Member	Feb-15

Appendix 2: Grain size data

Per cent frequency table

Sample	-2 ϕ	-1.5 ϕ	-1 ϕ	-0.5 ϕ	0 ϕ	0.5 ϕ	1 ϕ	1.5 ϕ	2 ϕ	2.5 ϕ	3 ϕ	3.5 ϕ	4 ϕ	4.5 ϕ	5 ϕ	5.5 ϕ	6 ϕ	6.5 ϕ	7 ϕ	7.5 ϕ	8 ϕ	8.5 ϕ	9 ϕ	9.5 ϕ	10 ϕ	Rest
CC6	0.00	0.00	0.00	0.00	0.00	0.00	0.00	0.00	0.02	0.00	0.04	0.13	0.76	2.06	3.21	4.11	5.09	5.78	6.36	7.15	7.54	7.05	5.68	4.89	4.11	36.12
TA1	0.00	0.00	0.43	0.48	0.86	1.69	2.73	3.76	7.04	12.09	16.96	8.66	5.40	2.52	2.03	2.75	2.91	2.61	2.42	2.42	2.38	2.38	2.09	1.71	1.75	12.00
TA2	0.00	0.00	0.04	0.00	0.04	0.06	0.12	0.19	0.76	6.05	19.01	11.61	12.28	5.35	4.74	4.46	3.62	3.18	2.87	2.30	2.25	2.43	1.85	1.81	1.94	13.02
TA3	11.68	4.33	3.94	4.40	3.42	3.44	2.71	1.65	1.50	1.64	3.63	8.01	4.33	1.07	1.53	1.56	1.38	1.65	1.61	1.83	1.74	1.87	1.92	1.78	1.74	25.64
TA5	0.00	0.00	0.00	0.00	0.05	0.07	0.07	0.07	0.05	0.09	0.16	0.38	1.95	1.78	3.57	4.25	5.12	6.08	6.28	6.66	7.05	6.57	5.02	4.54	4.54	35.63
TA6	0.00	0.00	0.00	0.27	0.31	0.38	0.44	0.47	0.45	0.44	0.67	5.70	17.99	13.32	10.66	10.87	6.30	3.63	2.42	2.10	2.10	1.65	1.46	1.65	1.46	15.20
TA7	0.00	0.00	0.00	0.00	0.02	0.08	0.08	0.11	0.20	0.99	25.08	26.92	11.48	2.96	2.20	2.55	2.32	2.03	1.77	1.80	1.93	1.83	1.50	1.31	1.18	11.65
07A	0.00	0.00	0.00	0.00	0.00	0.00	0.00	0.08	0.15	0.13	0.15	0.25	0.87	0.58	0.88	2.44	3.52	4.10	5.27	5.57	6.06	6.74	5.96	5.37	5.57	46.30
BC1	0.00	0.00	0.00	0.00	0.03	0.08	0.11	0.13	0.17	0.16	0.25	0.77	2.99	3.10	4.12	5.06	5.53	5.90	6.28	6.00	6.09	5.53	5.44	3.94	4.31	34.21
BC5	0.00	0.00	0.00	0.00	0.02	0.03	0.07	0.18	0.25	0.18	0.13	0.13	0.15	0.03	0.69	2.47	3.56	4.65	4.05	5.04	6.72	7.02	6.72	5.73	6.03	46.16
19A	0.00	0.00	0.00	0.09	0.09	0.07	0.13	0.15	0.20	0.31	0.54	2.20	5.50	6.94	4.58	5.27	5.34	5.34	5.34	5.50	5.90	5.66	4.85	4.13	3.88	28.07
18A	0.00	0.00	0.00	0.09	0.07	0.11	0.22	0.29	0.44	0.51	1.04	3.00	4.95	4.20	2.16	1.75	2.41	2.49	3.16	3.99	5.57	6.65	6.56	6.15	5.98	38.22

Summary statistics

Sample	Percentiles								Graphic				Moment			
	1	5	16	25	50	75	84	95	Mean	SD	Skew	Kurt	Mean	SD	Skew	Kurt
CC6	4.01	4.81	6.05	6.80	8.56	10.63	11.14	11.76	8.58	2.33	-0.03	0.74	9.11	2.83	0.01	1.59
TA1	-0.45	0.78	1.93	2.33	3.23	6.93	8.85	11.53	4.67	3.36	0.58	0.96	4.81	3.64	0.99	2.85
TA2	1.87	2.31	2.73	2.97	3.99	7.14	9.23	11.80	5.32	3.06	0.63	0.93	5.49	3.31	1.10	2.94
TA3	-2.46	-2.29	-1.50	-0.40	3.48	10.14	12.14	14.57	4.70	5.96	0.29	0.66	4.83	5.50	0.24	1.57
TA5	3.51	4.54	5.84	6.60	8.48	10.67	11.23	11.92	8.52	2.46	-0.02	0.74	8.99	2.95	-0.06	1.76
TA6	0.54	3.14	3.69	3.94	4.95	7.17	9.75	12.91	6.13	3.00	0.61	1.24	6.08	3.15	1.06	3.06
TA7	2.26	2.57	2.79	2.97	3.44	6.01	8.41	12.06	4.88	2.84	0.79	1.28	5.02	3.20	1.46	3.75
07A	3.63	5.39	6.77	7.58	9.67	10.96	11.36	11.86	9.27	2.13	-0.29	0.79	9.84	2.73	-0.42	1.92
BC1	3.05	4.05	5.40	6.21	8.29	10.62	11.24	11.99	8.31	2.66	-0.03	0.74	8.74	3.09	-0.03	1.73
BC5	3.56	5.59	6.93	7.75	9.68	10.85	11.21	11.65	9.27	1.99	-0.32	0.80	9.90	2.67	-0.47	2.15
19A	2.44	3.61	4.48	5.40	7.70	10.23	10.91	11.75	7.70	2.84	0.00	0.69	8.11	3.23	0.13	1.80
18A	1.75	3.37	4.75	6.70	9.03	10.61	11.02	11.52	8.27	2.80	-0.38	0.86	8.99	3.31	-0.43	2.04

Grain size histograms

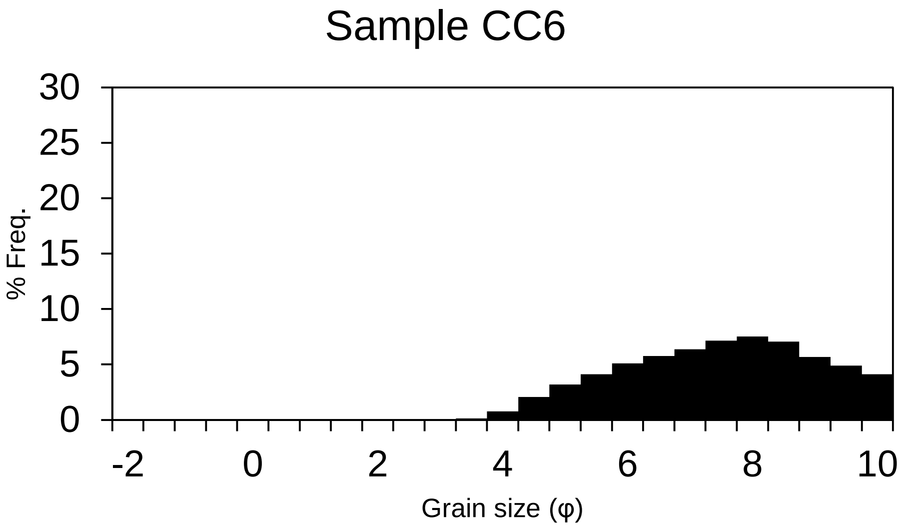

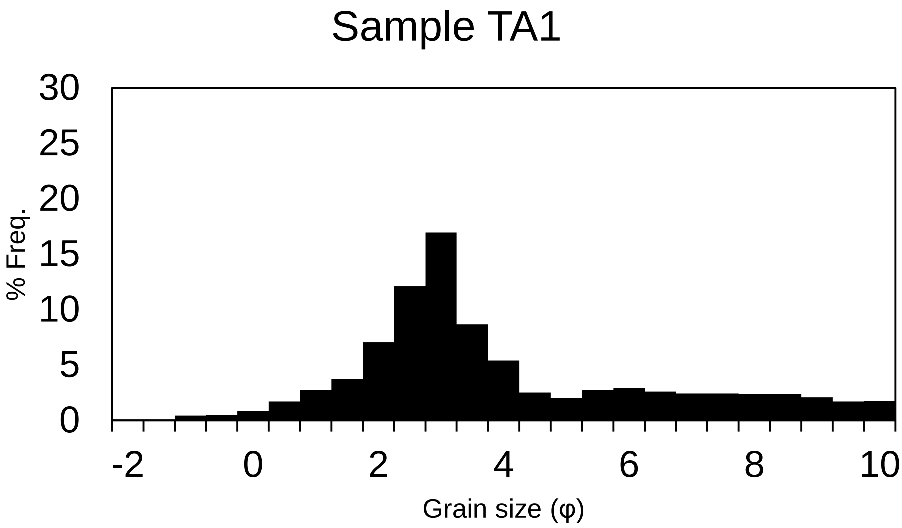

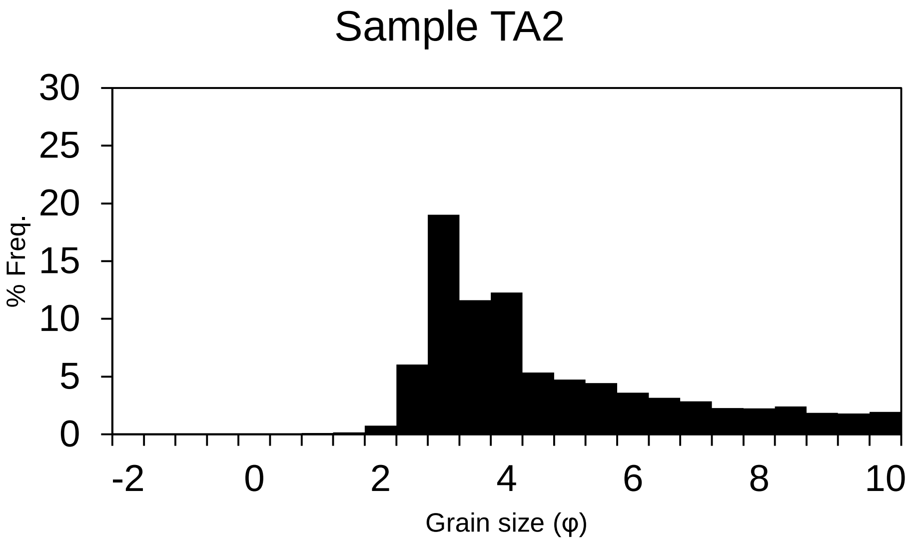

Sample TA3

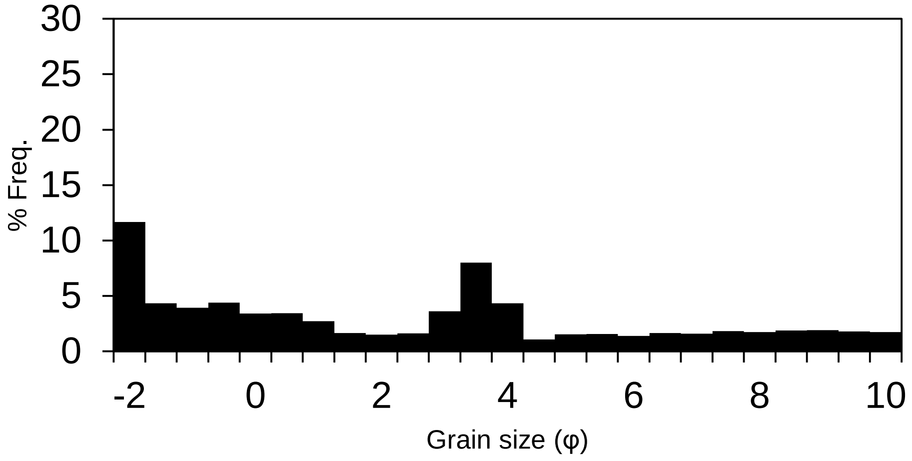

Sample TA5

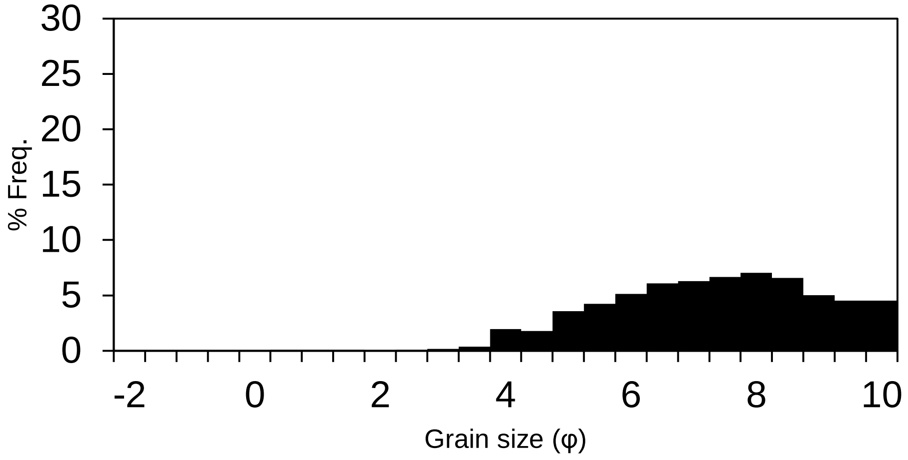

Sample TA6

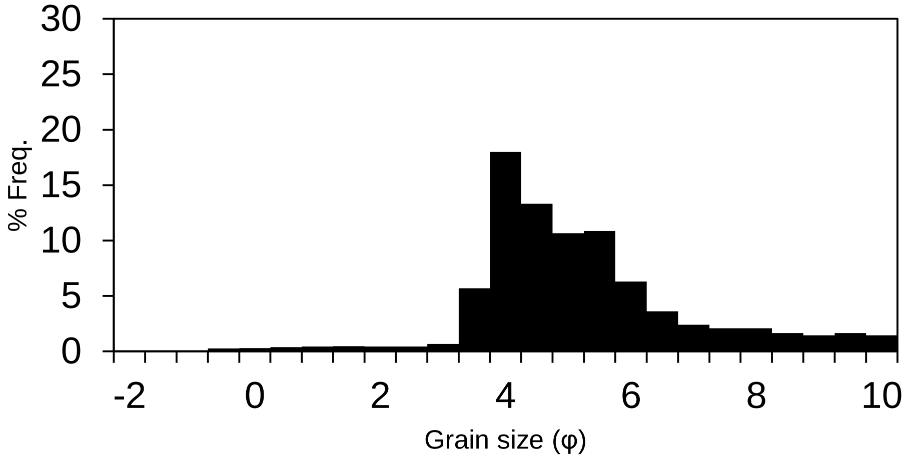

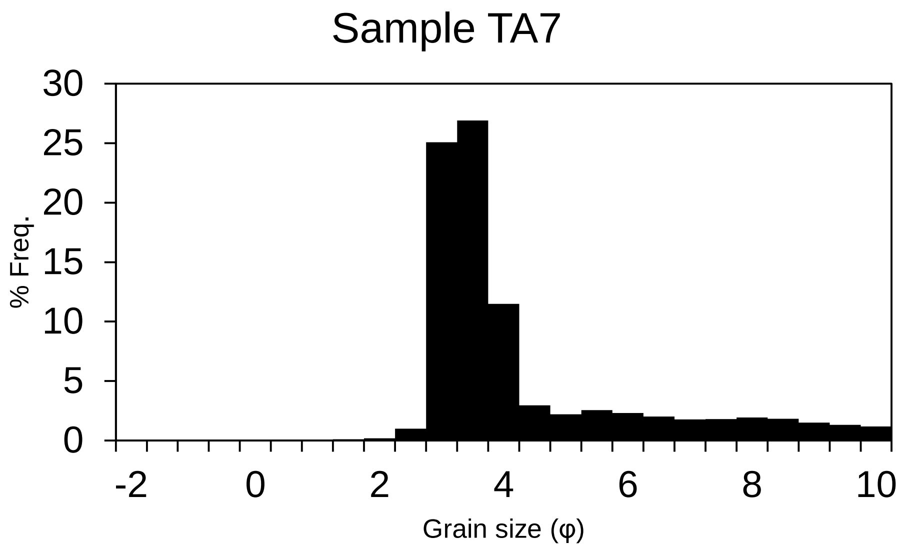
Sample TA7
30
25
20
15
10
5
0
% Freq.
-2
0
2
4
6
8
10
Grain size (φ)

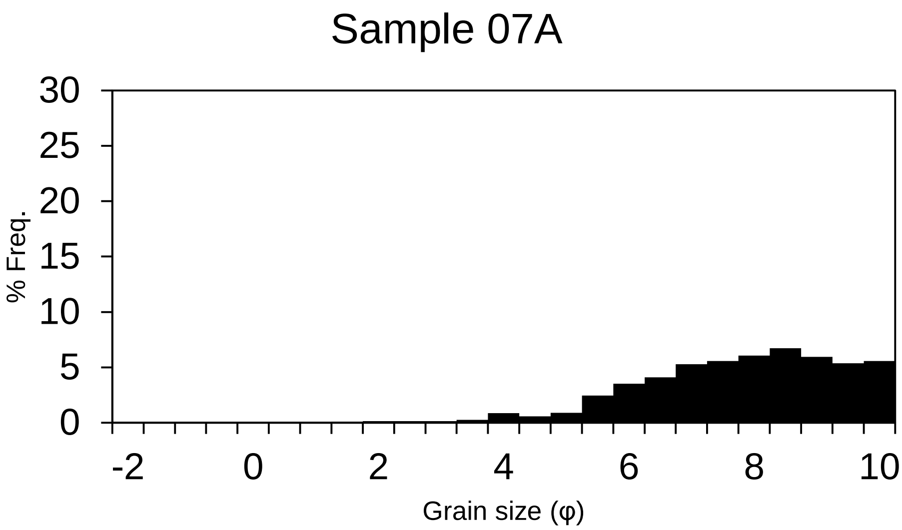
Sample 07A
30
25
20
15
10
5
0
% Freq.
-2
0
2
4
6
8
10
Grain size (φ)

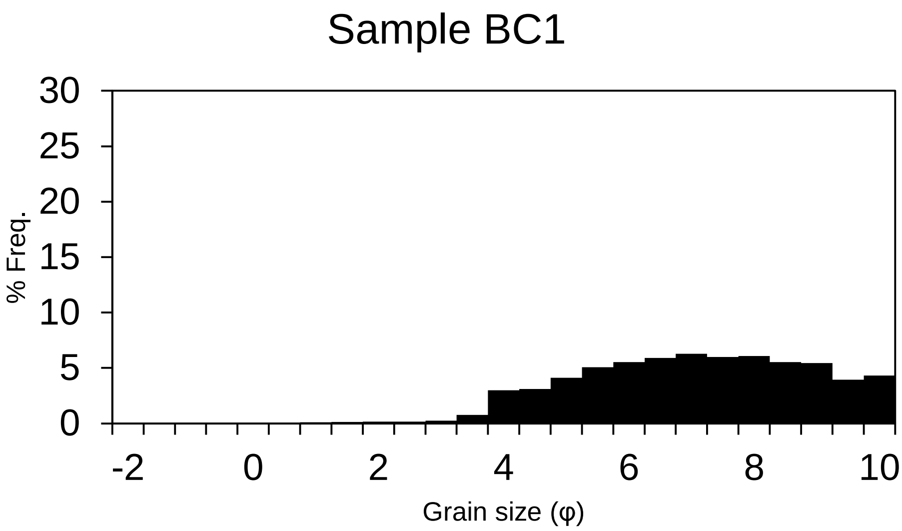
Sample BC1
30
25
20
15
10
5
0
% Freq.
-2
0
2
4
6
8
10
Grain size (φ)

Sample BC5

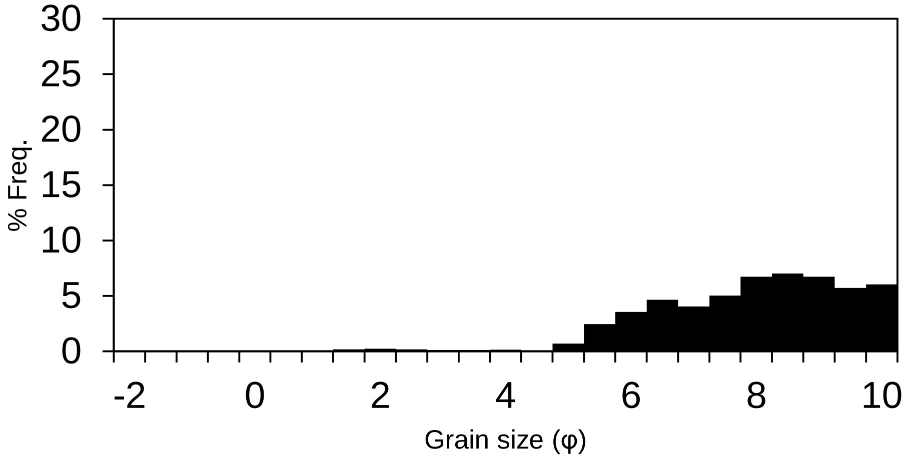

Sample 19A

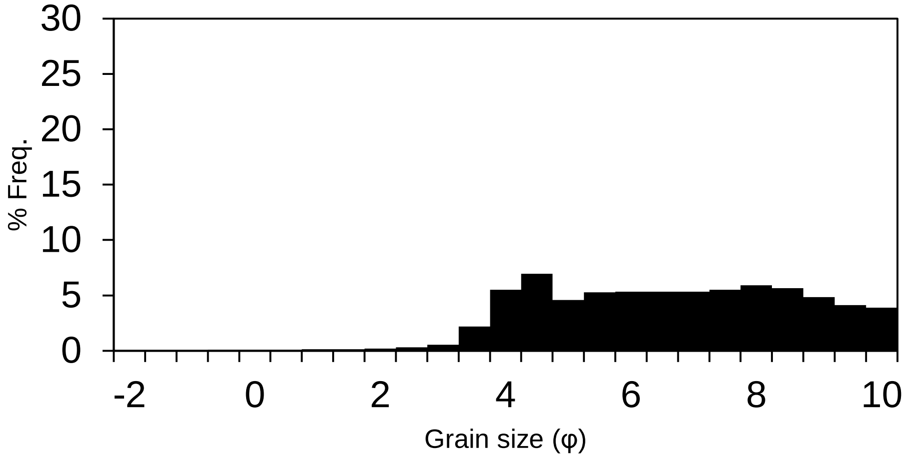

Sample 18A

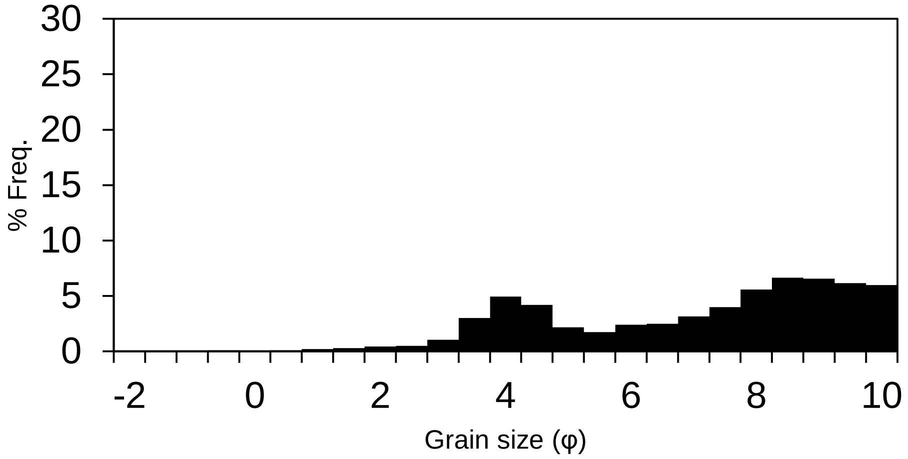

Appendix 3: New Zealand Geological Timescale

Stages for the Cenozoic Era, from Raine et al. (2015)

NEW ZEALAND GEOLOGICAL TIMESCALE 2015/1

NZ Series or International unit	Symbol	Stage	Symbol	Substage (informal)	Symbol	Base age, Ma				Duration, Ma	Lower boundary defining event (and currently used proxy)	Boundary stratotype or (reference section)	SSP?
						2004	2010	2012	2015				
Wanganui Series	W	Haweran	Wq			0.34	0.34	0.34	0.34	0.34	Base of Rangitawa Tephra	Rangitawa Stream, Rangitikei Valley	SSP
		Castlecliffian	Wc			1.63	1.63	1.63	1.63	1.29	Base of Ototoka Tephra	Wanganui coast, Ototoka Stream	SSP
		Nukumaruan	Wn			2.40	2.4	2.4	2.40	0.77	LO *Zygochlamys delicatula*	Base Hautawa Shellbed, Old Hautawa Road, Rangitiki Valley SSP (provisional)	SSP
		Mangapanian	Wm			3.00	3.0	3.0	3.00	0.60	LO *Phialopecten thompsoni*	Base Mangapani Shellbed, Mangapunipuni Stm, Waitotara	SSP
		Waipipian	Wp			3.60	3.6	3.7	3.70	0.70	HO *Reticulofenestra pseudoumbilica* (provisional)		
		Opoitian	Wo	(upper)		(4.25)			4.30	0.60	LO of *Globoconella inflata*		
				(lower)		5.28	5.33	5.3	5.33	1.03	LO *Globoconella puncticulata s.s.*	(Mangapoike River, Hawkes Bay)	
Taranaki Series	T	Kapitean	Tk	(upper)		5.53	5.6		5.6	0.27	LO *Globoconella sphericomiozea* s.s		
				(lower)		6.5	7.2	7.2	7.2	1.60	LO *Sectipecten wollastoni* (LO *Globoconella conomiozea*)		
		Tongaporutuan	Tt	(upper)		8.88	8.96		8.96	1.76	HO *Globoquadrina dehiscens*		
				(lower)		10.92	11.01	11.0	11.04	2.08	Base *Globoconella miotumida* Kaiti Coiling Zone		
Southland Series	S	Waiauan	Sw	(upper)					11.67	0.63	LO *Bolboforma subfragoris* s.l.		
				(lower)		12.7	12.98	12.7	13.05	1.38	HO *Globoconella conica* (provisional)	(Bryce Burn, Waiau Valley, Southland, provisional)	
		Lillburnian	Sl			15.1	15.1	15.1	15.1	2.05	LO *Orbulina suturalis*	(Clifden, Waiau River, Southland)	
		Clifdenian	Sc			15.9	15.9	15.9	15.9	0.8	LO *Praeorbulina curva*	(Clifden, Waiau River, Southland)	
Pareora Series	P	Altonian	Pl	(upper)		16.7	16.7		16.7	0.8	LO *Globoconella miozea*		
				(middle)		18.5	18.2		18.2	1.5	LO *Globoconella zealandica*		
				(lower)		19.0	19.0	18.7	18.7	0.5	LO *Globoconella praescitula*		
		Otaian	Po			21.7	21.7	21.7	21.7	3.0	LO *Ehrenbergina marwicki* lineage	(Bluecliffs, Otaio River, south Canterbury)	
Landon Series	L	Waitakian	Lw			25.2	25.2	25.2	25.2	3.5	LO *Globoquadrina dehiscens*	Trig Z, Otiake, Waitaki Valley	SSP
		Duntroonian	Ld			27.3	27.3	27.3	27.3	2.1	LO *Notorotalia spinosa*	(Landon Creek, Oamaru)	
		Whaingaroan	Lwh	(upper)		30.0	30.1		29.8	2.5	HO *Subbotina angiporoides*		
				(lower)		34.3	34.5	34.6	34.6	4.8	HO *Globigerinatheka index*	Point Elizabeth, Westland	SSP
Arnold Series	A	Runangan	Ar			36.0	36.0	36.4	36.7	2.1	LO *Bolivina pontis*	Sea cliffs, north of Point Elizabeth, Westland	SSP
		Kaiatan	Ak			37.0	38.4	39.1	39.1	2.4	HO *Acarinina primitiva*	Hampden coastal section, Otago	SSP
		Bortonian	Ab			43.0	42.77	42.6	42.6	3.5	LO *Globigerinatheka index*	Hampden coastal section, Otago	SSP
Dannevirke Series	D	Porangan	Dp			46.2	45.3	45.7	45.7	3.1	LO *Elphidium saginatum*	(Te Uri Stream, southern Hawkes Bay)	
		Heretaungan	Dh			49.5	49.3	49.2	48.9	3.2	LO *Elphidium hampdenensis*	(Te Uri Stream, southern Hawkes Bay)	
		Mangaorapan	Dm			53.0	53.3	53.7	52.0	3.1	LO *Morozovella crater*	(Te Uri Stream, southern Hawkes Bay)	
		Waipawan	Dw			55.5	55.8	56.0	56.0	4.0	Onset of PETM carbon isotope excursion	Tawanui Stream, southern Hawkes Bay	SSP
		Teurian	Dt	(upper)		59.7	60.48		61.5	5.5	LO *Fasciculithus tympaniformis*		
				(lower)		65.0	65.5	66.0	66.0	4.5	Base of Boundary clay and iridium anomaly	Flaxbourne River, Marlborough	SSP

Appendix 4: Biostratigraphic data

HH1

Foraminifera

Gaudryina convexa
Spiroplectinella proxispira
Textularia barnwelli
Textularia cf. *kapitea*
Textularia cf. *miozea*
Textularia cf. *subrhombica*
Textularia sp.
Siphotextularia sp.
Lenticulina calcar
Lagena striata
Fissurina clathrata
Fissurina spp.
Favulina spp.
Globigerinoides triloba
Globigerina bulloides
Globigerina falconensis
Turborotalita quinqueloba
Globoconella conomiozea
Globoconella miotumida
?Paragloborotalia sp.
Neogloboquadrina cf. *acostaensis*
Neogloboquadrina pachyderma
Orbulina universa
Bolivina petiae
Rectobolivina striatula
Rectobolivina parvula
Cassidulina laevigata
Cibicides deliquatus
Cibicides finlayi
Trifarina bradyi
Cibicides molestus
Discorbinella ?complanata
Cassidulina carinata
Planulina sp.
Laticarinina altocamerata
Pileolina cf. *zelandica*
?Rosalina sp.
Melonis sp.
?Zeaflorilus parri
Notorotalia cf. *finlayi*
Notorotalia taranakia

Mollusca

Pectinidae indet.
Crassostrea ingens
Juvenile *Osteridae* indet.

Brachiopoda

Notosaria nigricans
Neothyris sp.
Micro brachiopods indet.

Other

Barnacle plates
Bryozoa (bryoliths)
Ostracods

HH2

Foraminifera

Karreriella ?cylindrica
Martinottiella communis
Siphotextularia wairoana
Haeuslerella morgani
Haeuslerella pliocenica
Textularia spp.
Sigmoilopsis schlumbergi
Spiroloculina communis
Amphicoryna hirsuta
Laevidentalina communis
Nodosaria acuminata
Dentalina spp.
Neugeborina longiscata
Mucronina sp.
Lenticulina calcar
Lagena cf. *desmorphora*
Lagena striata
Lagena laevis
Fissurina earlandi
Favulina hexagona
Fissurina spp.
Globoconella puncticulata
Globigerina falconensis
Neogloboquadrina pachyderma
Neogloboquadrina deutertrei
Globoconella pliozea

Orbulina suturalis
Globigerinoides triloba
Globigerina sp.
Globigerina bulloides
Globigerinita glutinata
Turborotalita quinqueloba
Rectobolivina striatula
Bolivina affiliata
Bolivina watti
Bolivina parri
Cassidulina carinata
Globocassidulina subglobosa
Globocassidulina cuneata
Ehrenbergina mestayerae
Bulimina aculeata
Uvigerina cf. *mioschwageri*
Uvigerina ?delicatula
Uvigerina cf. *zeacuminata*
Neouvigerina bellula
Trifarina bradyi
Sphaeroidina bulloides
Laticarinina altocamerata
Laticarinina sp.
Cibicides deliquatus
Cibicides molestus
Dyocibicides biserialis
Nonionella cf. *magnalingua*
Gyroidina soldanii
Pullenia bulloides
?Osangularia bengalensis
Discorbinella bertheloti
?Anomalinoides sphericus
Anomalinoides sp.
Pullenia quinqueloba
Planulina sp.
Astrononion cf. *stelligerum*
Notorotalia cf. *finlayi*
Notorotalia cf. *zelandica*
Notorotalia cf. *rotunda*

Other

Ostracods
Barnacle plates
Fish scales
Bryozoa

HH3

Foraminifera

Gaudryina convexa
Sigmoidella pacifica
Bifarilaminella advena
Amphicoryna hirsuta
Globoconella pliozea
Globoconella puncticulata
Globoconella cf. *inflata*
Globigerinita glutinata
?Paragloborotalia sp.
Globigerina bulloides
Globigerina falconensis
Orbulina suturalis
Neogloboquadrina pachyderma
Turborotalita quinqueloba
Bolivina cf. *vellai*
Rectobolivina striatula
Globocassidulina cuneata
Globocassidulina subglobosa
Ehrenbergina mestayeri
Bulimina aculeata
Uvigerina ?delicatula
Patellinella inconspicua
Cibicides deliquatus
Gyroidina soldanii
Cibicides molestus
?Alabaminella weddellensis
Planulina sp.
?Dyocibicides sp.
Notorotalia taranakia
Cassidulina laevigata
Rotaliina indet., various

Other

Ostracods
Talochlamys gemmulata (bored)
Neothyris sp.

TA3

Foraminifera

Globigerina bulloides
Neogloboquadrina pachyderma
Globoconella cf. *miotumida*
Bolivina petiae

Rectobolivina striatula
?Quinqueloculina sp.
Cassidulina carinata
Globocassidulina cuneata
Trifarina bradyi
Cibicides deliquatus
Cibicides molestus
Gyroidina soldanii
?Cibicides sp.

Other

Bryozoan fragmenta
Sponge spicules
Shark teeth

TA4

Foraminifera

Gaudryina convexa
Textularia kapitea
Textularia spp.
?Martinottiella sp.
Corunspira sp.
Sigmoidella sp.
Dentalina sp.
?*Nodosaria vertebralis*
Lenticulina calcar
Saracenaria latifrons
Favulina hexagona
Fissurina cf. *orbignyana*
Fissurina sp.
Globoconella miotumida
Globoconella conomiozea
Neogloboquadrina pachyderma
Globigerina bulloides
Globigerina falconensis
Zeaglobigerina woodi
?Paragloborotalia sp.
Bolivina watti
Bolivina parri
Bolivina sp.
Rectobolivina striatula
Rectobolivina parvula
Cassidulina carinata
Ehrenbergina sp.
Ehrenbergina cf. *mestayeri*
Uvigerina ?delicatula
Trifarina bradyi
Patellinella inconspicua
Cibicides deliquatus
Cibicides molestus
Dyocibicides sp.
Pileolina sp.
Nonionella flemingi
Gyroidinoides zelandica
Rosalina sp.
Planulina sp.
Elphidium novozealandicum
Notorotalia ?hurupiensis
?Neoconorbina sp.

Other

Ostracods
Bryozoan fragments
Sponge spicules

TA5

Foraminifera

Gaudryina convexa
?Siphotextularia sp.
Nodosaria longiscata
Mucronina advena
Parafrondicularia antonina
Lenticulina calcar
Amphicoryna hirsuta
Nodosaria vertebralis
Zeaglobigerina woodi
Globoconella puncticulata
Truncorotalia crassaformis
?Paragloborotalia sp.
Globigerina bulloides
?Tenuitellinata angustiumbilicata
Turborotalita quinqueloba
Neogloboquadrina pachyderma
Globigerinita glutinata
Bolivina spathulata
Bolivina watti
Bolivina affiliata
Ehernbergina mestayeri
Bulimina striata
Cassidulina laevigata

Globocassidulina cuneata
Globocassidulina subglobosa
Bulimina aculeata
Uvigerina ?delicatula
Uvigerina cf. *zeacuminata*
Uvigerina cf. *mioschwageri*
Trifarina bradyi
Neouvigerina bellula
Neouvigerina eketahuna
Stilostomella sp. (spined var.)
Sphaeroidina bulloides
Cibicides molestus
Laticarinina pauperata
Cibicides finlayi
Cibicides deliquatus
Anomalinoides parvumbilia
Gyroidina soldanii
Melonis sp.
Pullenia bulloides
Nonionella novozelandica
Notorotalia depressa
Planulina sp.

07A

Foraminifera

Textularia sp.
?*Haeuslerella* sp.
Nodosaria sp.
Lagena cf. *laevis*
?Saracenaria sp.
Globoconella puncticulata
Truncorotalia crassaformis
Neogloboquadrina pachyderma
Zeaglobigerina woodi
Orbulina universa
Globigerina bulloides
Globigerinita glutinata
Bolivina cf. *affiliata*
Bolivina sp.
Chilostomella ovoidea
Ehrenbergina sp.
?*Uvigerina* sp.
Sphaeroidina bulloides
Nonionella sp.
Pullenia quinqueloba
?Cassidalinoides orientalis
Bolivinita sp.
Various indet.

BC1

Foraminifera

Siphotextularia sp.
Textularia cf. *miozea*
?Dentalina sp.
Mucronina subtregonata
Neugeborina longiscata
Parafrondicularia antonina
Stilostomella sp. (spined var.)
Lenticulina calcar
Saracenaria latifrons
Amphicoryna hirsuta
Globoconella miotumida
Globigerina bulloides
Zeaglobigerina woodi
Globigerinita uvula
Globigerinita glutinata
Bolivina affiliata
Bolivina parri
Bolivina spathulata
Cassidulina cuneata
Bolivina petiae
Bolivina vellai
Bolivinita pohana
Bulimina striata
Uvigerina ?delicatula
Uvigerina cf. *zeacuminata*
Uvigerina cf. *mioschwageri*
Neouvigerina eketahuna
Trifarina bradyi
Trifarina angulosa
Sphaeroidina bulloides
Cibicides deliquatus
Cibicides finlayi
Cibicides sp.
Nonionoides turgida
Pullenia bulloides
Pullenia quinqueloba
Melonis sp.

Anomalinoides cf. *subnonionoides*
Gyroidinoides zelandica
Gyroidina soldanii

Spores, pollen, etc.

Nothofagidites type
Lateropora type
Fungal spore
Plant debris
Insect parts

Other

Otoliths

BC2

Foraminifera

Textularia cf. *kapitea*
Martinottiella communis
Siphotextularia cf. *awamoana*
Haeuslerella morgani
Karreriella sp.
Nodosaria sp.
Plectofrondicularia pohana
Stilostomella sp. (spined var.)
Lenticulina loculosa
Lenticulina calcar
Lenticulina orbicularis
Globoconella miotumida
Globoconella conomiozea
Neogloboquadrina pachyderma
Turborotalita quinqueloba
Globigerinita glutinata
Globigerinoides triloba
Zeaglobigerina woodi
Bolivina affiliata
Bolivina watti
Rectobolivina striata
Rectobolivina parvula
Bolivinita pohana
Cassidulina carinata
Cassidulina laevigata
Globocassidulina subglobosa
Ehrenbergina sp.
Uvigerina ?delicatula
Neouvigerina eketahuna
Trifarina bradyi
Cibicides finlayi
Cibicides deliquatus
Dyocibicides biserialis
Cibicides molestus
Cibicides cf. *subhadingeri*
Gavelinopsis praegeri
Gyroidina soldanii
?Anomalinoides sphericus
Anomalinoides parvumbilia
Pullenia bulloides
Planulina sp.
Notorotalia sp.
Rotaliina indet. various
Hoeglundina elegans

Mollusca

Tucetona laticostata
Mesopeplum sp.
Purpurocardia sp.
Brachiopoda
Notosaria nigricans
Neothyris ovalis

BC3

Foraminifera

Karreriella cushmani
Karreriella cylindrica
Martinottiella communis
Haeuslerella pliocenica
Textularia spp.
?Nodosaria vertebralis
Dentalina spp.
Parafrondicularia antonina
Lenticulina peregrina
?Marginulina sp.
Stilostomella sp. (spined var.)
Lenticulina loculosa
Lenticulina calcar
Lenticulina sp.
Lenticulina ?anaglypta
?Amphicoryna hirsuta
?Pseudonodosaria sp.
Globoconella puncticulata
Globoconella pliozea
Globoconella cf. *conomiozea*

Neogloboquadrina pachyderma
Neogloboquadrina cf. *acostaensis*
Orbulina universa
Globigerina bulloides
Globigerinita glutinata
Bolivina affiliata
Bolivina watti
Uvigerina ?delicatula
Uvigerina cf. *zeacuminata*
Uvigerina ?rodleyi
Neouvigerina eketahuna
Trifarina bradyi
Sphaeroidina bulloides
Laticarinina pauperata
Cibicides molestus
Cibicides deliquatus
Anomalinoides subnonionoides
Anomalinoides parvumbilia
Notorotalia sp.
Rotaliina indet.

BC4

Foraminifera
Karreriella cylindrica
Textularia cf. *lythostrota*
Siphotextularia sp.
Karreriella bradyi
Textularia spp.
Sigmoilopsis schlumbergi
Laevidentalina communis
Stilostomella sp. (spined var.)
Nodosaria sp.
Dentalina sp.
Laevidentalina sp.
Lenticulina loculosa
Nodosaria longiscata
Nodosaria vertebralis
Mucronina advena
Amphicoryna hirsuta
Fissurina submarginata
Globoconella puncticulata
Truncorotalia crassaformis
Neogloboquadrina pachyderma
Neogloboquadrina cf. acostaensis
?Paragloborotalia sp.
Globoconella cf. *sphericomiozea*
?Tenuitellinata angustiumbilicata
Globigerinella cf. *obesa*
Globigerina falconensis
Globigerina bulloides
Zeaglobigerina woodi
Globigerinita glutinata
Bolivina cf. *vellai*
Pleurostomella alternans
Uvigerina delicatula
Cassidulina carinata
Bulimina aculeata
Bulimina striata
Trifarina bradyi
?Rosalina bradyi
Sphaeroidina bulloides
Neouvigerina eketahuna
Neouvigerina bellula
Laticarinina pauperata
Patellinella inconspicua
Laticarinina altocamerata
Cibicides refulgens
Cibicides pachyderma
Cibicides deliquatus
Cibicides molestus
Melonis sp.
Pullenia bulloides
Anomalinoides parvumbilia
Oridosalis umbonatus
?Cibicides sp.
Notorotalia cf. *finlayi*
Notorotalia sp.
Gyroidinoides zelandica

BC5

Foraminifera
Martinottiella communis
Karreriella cylindrica
Textularia spp.
Sigmoilopsis schlumbergi
Dentalina sp.
Mucronina hasta
Parafrondicularia antonina

Amphicoryna hirsuta
Stilostomella sp. (spined var.)
Lagena spp.
Globoconella puncticulata
?Paragloborotalia sp.
Turborotalita quinqueloba
Hirsutella cf. *scitula*
Globigerinita glutinata
Globigerina bulloides
Globigerina falconensis
?Tenuitellinata angustiumbilicata
Globigerinoides triloba
Globigerinita uvula
?Globorotalia spp.
Bolivina affiliata
Bolivina spathulata
Bolivina compressa
Cassidulina carinata
Globocassidulina cuneata
Bulimina striata
Bulimina aculeata
Uvigerina delicatula
Uvigerina cf. *mioschwageri*
Trifarina bradyi
Neouvigerina eketahuna
Hoeglundina elegans
Cibicides molestus
Pullenia bulloides
Pullenia quinqueloba
Laticarinina altocamerata
Planulina sp.
Cibicides dispars
Nonionella sp.
Astrononion parki
Astrononion ?stelligerum
Siphonina sp.
Rotaliina indet. various

28A

Spores, pollen, etc.
Nothofagidites type
Asteraceae type
Rubiaceae type
Myrtaceae type
Assamiapollenites type
Haloragacidites type
Monosulcites type
Kuylisporites type
Liliacidites type
Swamp types (abundant)
Podocarpaceae type
Proteacidites type
Tricolpites type
Tetrad type
Fagaceae type
Apiaceae type
Plant debris

19A

Foraminifera
Karreriella cylindrica
Martinottiella communis
Siphotextularia awamoana
Siphotextularia subcylindrica
Siphotextularia cf. *ihungia*
Siphotextularia sp.
Haeuslerella morgani
Haeuslerella parri
Textularia miozea
Textularia spp.
Spiroloculina sp.
Biloculina sp.
Dentalina sp.
?Nodosaria vetrebralis
Nodosaria sp.
Lenticulina peregrina
Lenticulina calcar
Lenticulina cultrata
Amphicoryna hirsuta
Lagena spiratiformis
Fissurina sp.
Favulina melo
Globoquadrina dehiscens
Globoconella miotumida
Globoconella cf. *conomiozea*
Truncorotalia cf. *juanai*
Neogloboquadrina pachyderma
Neogloboquadrina cf. *acostaensis*

Globigerina bulloides
Globigerina falconensis
Globigerinoides triloba
?Paragloborotalia sp.
Zeaglobigerina woodi
Hirsutella scitula
Zeaglobigerina nepenthes
Turborotalita quinqueloba
Globigerinita uvula
Orbulina suturalis
Orbulina universa
Bolivina spathulata
Bolivina parri
Bolivina minuta
Bolivina affiliata
Bolivina albatrossi
Boilvinita pohana
Bolivinita quadrilatera
Fursenkoina vellai
Cassidulina carinata
Globocassidulina subglobosa
Cassidulina laevigata
Bulimina striata
Trifarina bradyi
Uvigerina cf. *pliozea*
Neouvigerina eketahuna
Chilostomella ovoidea
Cibicides deliquatus
Cibicides molestus
Discorbinella rarescens
Astrononion parki
Planulina sp.
Melonis sp.
Pullenia bulloides
Anomalinoides subnonionoides
Anomalinoides parvumbilia
Grroidinoides zelandica
Notorotalia finlayi
Notorotalia taranakia
Rotaliina indet., various
Hoeglundina elegans

Spores, pollen, etc.

Cyathea type
Lycopodium type
Monolete fern
Centrolepis type
Pimelea type
Nothofagidites type
Fungal spores
Plant debris

Other

Ostracods including *Bradleya* sp.
Gastropoda indet.
Otoliths

24A

Foraminifera

Gaudryina convexa
Spiroplectinella proxispira
Textularia sp.
Siphotextularia wairoana
Corunspira sp.
?Marginulina sp.
Lagena striata
Fissurina cf. *orbignyana*
Fissurina sp.
Globigerina falconensis
Globigerinita uvula
?Paragloborotalia sp.
Globigerinita glutinata
Globigerinoides triloba
Hirsutella cf. *scitula*
Bolivina subspinescens
Bolivina watti
Bolivina sp.
Bolivina affiliata
Cassidulina carinata
Cassidulina laevigata
Globocassidulina subglobosa
Trifarina bradyi
Patellinella inconspicua
Cibicides molestus
Cibicides cf. *novozelandicus*
Cibicides finlayi
Cibicides deliquatus
Cibicides sp.
Gyroidinoides zelandica
Dyocibicides biserialis
Planulina sp.

Nonionella sp.
Rosalina sp.
Siphonina sp.
Anomalinoides cf. *subnonionoides*
Astrononion parki
Nonionella flemingi
Rotaliina indet., various

23A

Foraminifera
Gaudryina convexa
Textularia cf. *pseudogramen*
Migros cf. *medwayensis*
Textularia kapitea
Spiroplectinella proxispira
Tectularia barnwelli
Textularia spp.
Lenticulina calcar
Lenticulina orbicularis
Fissurina spp.
Globigerina falconensis
Pileolina spp.
Cibicides deliquatus
Cibicides molestus
Cibicides sp.
Rosalinidae indet.
Melonis sp.
Anomalinoides parvumbilia
Laticarinina altocamerata
Cassidulina laevigata
Planulina sp.
Rotaliina indet. Various
Mollusca
Mesopeplum crawfordi
Crassostrea ingens
Fissidentalium solidum (not collected)
Other
Micro-brachiopods
Ostracods

25A

Mollusca
Mesopeplum burnetti

35B

Foraminifera
Gaudryina convexa
Spiroplectinella proxispira
Haeuslerella morgani
Lenticulina sp.
?Spirillina sp.
Fissurina cf. *submarginata*
Truncorotalia juanai
Globoconella miotumida
Globoconella cf. *conomiozea*
Turborotalita quinqueloba
Neogloboquadrina pachyderma
Globigerina bulloides
Globigerinoides triloba
Bolivina spathulata
Bolivina subspinescens
Bolivina watti
Rectobolivina striatula
Cassidulina laevigata
Cassidulina carinata
Ehrenbergina cf. *marwicki*
Trifarina bradyi
Cibicides deliquatus
Dyocibicides biserialis
Cibicides finlayi
Cibicides molestus
?*Rosalina* sp.
Elphidium novozealandicum
Rotaliina indet., various
Hoeglundina elegans

35A

Foraminifera
Lenticulina sp.
Mollusca
Phialopecten marwicki
Other
Barnacle plates

18A

Foraminifera

Karreriella cylindrica
Haeuslerella morgani
Sigmoilopsis schlumbergi
Nodosaria spp.
Laevidentalina communis
Stilostomella sp. (spined var.)
Lenticulina calcar
Saracenaria italica
Globoconella conomiozea
Globoconella cf. *miotumida*
Truncorotalia cf. *juanai*
Globigerina bulloides
Zeaglobigerina woodi
Globigerinoides triloba
Globigerinita glutinata
Globigerina falconensis
?Tenuitellinata angustiumbilicata
Neogloboquadrina pachyderma
Bolivina affiliata
Bolivina cf. *petiae*
Bolivina watti
Bolivinita pliozea
Cassidulina laevigata
Globocassidulina cuneata
Ehrenbergina cf. *mestayeri*
Bulimina striata
Bulimina aculeata
Uvigerina ?delicatula
Uvigerina cf. *mioschwageri*
Uvigerina cf. *zeacuminata*
Neouvigerina eketahuna
Siphouvigerina proboscidea
Trifarina bradyi
Patellinella inconspicua
Cibicides deliquatus
Cibicides finlayi
Cibicides molestus
Pullenia quinqueloba
Pullenia bulloides
Planulina sp.
Gyroidinoides zelandica
Gyroidina soldanii
Cibicides sp.
?Nonionoides grateloupi
Dentalina sp.
Pleurostomella alternans
Notorotalia sp.
Notorotalia taranakia